UTION TEST CHART

②

TECHNICAL REPORT GL-88 6

GEOPHYSICAL INVESTIGATION IN SUPPORT OF BEAVER DAM COMPREHENSIVE SEEPAGE INVESTIGATION

by

Jose L. Llopis, Dwain K. Butler

Geotechnical Laboratory
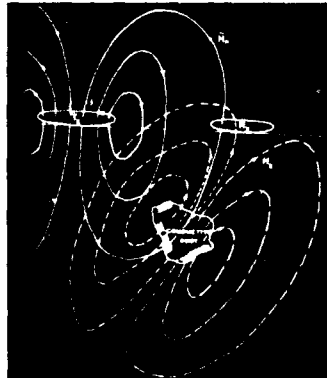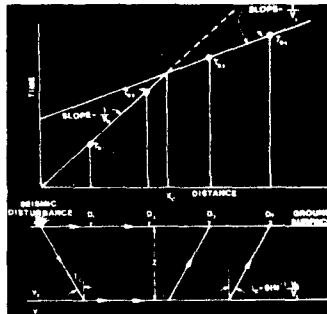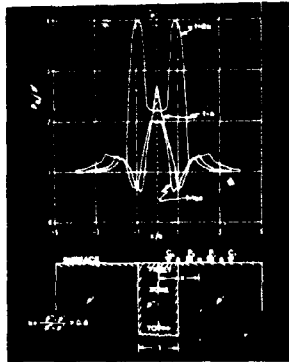
DEPARTMENT OF THE ARMY
US Army Engineer Waterways Experiment Station
PO Box 631, Vicksburg, Mississippi 39180-0631

US Army Corps of Engineers

AD-A195 588

DTIC
S **ELECTE**
D
JUN 0 1 1988
D

May 1988
Final Report

Approved For Public Release; Distribution Unlimited

88 6 1 039

REPORT DOCUMENTATION PAGE

Form Approved
OMB No. 0704-0188

1a. REPORT SECURITY CLASSIFICATION Unclassified	1b. RESTRICTIVE MARKINGS

2a. SECURITY CLASSIFICATION AUTHORITY	3. DISTRIBUTION/AVAILABILITY OF REPORT
2b. DECLASSIFICATION/DOWNGRADING SCHEDULE	Approved for public release; distribution unlimited.

4. PERFORMING ORGANIZATION REPORT NUMBER(S) Technical Report GL-88-6	5. MONITORING ORGANIZATION REPORT NUMBER(S)

6a. NAME OF PERFORMING ORGANIZATION USAEWES Geotechnical Laboratory	6b. OFFICE SYMBOL (If applicable) CEWES-GH	7a. NAME OF MONITORING ORGANIZATION

6c. ADDRESS (City, State, and ZIP Code) PO Box 631 Vicksburg, MS 39180-0631	7b. ADDRESS (City, State, and ZIP Code)

8a. NAME OF FUNDING/SPONSORING ORGANIZATION US Army Engineer District, Little Rock	8b. OFFICE SYMBOL (If applicable)	9. PROCUREMENT INSTRUMENT IDENTIFICATION NUMBER

8c. ADDRESS (City, State, and ZIP Code)
PO Box 867
Little Rock, AR 72203-0867

10. SOURCE OF FUNDING NUMBERS

PROGRAM ELEMENT NO.	PROJECT NO.	TASK NO.	WORK UNIT ACCESSION NO.

11. TITLE (Include Security Classification)

Geophysical Investigation in Support of Beaver Dam Comprehensive Seepage Investigation

12. PERSONAL AUTHOR(S)
Llopis, José L.; Butler, Dwain K.

13a. TYPE OF REPORT Final report	13b. TIME COVERED FROM_____ TO_____	14. DATE OF REPORT (Year, Month, Day) May 1988	15. PAGE COUNT 103

16. SUPPLEMENTARY NOTATION
Available from National Technical Information Service, 5285 Port Royal Road Springfield, VA 22161.

17. COSATI CODES			18. SUBJECT TERMS (Continue on reverse if necessary and identify by block number)
FIELD	GROUP	SUB-GROUP	Beaver Dam Seepage
			Dams
			Geophysical investigation

19. ABSTRACT (Continue on reverse if necessary and identify by block number)

A comprehensive seepage assessment of Beaver Dam, AR, was performed using a suite of geophysical methods. The Boone Formation, a severely weathered limestone, underlies Dike 1 and has been experiencing seepage since initial filling of the reservoir in 1966. Between the period 1968 and 1971 a grout curtain was constructed at Dike 1 to curtail this seepage. Although the grout curtain reduced the Dike's foundation leakage, recently discovered seeps and boils on the downstream toe of Dike 1 suggest that leakage is increasing to pregrouting levels.

Following a recommendation of the May 1984 Dam Safety Assurance Program Reconnaissance Report, a geophysical investigation was undertaken to assess and delineate seepage paths and to map fault zones believed to behave as hydraulic conduits. The geophysical investigation conducted at Dike 1 consisted of self potential (SP), seismic refraction,

(Continued)

20. DISTRIBUTION/AVAILABILITY OF ABSTRACT ☐ UNCLASSIFIED/UNLIMITED ☒ SAME AS RPT. ☐ DTIC USERS	21. ABSTRACT SECURITY CLASSIFICATION Unclassified
22a. NAME OF RESPONSIBLE INDIVIDUAL	22b. TELEPHONE (Include Area Code) 22c. OFFICE SYMBOL

DD Form 1473, JUN 86   Previous editions are obsolete.   SECURITY CLASSIFICATION OF THIS PAGE

19. ABSTRACT (Continued).

electrical resistivity, electromagnetic induction, magnetic, downhole water conductivity, and downhole water temperature surveys.

Results indicate that the geophysical tests were successful in determining the locations and strike of two faults bounding Dike 1. Results also indicate that seepage is pervasive rather than occurring in a few well defined conduits. Geophysical evidence suggests that the south bounding fault may act as a broad conduit for flow. The seismic refraction surveys indicate that the contact between the weathered limestone (Boone Formation) and the underlying more competent limestone is highly variable in depth. SP results indicate a correlation between SP values and pool elevation.

PREFACE

A geophysical seepage investigation at Beaver Dam was authorized by the US Army Engineer District, Little Rock (SWL), under IAO Nos. 85-0024, 85-0038, 85-0045, 86-0024, and 87-78, dated 1 November 1984, 8 January 1985, 19 February 1985, 7 November 1985, and 13 February 1987, respectively.

This report was prepared by Mr. J. L. Llopis and Dr. D. K. Butler, Earthquake Engineering and Geophysics Division (EEGD), Geotechnical Laboratory (GL), US Army Engineer Waterways Experiment Station (WES), Vicksburg, MS under the direct supervision of Mr. J. R. Curro, Jr., EEGD. The work was performed under the general supervision of Drs. A. G. Franklin, Chief, EEGD, and W. F. Marcuson III, Chief, GL.

Field work was performed by Dr. D. K. Butler, Messrs. J. R. Curro, Jr., J. L. Llopis, D. E. Yule, and M. K. Sharp, EEGD. Messrs. C. M. Deaver and S. C. Hartung, SWL, supervised the installation of the SP arrays and acquired SP data during the study period. Messrs. Deaver and Hartung also provided invaluable technical and field assistance.

COL Dwayne G. Lee, CE, was the Commander and Director of WES. Dr. Robert W. Whalin was the Technical Director.

Accesion For	
NTIS CRA&I	☑
DTIC TAB	☐
Unannounced	☐
Justification	
By	
Distribution /	
Availability Codes	
Dist	Avail and / or Special
A-1	

1

CONTENTS

CONVERSION FACTOR, NON-SI TO SI (METRIC)
UNITS OF MEASUREMENT

Non-SI units of measurement used in this report can be converted to SI (metric) units as follows:

Multiply	By	To Obtain
cubic feet	0.02832	cubic metres
Fahrenheit degrees	5/9	Celsius degrees or Kelvins*
feet	0.3048	metres
gallons per minute	3.785	liters per minute
miles (US statute)	1.609347	kilometers
millimhos per foot	3.28	millimhos per meter
ohm-feet	0.3048	ohm-metres
pounds (force) times seconds per square foot	14.88164	poise
pounds (force) per square foot	47.88026	pascals

---

* To obtain Celsius (C) temperature readings from Fahrenheit (F) readings, use the following formula: $C = (F - 32) * (5/9)$. To obtain Kelvin (K) readings, use: $K = (F - 32) * (5/9) + 273.15$.

GEOPHYSICAL INVESTIGATION IN SUPPORT OF BEAVER DAM
COMPREHENSIVE SEEPAGE INVESTIGATION

INTRODUCTION

1. **Background.** Geophysics is the application of physics to the study of the earth. In recent years it has been shown that the role of applied geophysics in geotechnical studies is very important. The use of geophysics in geotechnical projects can save time and money and also provide comprehensive information of subsurface conditions that can supplement more traditional methods of investigation, i.e. drilling, and can eventually lead to a better designed and managed project. The results obtained from performing a geophysical investigation can be an aid in planning a more logical and economical study. It is important to realize that the role of geophysics is to supplement and/or complement more conventional types of geotechnical testing, not to replace them.

2. The U.S. Army Corps of Engineers District, Little Rock (SWL), sponsored a comprehensive investigation of seepage conditions at Beaver Dam, Arkansas, by the U.S. Army Engineer Waterways Station (WES) beginning in March 1985. As part of the seepage study, WES proposed a suite of geophysical tests to aid in the investigation. The test methods included self potential (SP), borehole water temperature and conductivity measurements, electrical resistivity, magnetic, and electromagnetic induction profiling, and seismic refraction. The results of the geophysical investigation were deemed to be necessary input by SWL personnel for planning the future placement of piezometers and exploratory borings and for determining the most appropriate remedial measure to abate seepage at the site.

3. **Purpose.** The purpose of this report is to describe the conduct of an in-situ geophysical seepage investigation performed on the foundation materials of Dike 1, Beaver Dam, Arkansas and how these survey results were integrated with a seepage assessment program. The objectives of the geophysical investigation were as follows:

> 1. Detect, map, and monitor seepage through the
>   foundation of Dike 1.

2. Delineate geologic structure beneath and
   immediately adjacent Dike 1, especially to
   locate fault zones in the bedrock beneath and
   immediately adjacent to Dike 1.

3. Provide input to the rational planning of
   remedial measures.

4. To evaluate the effectiveness of each of the
   above geophysical methods for detecting
   seepage detection and/or geologic mapping.

4. **Location.** Beaver Dam is located on the White River at river mile
609.0 in Carroll County, Arkansas, approximately 6 miles northwest of Eureka
Springs, Arkansas, as shown in Figure 1. Beaver dam is a straight,
gravity-type, concrete structure flanked to the north by an earth embankment
(main embankment) and three saddle dikes. The location of Dike 1 relative to
the main dam and main embankment is shown in Figure 2. The reservoir is used
for flood control, power generation, and water supply. Construction of the dam
was started in November 1960 and completed in June 1966. Dike 1 is
approximately 1,000 ft in length and 30 ft high. The top of the conservation
pool is elevation 1,120 ft while the top of the dike is elevation 1,142 ft.
Dike 1 is built on intensely weathered limestone and is experiencing severe
seepage which is evident from various discharge or leakage points on the
downstream toe and left abutment/dike contact.

GEOLOGY

Regional Geology

5. **General geology.** Beaver Dam and reservoir area are located in an area known as the Ozark uplift, a region consisting of flat-lying sedimentary rocks composed chiefly of limestone and dolomitic limestone. The strata are nearly horizontal over the greater part of the area but are locally deformed by simple dislocations along southwest-northeast trending normal faults and shallow basins that in places are of considerable magnitude.

6. **Physiography.** The upland area around the dam is a part of the Springfield Plateau, the surface of which is developed at approximate elevation 1,500 ft on the cherty limestone of the Boone Formation. In the dam and reservoir area, the White River has cut a channel of approximately 600 ft in depth. This incision into the Plateau surface has resulted in a deeply and intricately dissected type of topography. The entrenched river follows a meandering course across the area.

7. **Stratigraphy.** Five formations are exposed at the dam site. They are (moving upsection) the Powell, the Cotter and the Jefferson City Formations of the Jefferson City Group which is of Ordovician age, the Chattanooga Formation of Devonian age, and the Boone Formation of Mississippian age (Figure 3). The Chattanooga and the Boone Formations are generally above reservoir level except in the vicinity of the left abutment of the dam and Dike 1 where the units are downfaulted. In the vicinity of the dam site, the Boone Formation caps the higher ridges and forms the sides of the valley down to approximate elevation 1,200 ft. Beneath this lies the Chattanooga Shale member (Chattanooga Formation), which in turn is underlain by its Sylamore Sandstone member. Beneath these and forming the valley walls below elevation 1,180 ft and underlying the greater part of the valley bottom are limestones and dolomitic limestones of the Jefferson City Group (Design Memorandum No. 5, 1959).

6

8. <u>Structural geology.</u> The general structural geology of the region is that of flat lying rocks which are locally deformed by simple dislocations along southwest-northeast trending normal faults that extend for considerable distances, and by monoclines, low domes, and shallow basins. The Beaver Dam site lies near the northeast end of a very gentle, shallow, elongate, northeast-southwest trending structural basin known as the Price Mountain syncline. This basin is often faulted in areas where the downfolding is most pronounced. In the greater part of the lower end of the reservoir, Ordovician strata underlie the valley floor and extend up the sides of the valley to about elevation 1,180 ft. Overlying these and almost everywhere above pool level are formations of Devonian and Mississippian age. In localized areas, these units have been downfaulted to form a part of the foundation under the topographically desirable dam sites in the valley. This is the case at Dike 1.

Dike 1

9. <u>Foundation materials.</u> Figure 4 shows the foundation materials underlying Dike 1. Dike 1 is founded on a downfaulted block (graben) of the Boone Formation. This downfaulted block extends approximately between station 63+00 at the northern end to approximate station 75+00 at the southern end, a total distance of approximately 1,200 ft. The graben is bounded by steeply dipping normal faults on either side trending roughly in a northeast-southwest direction. The vertical displacement of these faults is approximately 200 ft. Cores of the rock adjacent to the northern fault zone show evidence of fracturing within the fault; however, the fractures appear to be filled or cemented and sound. Boring information from the southern fault zone area indicates the presence of many clay-filled cavities. The southern fault gouge does not appear to have the same degree of soundness as the northern fault zone. The Boone Chert which makes up the foundation of Dike 1 can be divided into two distinct subunits (Figure 3). The uppermost unit (estimated thickness, 100 ft) is composed of calcium carbonate and chert which upon weathering has resulted in the removal of calcium carbonate and left a spongy, vuggy, residual material that is predominately chert. The lower zone (estimated thickness, 60 ft) is also composed of calcium carbonate and silica. However, this zone is characterized as being slightly weathered to unweathered

and contains more crystalline calcium carbonate. The second zone is moderately to closely jointed. This jointing has allowed the passage of water and has led to the dissolution of calcium carbonate which in turn has resulted in open channels and cavities.

10.   Underlying the Boone Chert Unit is the St. Joe Limestone, described as non-cherty, gray to green-gray, crystalline, very fossiliferous, and containing numerous thin shale seams and partings. Underlying the St. Joe Limestone is the Chattanooga Shale (Chattanooga Formation) described as black, firm, and fissile. The shale is considered to be an effective barrier to any downward movement of ground water.

11. **Pre-construction grout curtain.** The foundation materials of Dike 1 were recognized as being susceptible to seepage during the early phases of the site selection. In June 1959 it was decided that an economical solution to prevent a potential seepage problem was to install a grout curtain. The grout curtain consisted of two lines of holes spaced 5 ft apart with 10-ft hole spacings and extended to a depth of 5 ft below the top of sound or unweathered rock at all locations except between stations 72+70 and 74+70 where the grout curtain was extended deeper (16 to 65 ft) into sound rock. The grout was placed by gravity flow (Reconnaissance Report, Beaver Dam, 1984).

12. During initial filling of the reservoir (April 1966) seepage was detected in a small valley downstream of Dike 1. The reservoir pool elevation at this point was 1,102+ ft and the seep was flowing at a rate of 150-200 gpm. By June 1966 the reservoir elevation was 1,114 ft and eight additional seeps were detected with a combined flow rate of approximately 400 gpm. By the time remedial grouting operations had been undertaken in 1968 the combined flow rate of these seeps had risen to approximately 800 gpm. Conclusions from studies conducted at Dike 1, including flow measurements and dye tracing, indicated seepage was coming from the lake through two possible passages, either beneath the grout curtain through open cavities in the foundation rock, or along the top of rock or both. Seepage was occurring along the entire length of Dike 1 with the most concentrated flow occurring in the vicinity of station 71+00 near the southern portion of the dike (Reconnaissance Report, 1984).

13. There are numerous reasons why the pre-construction grout curtain did not perform satisfactorily. Some of the possible reasons for its ineffectiveness are as follows:

    a. Grout holes were not drilled deep enough into sound rock to intercept open joints.

    b. Grout was placed by gravity flow, therefore it is possible many small cavities and joints were not filled.

    c. Grout was too thick to enter some of the cavities and joints.

9

d. Drilling was done with tricone roller bits using
   compressed air to remove cuttings. It is believed
   that some of these cutting could have plugged some
   of the cavities preventing them from being grouted.

e. Many cavities and joints could have been missed
   altogether because of the grout hole spacing.

14. **Early Seepage Flow Studies.** Flow measurements, exploratory
drilling, pressure tests, and dye and temperature tests were conducted from
the time of leakage (1966) until 1968 to determine the extent and routes of
seepage through and beneath the dike, and formulate possible remedial
measures. These measurements were accomplished by installing two weirs, a
Parshall flume, and twenty-seven piezometers. The data suggested that the
leakage was issuing both through cavities below the original grout curtain and
along the top of crystalline/weathered rock interface. It was concluded that
seepage occurred along the entire length of Dike 1 and to the fault zone
beneath the main embankment at station 73+00, with the greatest seepage
occurring along the shortest flow path in the vicinity of station 71+00.

15. **Post-construction grout curtain.** During the period July 1968 to
December 1971 an extensive grouting program was conducted in an effort to
abate the seepage occurring at the dike. The program consisted of 30,040
linear ft being drilled in 228 holes. Also, 38,900 cubic ft of grout solids
were pressure injected into these holes with the heaviest grout takes
occurring in an area between stations 70+50 and 72+00. Problems encountered
during the grouting operations were collapsing boring walls (cave-in),
insufficient seating of casing, and incapability of grout pump to grout some
large cavities to refusal.

16. As a result of the remedial grouting program, seepage was reduced
to approximately 450 to 500 gpm for mid-pool elevations (1,120-1,130 ft), a
decrease in flow of 30 to 35 percent. During the period 1971 through 1984
piezometers were manually read approximately twice a year by SWL personnel
while the Parshall flume was read on a monthly basis by project personnel.
During a periodic inspection in 1980, a new seepage area was located on the
downstream right abutment of the dike. This prompted SWL personnel to
undertake an effort to locate, inspect, and describe all known seepage exits.

10

17. **Dam Safety Assurance Program.** When the U.S. Army Engineer Southwest Division's (SWD) Division-wide Master Plan for the Dam Safety Assurance Program was submitted in 1983, Beaver Dam was listed as requiring studies for a Reconnaissance Report under designated priorities of spillway adequacy and major seepage. The Reconnaissance Report, prepared by SWL, was submitted to SWD in May 1984. The report concluded that seepage at Dike 1 would increase to near pre-grouting flows (800+ gpm) during a Spillway Design Flood (Probable Maximum Flood, pool elevation 1,139.9 ft) and continue flowing at this rate even after the flood receded due to expansion of existing cavities. This conclusion was proven to be valid on 23 December 1984 when a Pool of Record (el. 1,130.4 ft) occurred. During the emergency flood procedure inspection on that date, the project superintendent observed a new seepage exit 500 feet downstream from Dike 1 with a flow rate of approximately 25 gpm. The alarming factor at the newly discovered exit however, was the large amounts of detrital material (sediment), ranging from clay- to gravel-size being discharged in the flow, i.e. muddy water. Another new seep was discovered on 2 January 1985 near the left dike/abutment contact at approximate elevation 1,106 ft. Water from this new seep was described as jetting vertically with a flow rate of approximately 7 gpm at pool elevation 1,125.1 ft (Feature Design Memorandum, 1987). The 1984 Reconnaissance Report recommended that a seepage investigation be undertaken to determine the location and extent of seepage and develop remedial measures to control seepage at Dike 1.

18. After approval of the Reconnaissance Report, a combined SWD/WES/SWL meeting was held at Beaver Dam during the period 14-16 January 1985 to discuss the proposed seepage investigations, which were initiated in February 1985. During the meeting results of monitoring and testing of the new seepage exit were reviewed. This review not only substantiated the need for seepage investigations, but also added an element of urgency and a necessity to expedite the investigations, and recommendations of measures to control seepage. In 1985 the monitoring/inspection of instrumentation and seepage was revised to more frequent scheduling, especially for pool levels above elevation 1,128 ft. The action having the greatest impact on project operations, due to severe seepage, is the request and approval for a deviation (loss) of the authorized flood storage pool in Beaver Lake from elevation 1,130 to 1,128 ft until the seepage the seepage problem is resolved. As

recommended in the 1984 Reconnaissance Report, SWL initiated a comprehensive seepage investigation of Dike 1. This program consisted of examining the project history, mapping and topographic surveying, surface geophysical testing, extending the piezometer network, including drilling, sampling and testing, exploratory drilling, seepage flow measurements, planning for and installing an automated piezometer and flow measurement data acquisition system, and remedial measure analysis. In support of this effort WES was requested to perform a geophysical investigation of the dike and its foundation. The geophysical investigation in support of the overall seepage assessment program is described below.

GEOPHYSICAL INVESTIGATION

Geophysical Methodology and Survey Program

Strategy of Geophysical Seepage
Mapping and Monitoring.

19. Geophysical methods are applied to seepage problems by attempting to detect, and map (1) anomalous conditions in the foundation, abutments, or the dike which may be conducive to the flow of water and/or (2) anomalies created by the flow of water. In the first case seepage conduits such as faults or fracture zones, gravel and sand layers, etc. are targets of the investigation. In the second case anomalous conditions generated by the streaming or flowing of water are the targets. It is important that a distinction be made between these two cases. In the first case the anomaly may be independent of the presence of water while in the second case the anomaly will exist only when seepage is occurring.

20. Detection refers to determining the existence of an anomaly at a given point, which may be due to seepage paths, seepage, or both. Mapping, on the other hand, refers to evaluating the extent of anomalous features at a given time (Greenhouse and Monier-Williams, 1985). Mapping is accomplished by using multiple geophysical survey lines and correlating anomalous conditions. This allows the projecting or mapping of anomalous conditions or flow paths in plan and depth in some cases. If these same surveys are conducted periodically (monitoring), then anomaly patterns around the site can be studied as a function of time. If these time-dependent anomalies exhibit a positive correlation with reservoir pool level, then the anomaly changes can be assumed to be attributed to changes in seepage conditions i.e. new flow path activated, increased flow along an existing flow path, or change in water chemistry or temperature. Monitoring allows for a more unambiguous interpretation of anomalous conditions. Self-potential (SP) and borehole water conductivity and temperature surveys were conducted periodically for this investigation.

13

Geophysical Methods

21. The geophysical methods used for the investigation are listed below. Also shown in the tabulation are the primary and secondary applicability of the methods (relevant to objectives 1 and 2).

Method	Primary Applicability	Secondary Applicability
Self Potential (SP)	Seepage Detection, Mapping and Monitoring	Geologic Mapping
Electrical Resistivity	Geologic Mapping	Seepage Mapping
Electromagnetic Conductivity (EM)	Geologic Mapping	Seepage Mapping
Seismic Refraction	Geologic Mapping	-------
Magnetic Profiling	Geologic Mapping	-------
Borehole Fluid Conductivity	Seepage Mapping	-------
Borehole Fluid Temperature	Seepage Mapping	-------

Survey Program

22. Six survey lines were established at Dike 1 as shown in Figure 5. The lines are designated by letters A through H. The following tabulation summarizes the geophysical program:

Survey Line	Applied Geophysical Method
A	SP
B	SP, Electrical Resistivity, Magnetic Profiling
C	SP, Electrical Resistivity, EM, Seismic Refraction, Magnetic Profiling
D	SP, Magnetic Profiling
E	SP, Magnetic Profiling
H	Electrical Resistivity, EM, Magnetic Profiling

Borehole water conductivity and temperature measurements were made in piezometer borings at the site which provided access for the downhole conductivity/temperature probe. SP measurements were made on most survey lines on numerous occasions by SWL and WES personnel; all other geophysical surveys were performed only once.

Principles and Field Procedures

23. The geophysical survey procedures, including a brief description of each survey type as it pertains to the investigation, are given below.

24. **SP Surveys.** SP refers to the spontaneous electrical potentials generated in the ground by the flow of fluid through a porous medium in response to a pressure differential. The electrokinetic or streaming potential, V, generated by the the flow of fluid in a porous medium as it interacts with the Helmholtz double layer at the pore surface is described by the Helmholtz-Smoluchoski equation:

$$V = \frac{\rho\, \epsilon\, \zeta}{4\pi\, \mu}\, \Delta P \qquad (1)$$

where   V = streaming potential (stat volts)

   ϵ = dielectric constant of the fluid
   (stat coulomb per stat volt-feet)

   ζ = electrokinetic or zeta potential (stat volts)

   ρ = resistivity of the fluid (stat volt-second-ft
   per stat coulomb)

   ΔP = pressure drop along flow path
   (pound force per square foot)

   μ = viscosity of the fluid
   (pound-second per square foot)

25. Water possesses a dipolar molecular structure in which there is a region that is positively charged (oriented between the two hydrogen atoms) and a negative region (oriented towards the oxygen atom). Electrostatic forces between materials with a negative net charge, such as silica-based minerals and carbonates, and the positively charged pole of the water molecule causes a layer of water to affix itself to the material surface leaving a more weakly charged region exterior to that first water layer. In a non-flowing water-solid system, the thermal motion inherent to the individual water molecules prevents more than two layers to be electrostatically bound to the material surface. If the water phase in the system is allowed to flow past the material under a pressure gradient, then some of molecules of the more weakly bound outer layer of molecules are swept away. The electrostatic charge imbalance that remains near the material surface is negatively charged and is observed as an electric potential (Warriner and Taylor, 1982).

16

26. Equation (1) holds true for capillary tubes, but it may be violated when flow is turbulent as in large fissures (Ogilvy et al., 1969). Presently, not enough is understood about the behavior of ρ, ξ , and μ in porous media, such as rocks and soil, to allow an accurate determination of the electrokinetic coupling coefficient $V/\Delta P$ (Corwin and Hoover, 1969).

27. The SP method of exploration has been in use for more than 50 years chiefly as a tool in mineral exploration, especially for sulfide ores. However, the SP method has been used with more frequency in recent years for geothermal exploration and seepage investigations. For many years the Russian literature has reported the use of the SP method in hydrological and geotechnical applications such as determining seepage paths at reservoirs and dams (Ogilvy et al., 1969; Bogoslovsky and Ogilvy, 1973). WES has recently used the SP method for mapping and monitoring subsurface seepage particularly at dam sites (Cooper et al., 1982; Koester et al., 1984; and Yule et al., 1985).

28. The SP survey is performed by installing copper-clad steel electrodes (grounding rods) into the ground, in either a grid or profile array, and measuring the electric potential between each rod and a reference electrode using a high impedance digital multimeter. The reference electrode is installed in an area believed to have a small potential gradient. Figure 6 diagramatically shows the generation of an SP anomaly. In this study the reference electrode was placed north of Dike 1 as shown in Figure 7. The ground, or negative clip lead, was always connected to the reference electrode to maintain a standard polarity convention. The reference electrode was connected to each electrode by a wire left in place between measurements.

29. In this study, five permanent SP electrode profiles were installed as shown in Figure 7. The SP survey lines were installed by SWL personnel in consultation with WES personnel. SP electrode spacings were 25 ft for line C and 50 ft for the remaining SP survey lines. Survey line A was unusual in that most of the electrodes were underwater; the underwater electrodes were installed by divers and were covered with sandbags to minimize reservoir water motion around the electrodes. Electrical connection to the underwater electrodes were made at two junction boxes located on either side of the embayment west of the dike. Each electrode was wired to the nearest junction box. In places where the reference wire crosses roads or parking areas, the

wire was taken up and coiled when measurements were completed; also in some areas the reference wire was buried in shallow trenches to reduce the possibility of vandalism.

30. Several measurements were obtained by WES personnel during the March 1985 field work to determine SP character and variability and establish baseline profiles. Subsequent data sets were obtained by SWL personnel periodically and when there were significant pool level changes. The data were forwarded to WES for analysis and interpretation.

31. Electrical Resistivity Surveys. The electrical resistivity survey method allows for the investigation of the electrical properties of subsurface materials from the ground surface. When a current is introduced into a homogeneous earth through a pair of electrodes, the current radiates out through the ground from one electrode and current paths converge on the second electrode through which current leaves the ground. In a homogeneous earth model, the potential drop will be equal for all points equidistant from the point of current entry or exit. Differences in the electrical properties of the underlying materials perturb the distribution of the equipotential surface. In the resistivity method a known current is introduced in the ground by means of two electrodes emplaced in the ground and a potential difference is measured at two other electrodes. Earth resistivity methods are widely used in geotechnical investigations, ground water exploration, and for locating shallow mineral deposits (Dobrin, 1960).

32. Earth resistivity is calculated from the current (known) and the potential difference (measured) using Ohm's Law. The resistance, R, in ohms, between two surfaces of constant potential is defined by Ohm's law as:

$$R = \Delta V/I \tag{2}$$

where I = current in a conducting body

ΔV = potential difference between two surfaces of constant potential.

Also, for a conducting cylinder, the resistivity (ρ) of the material is defined as:

$$\rho = RA/L \tag{3}$$

where A = the cross-sectional area of the cylinder

L = the length of the cylinder.

The objective of the electrical resistivity surveys is the determination of the electrical resistivity, ρ , or variations in resistivity of subsurface geological materials. Electrical resistivity is a fundamental property of materials and often has engineering significance because it depends not only on mineralogy but also on soil/rock structure, porosity, degree of saturation, and chemistry of the pore fluid. Referring to Figure 8, if a current I is introduced at electrodes A and B and a potential drop is measured between electrodes C and D then the potential at electrode C will be

$$V_c = \frac{I\rho}{2\pi}\left(\frac{1}{r1} - \frac{1}{r2}\right) \tag{4}$$

where r1 is the distance from potential electrode C to current electrode A and r2 is the distance to current electrode B. The potential at electrode D is

$$V_D = \frac{I\rho}{2\pi}\left(\frac{1}{R1} - \frac{1}{R2}\right) \tag{5}$$

where R1 is the distance from potential electrode D to current electrode A and R2 the distance to current electrode B. The potential difference between C and D is VC-VD or

$$\rho = \frac{2\pi V}{I}\left(\frac{1}{r1} - \frac{1}{r2} - \frac{1}{R1} + \frac{1}{R2}\right) \tag{6}$$

The quantity in the parenthesis is a function of the electrode spacing or spacings and can be described as 1/k. Thus, solving for ρ ,

$$\rho = 2\pi k\left(\frac{V}{I}\right) \tag{7}$$

19

Therefore, from the measured values of V, I, and k (the geometric factor), the resistivity of the material can be determined. For a homogeneous earth, the resistivity determined by equation (7) will be the true resistivity of the material. For subsurface conditions which vary vertically and laterally, the resistivity given by equation (7) will be an apparent resistivity (denoted by ρ_a) which is a complicated volume average of the resistivities and dimensions of materials within the "depth of investigation" of the array.

33. There are basically two types of of resistivity surveys, vertical electrical sounding and resistivity profiling, and they are more or less complementary to each other. In the vertical electrical sounding technique the resistivity of the material as a function of depth is obtained below a given point on the earth's surface. In resistivity profiling lateral variations in the resistivity of the subsurface to a near constant depth are mapped. The resistivity profiling technique was the method of choice at Beaver Dam. In the profiling resistivity technique a specified electrode separation is chosen depending on the depth of investigation required. The electrodes are usually laid out in advance at a chosen uniform separation, designated "a". A resistivity reading is taken at the first station and then the array is advanced to the next station usually by a distance "a" or a multiple of "a" and another reading taken. This process continues until the end of the planned profile line is reached. The resistivity readings are then plotted versus distance or if there are multiple profile lines a resistivity map can be produced. Any resistivity variations existing in the subsurface within the depth of investigation should be indicated on the plot or map. Resistivity variations may be indicative of subsurface anomalous conditions such as fault zones or lateral changes in material type such as increased degree of saturation, changes in pore water chemistry, etc.

34. The horizontal resistivity profiling conducted at Beaver Dam was accomplished using the Wenner type electrode arrangement as shown in Figure 9. In this type of electrode configuration the electrodes are equally spaced and the array is characterized by the spacing "a". For the Wenner array As a rule of thumb, in the case of the Wenner array, the depth of investigation is characterized by the electrode separation "a". For example, as a rule of thumb, the depth of investigation for an electrode spacing 2a is twice the depth of investigation for an array with spacing a. Some of the

existing electrode arrays used for the SP surveys were also employed for conducting the resistivity profile survey. Figure 10 shows the location of the resistivity profile lines. For line B, run along the crest of Dike 1, resistivity profiles were obtained for a - 50 ft and a - 100 ft. For line C, run along the downstream berm of the dike, and line H, located northeast of the dike, profiles were obtained for a - 25 ft and a - 50 ft. The purpose of conducting surveys along line H was to attempt to detect and project the trace of the north fault zone downstream of the dike.

35. **Electromagnetic (EM) Surveys.** Although the EM surveying technique has been in use for many years, chiefly for detecting conductive ore bodies, it has in the past few years, gained much popularity in the field of civil engineering as a tool for conducting site investigations and hydrologic studies (Zalasiewicz, et. al.,1985).

36. Basically, the EM technique is used to measure differences in terrain conductivity. Like electrical resistivity, conductivity is affected by differences in soil porosity, water content, chemical nature of the ground water and soil, physical nature of the soil, etc. (McNeil, 1980). In fact for a homogeneous earth the true resistivity is the reciprocal of the true conductivity. The EM technique is also useful for determining the configuration of subsurface structures (McNeil, 1980). Some advantages of using the EM technique over the resistivity method to measure the ground conductivity are (a.) it is less sensitive to localized resistivity inhomogeneities, (b.) no direct contact with the ground is required thus, there are no current injection problems, (c.) a smaller crew can be used, and (d.) it provides easy, rapid measurements (McNeil, 1982). However, due to the inherent limitations of the electronic instrumentation, the use of the EM method is not suggested in terrains having very high or very low conductivities. Thus, the use of the Wenner resistivity method is required in such terrain to supplement the EM technique.

37. The EM equipment used at Beaver Dam consisted of two coils, connected by a cable. One coil was a transmitter and the other coil was a receiver. The transmitter coil (energized with an alternating current (AC) at an audio frequency) was placed on the ground and the receiver coil placed a small distance away (33-, 66-, or 132 ft). The purpose for conducting the

21

survey using multiple spacings was to determine whether an anomaly, if present, was relatively shallow or deep, since the greater the intercoil spacing the greater the depth of investigation. The transmitter coil created a primary time-varying magnetic field which induced small eddy currents in the ground. These currents then generated a secondary magnetic field which was sensed together with the primary field by the receiver coil. Figure 11 illustrates the EM principle. The ratio of the secondary to the primary magnetic field is linearly proportional to the terrain conductivity, making it possible to obtain a direct conductivity reading in millimhos/meter (McNeil, 1980). The readings obtained are presented in profile fashion (i.e. conductivity versus distance) or as isoconductivity contours if data are obtained in a grid form. A more thorough discussion of the EM induction theory and interpretation techniques is given by Keller and Frischknecht, 1970 and Butler, 1986.

38. Figure 12 shows the location of the two EM survey lines conducted at the site. EM profile line C, located on the downstream berm of Dike 1, was run with intercoil spacings of 33-, 66-, and 132 ft, while EM profile line H, downstream left abutment, was run with intercoil spacings of 33 and 66 ft.

39. Seismic Refraction Surveys. The seismic refraction method utilizes the fact that the velocity of seismic wave propagation in a material is dependent on its elastic properties. It is assumed that materials are locally homogeneous and isotropic. In this method of investigation, depth and location of bodies or layers having contrasting elastic properties are determined. In the seismic refraction method, energy is imparted into the ground usually by means of explosives or by striking a metal plate on the ground with a sledgehammer to produce a seismic disturbance. The location of the seismic disturbance is considered a point source and the disturbance is transmitted through the ground as a series of waves. In this investigation the compression-wave (P-wave) will be the elastic wave studied. Geophones (velocity transducers) are implanted into the ground surface and laid along a straight line spaced at regular intervals. The length of the survey line depends on the required depth of investigation; a common rule of thumb is that the length of the line should be from three to four times the depth of interest. The function of the geophones is to detect the arrival of the

22

P-wave. A geophone consists of a wire coil that moves relative to a magnet, thus generating an electrical signal. These signals are then transmitted via a cable to a seismograph where they are amplified and the time of arrival of the P-wave at each geophone location determined. Interpretation of seismic refraction data uses a plot of the P-wave arrival times versus the geophone distances from the seismic source. The slopes of the straight line segments drawn through the points correspond to the P-wave velocities of the materials (see Figure 13 for an example of a two-layer case). By the use of Snell's law,

$$\frac{SIN\ \alpha}{SIN\ \beta} = (V1/V2) \tag{8}$$

the depth to the horizontal interface separating the two layers can be determined by the following expression:

$$D = (X_c/2) * [(V2 - V1)/(V2 + V1)]^{1/2} \tag{9}$$

where:

$V1$, $V2$ — velocities of layers 1 and 2, respectively

α, β — angles the ray path makes with the normal to the boundary in the two respective layers

D — depth to layer 2

X_c — critical distance (distance corresponding to the intersection of straight line segments for velocities V1 and V2).

40. The analysis of seismic refraction for greater than two layers, dipping layers, and more complicated geological structures are described by Telford et. al. 1976, Redpath 1973, Department of the Army 1979, Grant and West 1965, and other standard geophysical references.

41. The seismic refraction survey conducted at Beaver Dam consisted of three end-to-end lines run along the downstream berm of Dike 1, as shown in Figure 14. Two 250 ft lines had 24 geophones at 10 ft spacings; and one 625 ft line had 24 geophones at 25 ft spacings. A two-component explosive consisting of ammonium nitrate and nitromethane was used to create the seismic

23

disturbance. The data were collected on a portable 24-channel seismograph and stored on magnetic tape for subsequent processing and interpretation. Descriptions and examples of the data processing and interpretation are given by Butler and Llopis, 1984; Zohdy et al., 1974; and the Department of the Army 1979.

42. **Magnetic Surveys.** The magnetic method of surveying is based on measuring the anomalies of the local geomagnetic field caused by the variations in the intensity of magnetization in the rock formations (Parasnis 1966). Magnetic anomalies are caused by two different types of magnetism: induced and remanent magnetization (Parasnis 1966 and Breiner 1973). Induced magnetism refers to the total field within a body. This total field consists of the sum of the external magnetic field and the magnetic field induced in the body by the external field. The magnetization of the body is proportional to the strength of the external field and also to the degree to which the material can be magnetized, a property known as magnetic susceptibility. The magnetic susceptibility of a material depends on the nature and the quantity of magnetic minerals present, mainly magnetite, sometimes ilmenite or pyrrhotite (Parasnis 1966 and Telford et. al.1973). In general, dark basic igneous rocks have a higher susceptibility than lighter acid igneous rocks which in turn have higher magnetic susceptibilities than sedimentary rocks.

43. Some rocks have permanent magnetic fields of their own referred to as natural remanent magnetism. This property depends on the thermal and magnetic history of the body, and is independent of the field in which it is measured (Breiner 1973). Remanent magnetism may be greater than the induced magnetism and a body with a high degree of remanent magnetization may be magnetized in a different direction than that of the earth's main magnetic field causing uncertainties in interpretation.

44. A proton magnetometer with an accuracy of approximately 1 gamma was used for the conducting the surveys at Dike 1. A gamma is the unit used in geophysical work for measuring variations in the intensity of the Earth's magnetic field and is defined as 10^{-5} oersteds. For reference, the nominal Earth's magnetic field is approximately 50,000 gammas. The locations of the magnetic survey lines are shown in Figure 15. The proton magnetometer utilizes the precession of spinning protons (hydrogen nuclei) which are polarized in an

organic fluid rich in hydrogen to measure the total magnetic field. This is explained in more detail by Griffiths and King 1969, and Telford et. al. 1973. Magnetic total field strength measurements were taken along each line surveyed. Measurements were made at 25-ft intervals for lines C and H and at 50-ft intervals for the remainder of the lines. The data were stored in internal memory for subsequent processing and interpretation.

45. <u>Borehole Fluid Conductivity and Temperature Surveys.</u> The purpose for conducting these tests was to try to define and delineate seepage paths. The rationale behind this series of tests was that borings intercepting ground water with similar water conductivities and/or temperatures should lie along a flow path from a common source. It was felt that these tests, similar in concept to dye tracing, should proceed more rapidly. Conductivity and temperature measurements were made in each accessible well and piezometer in the vicinity of Dike 1. During the third series of measurements (January 1986), piezometers installed during the summer and fall of 1985 were accessible. Measurements were made by lowering a combination conductivity/temperature probe down each boring approximately 1 ft below the water surface, allowing it to equilibrate, and noting the readings on a conductivity/temperature meter at the surface. During each series of borehole measurements, the reservoir water conductivity and temperature were obtained in the reservoir adjacent to Dike 1.

Chronology of Geophysical Investigations

46. The following is a descriptive chronology of events related to the geophysical investigations at Beaver Dam Dike 1:

Date	Event
Nov 1984	Two WES personnel visit Beaver Dam for site inspection prior to planning geophysical program. Borehole conductivity/temperature measurements acquired in several piezometers.

25

Date	Event
Dec 1984	WES proposal for a geophysical seepage assessment program at Beaver Dam transmitted to SWL for consideration.
Jan 1985	Southwestern Division, SWL, and WES personnel meet at Beaver Dam for review of proposed geophysical program and site inspection.
Feb 1985	Funds to support geophysical program transmitted to WES. SWL personnel establish survey lines and install SP electrodes.
Mar 1985	Four WES personnel perform major geophysical field work as outlined above. Reservoir level between 1,124.94 and 1,125.00 ft.
Apr 1985	WES personnel perform preliminary interpretation of survey data and forward recommendations for new piezometer locations.
Aug 1985	WES personnel forward recommendations for exploratory boring locations to SWL.
Jan 1986	Program review meeting at Beaver Dam to assess the status of all on-going work related to the seepage assessment. Borehole conductivity and temperature measurements acquired. Reservoir level 1,118.35 ft.
Mar 1986 to Present	SWL personnel acquire SP data and forward tabulated data to WES for analysis. Reservoir level between 1,117.10 and 1,1129.00 ft.

RESULTS

Geologic Structure Mapping

47. As discussed above the four geophysical methods used for mapping
the geologic structure at the site were electrical resistivity,
electromagnetic, and magnetic profiling and seismic refraction. In order to
better define zones of seepage it was of prime importance to define the faults
north and south of Dike 1 and the thickness of the weathered part of the Boone
Chert.

48. Resistivity Surveys. A common technique used when profiling with
the resistivity, electromagnetic, and magnetic methods is to mathematically
model the site and calculate the effects certain geologic features would have
on each survey type. Figure 16 illustrates the effect a fracture zone has on a
resistivity profile using various electrode spacing to thickness ratios. The
fault zone is assumed to have a higher electrical resistivity than the
bounding material. The complicated shape of the resistivity profile results
from the changes in potential field distribution as the four electrodes
successively cross the vertical boundaries. The details of the resistivity
profile, such as the number and relative amplitude of the peaks, depend on the
relation of the electrode spacing "a" to the fracture zone thickness "t". In
practice the profile also depends on the spacing between measurement points.
Figures 17 through 19 show the results of the Wenner resistivity profile lines
conducted at the site. Figure 17 shows the results of the profile line run
along the upstream side of the crest of Dike 1. A-spacings of 50 and 100 ft
were used for this profile. A high resistivity peak can be seen centered about
station 64+50 in Figure 17. This resistivity peak is believed to be indicative
of the north bounding fault. According to the inferred fault zone shown in
Figure 10, it intersects profile line B between stations 64+00 and 64+40. Also
indicated in resistivity profile B are resistivity highs which are believed to
be caused by the shallow, more resistive bedrock. It can also be seen in
Figure 10 that the 100-ft a-spacing profile line tends to better define the
bedrock surface due to its greater depth of investigation and also because it

27

is less influenced by near surface effects. It is difficult, in this profile to discern the south bounding fault due to the superimposed effects of a bedrock knoll in the vicinity of the fault.

49. Resistivity profile line C was run along the downstream berm of Dike 1 as shown in Figure 10. Results are presented in Figure 18. A-spacings of 25 and 50 ft were used for profile line C. As in resistivity profile line B, the north bounding fault as well as the bedrock surface can be discerned. The resistivity high centered about station 64+00 is interpreted as being the northern fault. Shallow bedrock is interpreted at areas centered about station 69+00 and 73+00. The southern portion of the profile seems to exhibit the typical resistivity signature expected from a vertical fault zone. The inferred fault zone shown in Figure 10 crosses the profile line approximately between stations 73+00 and 74+50. Referring to Figure 18, an anomalous condition is recognized between stations 73+00 and 74+00. This portion of the profile line is deemed to be anomalous due to the crossing of the values from the 50 and 25 ft a-spacing lines. This may be indicative of a higher percentage of lower resistivity material (clay or saturated material) with increasing depth associated with the fault zone.

50. Wenner resistivity profile line H was run downstream of the left abutment of Dike 1 as shown in Figure 10. A-spacings of 25 and 50 ft were used for this profile line. The purpose for conducting this line was to try to project the location of the fault zone downstream. The results of line C are presented in Figure 19. Referring to Figure 19 it can be seen that resistivity values increase to the south and reach a peak value of approximately 3,000 ohm-ft at approximate station 61+40. This high resistivity anomaly may be caused by the fault zone or by resistive rock very close to the surface; however, the location of the high resistivity anomaly is appropriate for a straight line extension of the fault zone.

51. **Electromagnetic Surveys.** Figure 20 shows a typical response expected from an EM profile run across a low conductivity (high resistivity) fault zone. Conductivity line C was run along the downstream berm of Dike 1 as shown in Figure 12, and the results are presented in Figure 21. Intercoil spacings of 33-, 66-, and 132-ft were used for the survey. Being analogous to the resistivity profiling method, the greater the intercoil spacing the

28

greater the depth of investigation and volume of material averaged in the readings. The shorter intercoil spacings are affected more by the near surface materials than those at greater depths. This explains why the larger intercoil spaced lines appear to have a "smoother" appearance. A number of anomalous conductivity zones can be seen in Figure 21. The two bounding faults can be interpreted from the data and are indicated by conductivity lows. The northern fault zone is centered about station 64+00 while the southern fault zone is interpreted to be centered about station 73+50. Effects due to bedrock topography can be noted in the figure. An anomalous area is noted at station 75+50 which was not detected by the Wenner resistivity profile run in the same area. This anomaly is believed to be due to thickening of overburden material or an increase in clay and/or water content.

52. EM profile line H was run on the downstream left abutment as shown in Figure 12, and the results are presented in Figure 22. Referring to Figure 22, it can be seen that conductivity values decrease rapidly between stations 59+60 and 60+60, at which point the readings level out. The data indicates that the line was run across the northern fault zone.

53. Magnetic Surveys. The results of model studies, based on typical magnetic susceptibility values as given by Telford et al. 1976, Dobrin 1960, and Heiland 1940, showed that any anomalies due to the fault zones would be on the order of 10 gammas or less. Although the magnetometer used for this survey has the resolution to detect anomalies of this magnitude the background magnetic noise was such that it made detecting the fault zone improbable. However, it was felt that magnetic profiling could be useful in locating areas with anomalously high clay contents. Five magnetic profile lines were run at the site as indicated in Figure 15. The results of magnetic survey are presented in Figures 23 through 27. Figure 23 shows the result of magnetic survey line A run across the upstream toe of Dike 1 as shown in Figure 15. The base level reading is about 54,500 gammas. Between Stations 70+00 and 73+50 an anomalous zone is indicated. This may be partly due to susceptibility differences between man-placed dike material and natural material south of Station 70+00.

29

54. Figure 24 shows the data obtained from magnetometer survey line B which was run along the centerline of Dike 1 as shown in Figure 15. No useful information could be gathered from this particular survey line due to magnetic interference from metal guard rails on either side of the road that runs the entire length of the dike.

55. Magnetic survey line C was run along the downstream berm of Dike 1 as shown in Figure 15. The results are presented in Figure 25. The baseline reading for this survey line is on the order of 54,500 gammas. The spiked features that appear on this survey line and noted in the figure are due to metal piezometer riser pipes in the vicinity of the reading station. No structural features were discerned from line C.

56. Magnetic profile line D was run downstream of Dike 1, as shown in Figure 15, and the results are shown in Figure 26. As was seen in line C, the positive peaks can be attributed to metal piezometer riser pipes. An anomaly was clearly detected between stations 72+50 and 74+00 which is in the vicinity of the southern fault zone and is believed to be the source of the anomaly. The anomaly may be indicative of clay-filled zones associated with the fault zone.

57. Magnetic profile line E was run on the downstream toe of Dike 1 perpendicular to the axis of the Dike as shown in Figure 15; the results are presented in Figure 27. An anomalous area with low magnetic values is indicated between stations 31+00 and 32+50. This area occurs where the survey line intersects the southern fault zone. As was the case for profile line D, it is suspected that this anomalous magnetic signature may be due to fault related clay deposits.

58. **Seismic Refraction.** Figures 28 through 30 present the time-distance curves for seismic refraction lines 1 through 3, respectively. Figure 31 presents the P-wave velocity profile interpreted from the results of the three seismic refraction survey lines. Depths to the various layers were computed using the time delay method as described by Redpath, 1973. Figure 31 shows three layers between Stations 65+30 and 74+00 with average velocities of 1,325-, 3,625-, and 15,475-fps, corresponding to overburden material, severely weathered rock, and dense unweathered rock, respectively. Two velocity layers were interpreted between stations 74+00 and 76+00. The first layer has a

30

velocity of 2,400 fps corresponding to overburden material while the second layer has a velocity of 12,835 fps corresponding to hard, dense bedrock. Figure 31 shows the vertical and lateral extent of the severely weathered limestone (V = 3,625 fps) as well as the south bounding fault as interpreted from the refraction data.

Interpreted Fault Zones.

59. Based on the results of the resistivity, EM, and magnetic profile lines, as well as the results of the seismic refraction tests, the northern and southern fault zones were mapped as shown in Figure 32. The hachured zones indicate the inferred fault zones, detected by at least one geophysical method. The hachured areas are connected by dashed lines and indicate the strike of the fault. Information obtained from boring operations prior to construction indicated the presence of the northern and southern fault zones however, the exact widths of the fault zone and the trend of the fault were not precisely known. The fault zones and their respective widths, as inferred from drilling, and shown in the 1984 Reconnaissance Report are presented in Figure 32.

Seepage Detection and Delineation

60. SP Surveys. There are two hypotheses that determine the manner in which SP data are presented and analyzed: (a) that areas on the ground surface above active groundwater seepage or streaming should be areas of relative negative voltage anomaly; and (b) that changes, such as those induced by increased pool levels, that result in increased flow should also result in negative changes in potential, relative to a reference electrode. The SP data are examined in two ways: (a) in static profiles, i.e., plots of SP values versus distance for a given pool elevation; and (b) SP values versus pool elevation relative to low pool elevation (in this report 1,117 ft).

61. SP readings were taken over a period of approximately one year at pool elevations ranging between 1,117 and 1,129 ft. Table 1 shows the dates on which SP readings were taken with corresponding pool elevations. Figures 33 through 35 present the results of the SP survey conducted along line A

(underwater array) as shown in Figure 7. Figure 33 shows the unprocessed SP readings versus station for various pool elevations. The SP values for a particular pool level were the result of averaging the SP values obtained throughout the year for that particular pool level. Referring to Figure 33 it can be seen that the same general trend in the data exists for each pool level; however, the lines are shifted with respect to each other, i.e., the reference or base line level seems to have changed. Possible causes for these shifts in the data may be due to (1) changes in reference potential of the reference electrode, (2) changes in flow conditions, related to pool level, over broad zones which affect entire SP lines, (3) changes in soil moisture and/or temperature which affect the rod/soil electrochemical potential along the survey lines, and (4) possibly other factors which at this time are not fully understood, such as biological activity, elevation, and soil type (Ernstson and Scherer, 1986). In order to analyze and make meaningful comparisons between the SP values for the various pool levels it was necessary to minimize the time-induced effects which cause a relative shifting of the data. This was accomplished by computing the mean value for each SP data set corresponding to a particular pool elevation and subtracting the mean from each reading for that same line. Figure 34 shows the results of this process on the SP data collected for line A. At this point in the processing stage one can begin searching for anomalous SP readings. In this report anomalous values will be arbitrarily defined as any values greater than +100 mV or less than -100 mV. Using this definition and referring to Figure 34 one can define an anomalous negative SP zone between stations 66+00 and 71+00. Relative positive anomalies are indicated at stations 65+00 and between stations 72+00 and 73+50. Therefore, it would appear that seepage is occurring roughly between stations 66+00 and 71+00. In an attempt to correlate the effects of pool level on SP values the data were further processed, by subtracting SP values obtained for the various pool levels from a reference set of SP readings, in this case the 1,117 ft pool level data. The purpose of this processing was to determine if there existed areas along the profile line where SP values responded to pool level differences. Figure 35 presents the results of the change in SP values relative to the reference low pool elevation, 1,117 ft, for line A (difference plot). In this type of plot, it is assumed that any relatively constant factors which affect each data set in the same way will

32

cancel. The magnitude of the anomalies in this type of plot may be indicative of the amount of change in flow due to pool fluctuations. Relative negative anomalies occur at station 65+50, 70+00 and between stations 71+00 and 72+50. Positive anomalies can be seen occurring at stations 66+00, 70+50, and 73+00. Thus, it is reasonable to assume that these stations are affected most by pool level fluctuations. The rest of the SP lines were analyzed in the same manner and only the processed data plots will be presented.

62. Figures 36 and 37 present the SP data obtained along the crest of Dike 1, line B, as shown in Figure 7. Referring to Figure 36 it can be seen that negative SP values exist roughly between stations 63+00 and 73+00 with exceptions occurring at 68+00 and 69+00. No explanation can be given for these two recurring positive peaks. Positive anomalies are also seen between Stations 74+50 and 77+00. It is believed that these positive anomalies may be due to a change in bedrock type which may affect the hydrologic conditions in the vicinity and thus SP values. Figure 37 is the difference plot for line B. SP readings can be seen to be greatly affected by changes in pool elevation across the entire line however, this effect is most prominent between Stations 72+50 and 73+50. Note that the two peaks present in Figure 36 are not present in Figure 37.

63. Figures 38 and 39 present the SP data for line C, located along the downstream berm of Dike 1, as shown in Figure 7. A great amount of variability in the static SP values with respect to pool elevation can be seen in Figure 38. This amount of variability in the data may be due to line C being closer to the SP sources, in this case, flowing water through joints and bedding planes of the limestone underlying the dike. A broad zone of negative SP readings can be seen occurring between stations 66+00 and 73+50 with the exception being a positive anomaly at station 69+00. Other areas with negative anomalies occur at stations 63+50, 75+00, and 76+00. Additional locations having relatively positive SP readings are centered about stations 63+00, 64+50, 74+50, 75+50, and 76+25. In general, it can be said that a broad zone consisting of anomalously low SP values exists between stations 66+00 and 74+00 and this zone is bounded on both sides by more positive SP values. It appears that seepage is quite pervasive in this broad negative zone. Highly suspect areas are interpreted to occur at stations 63+50, 66+00, 70+50, 75+00, and 76+00. Figure 39 presents the difference plot for line C. The entire

33

length of the line shows that it is affected by fluctuations in pool level, though some areas are affected to a greater degree than others. Areas that seem to show abnormally high SP variations due to pool level changes are located at stations 62+50, 63+50, 65+50, 67+50 to 68+00, 70+00 to 74+00, 75+00, and 76+00.

64. Figures 40 and 41 present the data for SP line D run along the downstream toe of Dike 1 as shown in Figure 7. Figure 40, static profile, shows five areas with negative SP anomalies. These areas are located at stations 67+50, 69+00, 70+50 to 71+00, 72+00, and 73+50. Figure 41 shows the difference plot obtained for line D. It shows three areas with anomalous SP values. These occur at stations 67+00, 71+00, and 74+00. Stations 67+00 and 71+00 are located in gullies while station 74+00 is located near an area of known seepage.

65. Figures 42 and 43 present the static profile data for SP line E run downstream and perpendicular to the axis of Dike 1 as shown in Figure 7. The static plot for line E, presented in Figure 42, shows three anomalous SP zones. These zones occur at stations 29+25, 30+75, and 32+75. Areas most affected by pool level changes are shown in the difference plot, Figure 43. There are two significant anomalous areas, station 29+25 and station 30+75.

66. Figures 44 through 48 present plots of SP values versus pool elevation, pool elevation versus time, and SP values versus time for SP lines A through E, respectively. The SP values shown in the plots were obtained by averaging the SP line values recorded for a particular pool elevation. The plots of SP values versus pool elevation would lead one to believe that the higher the pool elevation the higher the the average SP readings however, the plots with the SP values and pool elevation plotted versus time indicate that in general as pool elevations decrease SP values also decrease. The exception for this case occurs approximately in the first two months of the study. It is believed that the copper-clad SP electrodes were achieving chemical equilibrium during this time and therefor were subject to fluctuations and inconsistencies.

67. <u>Borehole Fluid Conductivity and Temperature Survey.</u> The purpose for conducting these tests was to define probable seepage paths. As previously mentioned the rationale behind this test was that borings with similar water

34

conductivities and/or temperature could lie along a flow path from a common source. It was felt that these surveys, similar in concept to a dye tracer study, should proceed much more rapidly than a dye tracer study. Figures 49 through 51 present the results obtained from conducting downhole conductivity surveys on three different occasions in accessible piezometers in the vicinity of Dike 1. Figure 49 shows the results obtained on 16 November 1984. The reservoir water conductivity was not obtained on this occasion because the conductivity probe was lost in piezometer P-18. Also, as a result of the loss of the conductivity probe, no conductivity information was obtained for the northern portion of the dike. Measured water conductivities ranged between 1.7 and 5.8 mmhos/ft (resistivities from 588 to 172 ohm-ft). Referring to Figure 49, it can be seen that the water conductivities taken along the south ravine have a mean value of 4.4 mmhos/ft. Other locations with similar readings as those found in the southern ravine area are located at piezometers P-8, Exit 9 (near the Parshall flume), and the water well located at approximate coordinate (72+50,32+25) situated in the south fault zone. These areas with similar conductivities may be hydraulically interconnected. The arrows shown in Figure 49 indicate inferred seepage paths. Figure 50 presents data collected on 14 March 1985. Again, as in the previous set of readings, conductivity readings for seepage exits in the south ravine agree very well with each other. Values for exit 6 (new wet area) and the water well located in the southern fault zone (72+60,32+30) indicate similar values as those in the seepage exits in the south ravine. The arrows shown in Figure 50 indicate probable seepage paths as interpreted from conductivity data collected on 14 March 1985. Finally, Figure 51 presents the results of the downhole conductivity survey conducted on 29 and 30 January 1986. As in the previous surveys, values for the seepage exits agree very well with each other and with values for exit 6. This set of readings included values from recently installed piezometers. In Figure 51, inferred seepage paths are shown by arrows. Seepage appears to be occurring under the dike in the vicinity of Station 70+00 to 72+00 in an easterly direction. It also appears that some of this water may be flowing to the southeast where the southern fault is intercepted, from which point the water appears to flow along the fault axis where it exits to the east at exits 1-6.

68. The results of downhole temperature measurements taken in conjunction with the downhole conductivity surveys are presented in Figures 52 through 54. Figure 52 presents the downhole and seepage exit water temperatures taken in November 1984. As mentioned above, the conductivity/temperature probe was lost in one of the piezometers and thus, measurements were not taken for the northern piezometers or in the reservoir. Temperatures ranged between 57° and 66° F. The temperature measurements taken in the south ravine (seepage exits and piezometers) agree very well with each other. Due to insufficient water temperature readings no seepage paths were inferred for the north ravine area.

69. Figure 53 presents the results obtained from water temperature measurements in March 1985. Water temperatures ranged between 54.5° and 60° F. Seepage paths inferred from the temperature data are shown in Figure 53. The reservoir water temperature was recorded as 49.7° F.

70. Figure 54 presents the results obtained from water temperature measurements taken in January 1986. Recorded temperatures ranged between 50 and 65.5° F. A general temperature gradient is evident trending roughly in a northwest-southeast direction. The seepage areas in the south ravine and the piezometers in the southeastern part of the site have the lowest temperatures while the higher temperatures are found in the northwestern part of the site. Temperature measurements were taken at three different reservoir locations as shown. The average reservoir water temperature was 50.0° F. The average temperature for the seepage exits measured was 55.1° F. Using the information gathered from this temperature survey, seepage paths, indicated by arrows, were inferred and are shown in Figure 54.

Input to Piezometer and Exploratory Boring Placement.

71. At the request of the SWL, WES, in May 1985, provided four suggested locations for future piezometers. It was hoped that these piezometers would provide added information for determining the location of seepage paths and voids. The locations were based on preliminary interpretations of the electrical resistivity profiles and SP tests conducted during 9-15 March 1985. Figure 55 shows locations with anomalous low resistivity values along with anomalous negative and positive SP values. Based

36

on the results of these geophysical tests, seepage paths were inferred and piezometer locations recommended as shown in Figure 55. Piezometers were installed in the locations recommended by WES. A common difficulty in drilling the piezometer borings was heavy loss of drilling (circulation) fluid, with most borings having a total circulation loss at some point during drilling. The boring logs associated with these piezometers indicated excessive water losses and numerous cavities. Piezometer D-29.7 had significant water inflow (est. 5-10 gpm) at a depth of 31.2 ft. A dye tracer test conducted in piezometer D-29.6 indicated a seepage path between the piezometer and seepage Exit 2 located in the south ravine. Piezometer D-29.6 was located in material that was previously thought to be rather competent due to low grout takes during grouting operations in the 1960's, and the inferred seepage path (from D-29.6 to Exit 2) was not previously suspected. A downhole camera lowered into several of the piezometers in August 1985 indicated rock characteristics and features which contribute to subsurface seepage such as open cavities, channels, intensive fracturing, and weathering.

72. Twenty-five exploratory borings were drilled along the upstream crest of Dike 1 and its abutments during the period April 1986 to August 1987. The primary purpose of these borings was to delineate the limits and geologic characteristics of the downthrown faulted block of the Boone Formation beneath Dike 1 and the north and south fracture zones that bound the Dike. Originally, the boring locations were selected based on areas that had experienced high grout takes during the previous grouting program. However, locations for the borings were later changed to take advantage of information obtained from geophysical testing. Based on results of the SP, resistivity, and other geophysical testing and also considering previous grout takes, fault locations, and piezometer data, WES submitted a list of proposed locations for exploratory borings to SWL for approval. Figure 56 shows the WES suggested exploratory boring locations.

73. Extensive investigations were conducted on each of the borings, typically included soil sampling, diamond core drilling, detailed descriptive logging of rock core, dye testing at zones of drill fluid loss, pressure testing of rock, downhole geophysical logging, inspection with downhole video equipment, and laboratory testing of rock core samples.

37

74. The results of tests conducted in the exploratory borings determined that the northern fault zone has a vertical offset of 230 ft while the southern fault zone's vertical displacement measures approximately 146 feet. The unsound nature of the fault zones was evidenced during drilling by noting the complete loss of drill fluid and large core looses. This condition was substantiated by SWD laboratory personnel while performing "down-looking" and "side-wall looking" observations with a down-hole video camera. Numerous open cavities, channels, joints, and intensely fractured zones were encountered in the the fault zones as well as in the upper cherty Boone Formation. Subsurface flows through channels in rock were apparent in several borings where normally suspended fines could be seen moving rapidly.

Integrated Methods Seepage Map.

75. Based on the results of the tests described above and other pertinent information provided from geologic maps, boring logs, dye tracer tests, piezometers, and seepage flow measurements an integrated seepage map was produced as shown in Figure 56. This map indicates that seepage beneath the dike is flowing primarily in an easterly-southeasterly direction with the greatest amount of water movement occurring between Stations 69+00 and 73+00. The map also indicates the possibility of water movement along the southern fault zone.

CONCLUSIONS

Geophysical tests conducted at the site were successful in determining the locations and strikes of the north and south bounding faults. Seismic refraction surveys were used to map the extent, both laterally and vertically, of weathered rock (Boone Formation) underlying the dike. Results of the SP surveys indicate that seepage is occurring along the entire length of the dike. It appears that seepage is rather pervasive and not occurring in a few well defined conduits. Temperature and conductivity tests indicate that seepage is coming from the lake and a short seepage route exists beneath the dike at approximate Station 71+00. Evidence also suggests that there is seepage occurring along the southern fault zone. The northern fault zone is apparently "tight" and there is no evidence suggesting flow along or across this fault zone. Information obtained from the geophysical tests and substantiated by exploratory borings indicate that the southern fault zone, unlike the northern fault zone, is not "tight" but is instead allowing water to flow across the upper portion of the zone and also along its length.

Another conclusion that can be made from conducting this study is that the results of all the geophysical techniques need to be integrated in order to more accurately characterize a site. The usefulness of a particular geophysical test to a study depends on the sub-surface characteristics of the site. A test that may provide valuable information at one site may not do so at a different site because of different site conditions. In this study the electrical resistivity, EM, and seismic refraction tests were deemed to be more effective than the magnetic or SP method for mapping geologic structure. The SP method provided more useful information for seepage mapping than did the electrical resistivity, EM, borehole fluid conductivity, or borehole temperature tests.

References

Bogoslovsky, V. A. and Ogilvy, A. A. 1973. "Deformations of Natural Electric Fields Near Drainage Structures," Geophysical Prospecting, Vol 21, pp. 716-723.

Breiner, S. 1973. "Applications Manual for Portable Magnetometers", GeoMetrics, Sunnyvale, Calif.

Butler, D. K. 1986. "Military Hydrology; Report 10: Assessment and Field Examples of Continuous Wave Electromagnetic Surveying for Ground Water," Miscellaneous Paper EL-79-6, U.S. Army Engineer Waterways Experiment Station, Vicksburg, Miss.

Butler, D. K. and Llopis, J. L. 1984. "Military Hydrology; Report 6: Assessment of Two Currently "Fieldable" Geophysical Methods for Military Ground-Water Detection," Miscellaneous Paper EL-79-6, U.S. Army Engineer Waterways Experiment Station, Vicksburg, Miss.

Cooper, S. S., Koester, J. P., and Franklin, A. G. 1982. "Geophysical Investigation at Gathright Dam," Miscellaneous Paper GL-82-2, U.S. Army Engineers Waterways Experiment Station, Vicksburg, Miss.

Corwin, R. G. and Hoover, D. B. 1978. The Self-Potential Method in Geothermal Exploration, Geophysics Vol. 44, pp.226-245.

Department of the Army 1979. Geophysical Exploration, Engineer Manual EM 1110-1-1802, Office of the Chief of Engineers, Washington, DC.

Dobrin, M. B. 1960. Introduction to Geophysical Prospecting, McGraw-Hill Book Co., New York.

Ernston, K. and Scherer, H. U. 1986. "Self-Potential Variations with Time and their Relation to Hydrogeologic and Meteorological Parameters," Geophysics, Vol. 51, No. 10, pp. 1967-1977.

Grant, F. S., West, G. F. 1965. Interpretation Theory in Applied Geophysics, McGraw-Hill Book Company, New York.

Greenhouse, J. P. and Monier-Williams, M. 1985. "Geophysical Monitoring of Ground Water Contamination Around Waste Disposal Sites," Ground Water and Monitoring Review, Vol. 5, No. 4, pp. 63-69.

Griffiths, D. H., King, R. F. 1969. Applied Geophysics for Engineers and Geologists, Pergamon Press, New York.

Heiland, C. A. 1940. Geophysical Exploration, Prentice-Hall, New York.

Koester, J. P., Butler, D. K., Cooper, S. S., and LLopis J. L. 1984. "Geophysical Investigations in Support of Clearwater Dam Comprehensive Seepage Analysis," Miscellaneous Paper GL-84-3, U.S. Army Engineer Waterways Experiment Station, Vicksburg, Miss.

McNeil, J. D. 1980. "Electromagnetic Terrain Conductivity Measurement at Low Induction Numbers," Technical Note TN-6, Geonics Limited, Ontario, Canada.

McNeil, J. D. 1980. "EM-34-3 Survey Interpretation Techniques," Technical Note TN-8, Geonics Limited, Ontario, Canada.

McNeil, J. D. 1982. "Electromagnetic Resistivity Mapping of Contaminant Plumes in Management of Uncontrolled Hazardous Waste Sites," Hazardous Material Control Research Institute, Silver Springs, Md., pp 1-6.

Ogilvy, A. A., Ayed, M. A., Bogoslovsky, V. A. 1969. "Geophysical Studies of Water Leakages from Reservoirs," Geophysical Prospecting, Vol. 17, No. 1, pp. 36-62.

Parasnis, D. S. 1966. Mining Geophysics. Elsevier Publishing Company, New York.

Redpath, B. B. 1973. "Seismic Refraction Exploration for Engineering Site Investigations," Technical Report E-73-4, U.S. Army Engineer Waterways Experiment Station, Vicksburg, Miss.

Telford, W. M., Geldhart, L. P., Sheriff, R. E., and Keys, D. A. 1973. Applied Geophysics. Cambridge University Press, New York.

U.S. Army Engineer District, Little Rock 1984. Reconnaissance Report, Beaver Dam. Little Rock, Ark.

U.S. Army Engineer District, Little Rock 1959. Design Memorandum NO. 5 Geology and Soils. Little Rock, Ark.

Van Norstrand, R. G., and Cook, K. L. 1967. "Interpretation of Resistivity Data," US Geological Survey Professional Paper 499, Washington, DC.

Warriner, J. B. and Taylor, P. A. 1982. "Modeling of Electrokinesis," Miscellaneous Paper GL-82-13, U.S. Army Engineer Waterways Experiment Station, Vicksburg, Miss.

Yule, D. E., Llopis, J. L., and Sharp, M. K. 1985. "Geophysical Seepage Studies at Center Hill Dam, Tennessee," Miscellaneous Paper GL-85-29, U.S. Army Engineer Waterways Experiment Station, Vicksburg, Miss.

Zalasiewicz, J. A., Mathers, S. J., and Cornwell, J. D. 1985. "The Application of Ground Conductivity Measurements to Geological Mapping," Q. J. Eng. Geol., Vol.18, pp. 139-148, London.

Zohdy, A. A. R., Eaton, G. P., Mabey D. R. 1974. "Application of Surface Geophysics to Ground-Water Investigations," Techniques of Water-Resources Investigations of the United States Geological Survey, Chapter D1, U.S. Geological Survey, Washington, D.C.

TABLE 1

Pool Elevations for Days SP Readings Collected

DATE	POOL ELEVATION, ft
9 March 1985	1125.50
11 MARCH 1985	1124.94
12 MARCH 1985	1124.77
14 MARCH 1985	1125.05
15 MARCH 1985	1125.00
2 APRIL 1985	1129.25
3 APRIL 1985	1129.00
21 MAY 1985	1124.04
25 JUNE 1985	1123.60
27 JUNE 1985	1123.53
23 JULY 1985	1122.80
24 OCTOBER 1985	1119.70
21 NOVEMBER 1985	1127.83
10 DECEMBER 1985	1125.00
29 JANUARY 1986	1118.35
3 MARCH 1986	1117.10

LOCATION MAP
SCALE OF MILES
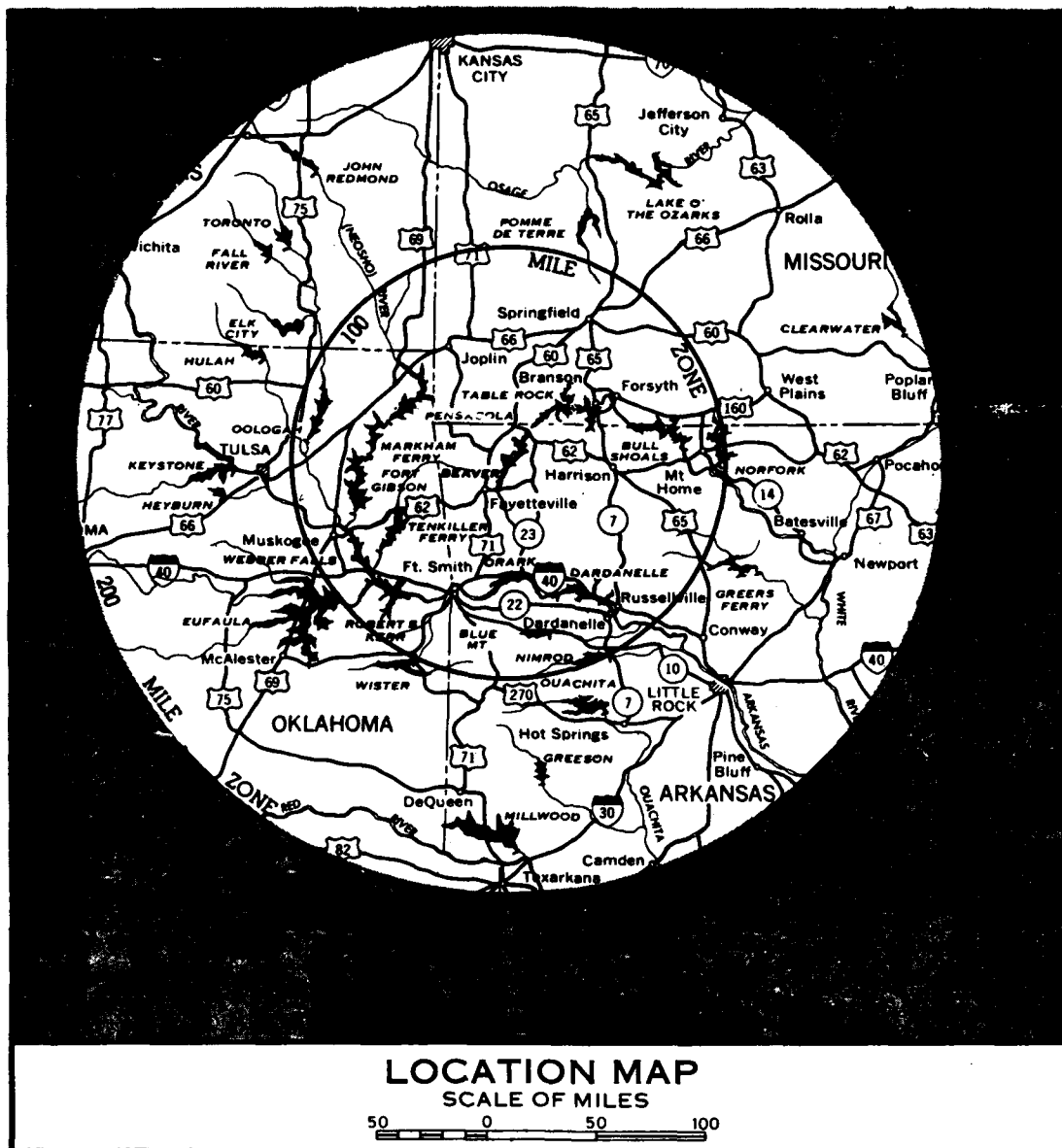
Figure 1. Site map
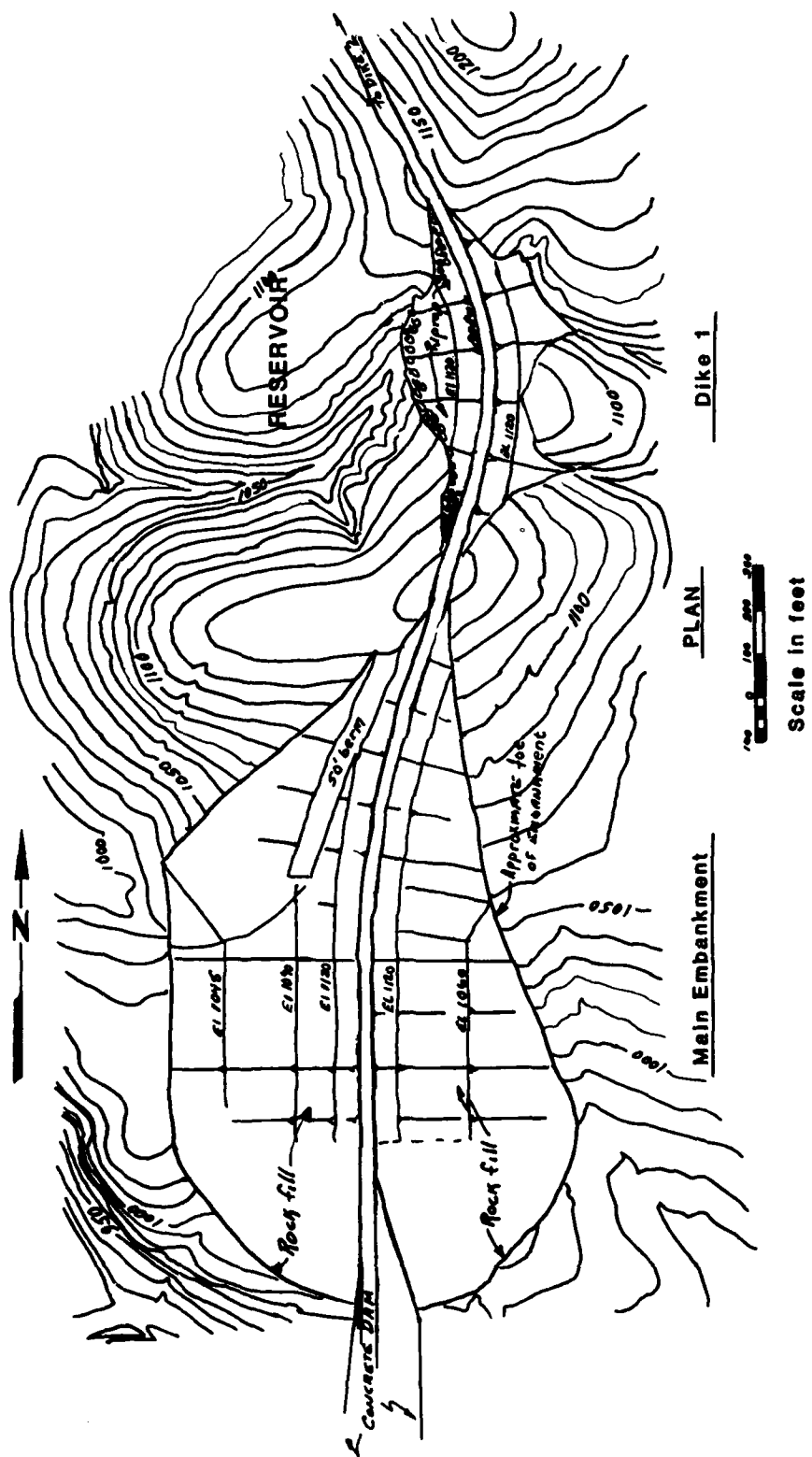
Figure 2. Plan view of Dike 1 and main embankment
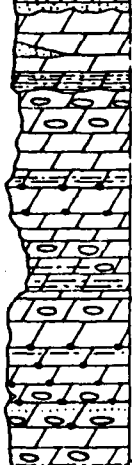
SYSTEM	GROUP	FORMATION	SECTION	THICKNESS IN FEET	UNIT	DESCRIPTION
MISSISSIPPIAN		BOONE			BOONE CHERT	LIMESTONE, CHERTY, LIGHT TO DARK GRAY, SLIGHTLY SHALY, FINE-GRAINED, HARD, THIN- TO MEDIUM-BEDDED. CHERT OCCURS AS THIN BEDS AND NODULES, SHALE OCCURS AS THIN LAMINATIONS.
				45 to 50	ST. JOE LIMESTONE	LIMESTONE, GRAY TO GREEN-GRAY WITH OCCASIONAL PINK HORIZONS, CRYSTALLINE, VERY FOSSILIFEROUS, CONTAINS NUMEROUS THIN SHALE SEAMS AND PARTINGS.
					CHAT. SHALE	SHALE, BLACK, FIRM, FISSILE.
DEVONIAN	CHATTA-NOOGA				SYLAMORE SS	SANDSTONE, WHITE TO YELLOW, MEDIUM- TO COARSE-GRAINED. VARIES FROM POORLY CEMENTED TO QUARTZITIC. USUALLY MASSIVE, LOCALLY THIN-BEDDED.
ORDIVICIAN	JEFFERSON CITY	POWELL		17±	1	LIMESTONE, LIGHT GRAY TO GREEN WHEN FRESH, AND TAN TO BUFF WHEN WEATHERED. IT IS DENSE, MODERATELY HARD, AND MEDIUM- TO MASSIVE-BEDDED. MARKER V, A GREEN ARGILLACEOUS ZONE CONTAINING NUMEROUS SHALE SEAMS AND INCLUSIONS FORMS THE BASE OF THE UNIT. Marker V
		COTTER		21±	2	LIMESTONE, DOLOMITIC, LIGHT GRAY TO GRAY-GREEN WHEN FRESH, AND TAN OR BUFF WHEN WEATHERED. IT IS DENSE AND MODERATELY HARD. THE UPPER HALF CONTAINS SCATTERED CHERT NODULES AND ANGULAR FRAGMENTS, WHICH ARE BANDED BLUE AND GRAY, NEAR THE MIDDLE OF THE UNIT IS A MOTTLED, OFTEN VUGGY ZONE. THE BEDS ARE THICK TO MASSIVE THROUGHOUT MOST OF THE UNIT BUT ARE THIN AND CONTAIN CLOSELY SPACED SHALE SEAMS AT THE BOTTOM.
				26±	3	LIMESTONE, DOLOMITIC, GRAY TO DARK GRAY WHEN FRESH AND TAN TO BUFF WHEN WEATHERED. THE UPPER HALF OF THE UNIT IS VERY FINELY CRYSTALLINE, HARD, THICK- TO MASSIVE-BEDDED, MOTTLED, AND OCCASIONALLY VUGGY. THE BOTTOM HALF IS DENSE, MEDIUM TO THICK-BEDDED, AND CONTAINS SCATTERED CHERT NODULES.
				41±	4	LIMESTONE, DOLOMITIC, BLUE-GRAY TO DARK GRAY WHEN FRESH, AND BROWN TO BUFF WHEN WEATHERED. THE PREDOMINANT TYPE OF ROCK IS HARD, MOTTLED, OFTEN VUGGY, AND FINELY CRYSTALLINE, BUT THERE ARE SEVERAL ZONES OF MODERATELY HARD, DENSE ROCK. THE BEDDING IS GENERALLY THICK TO MASSIVE. SCATTERED CHERT NODULES AND BANDS OCCUR THROUGHOUT. THE BASAL PORTION IS COMPOSED OF A DENSE, MODERATELY HARD ROCK WHICH BECOMES VERY SHALY AT ITS BASE. MARKER IV IS THE TOP OF THE SHALY HORIZON. Marker IV

Figure 3. Geologic column
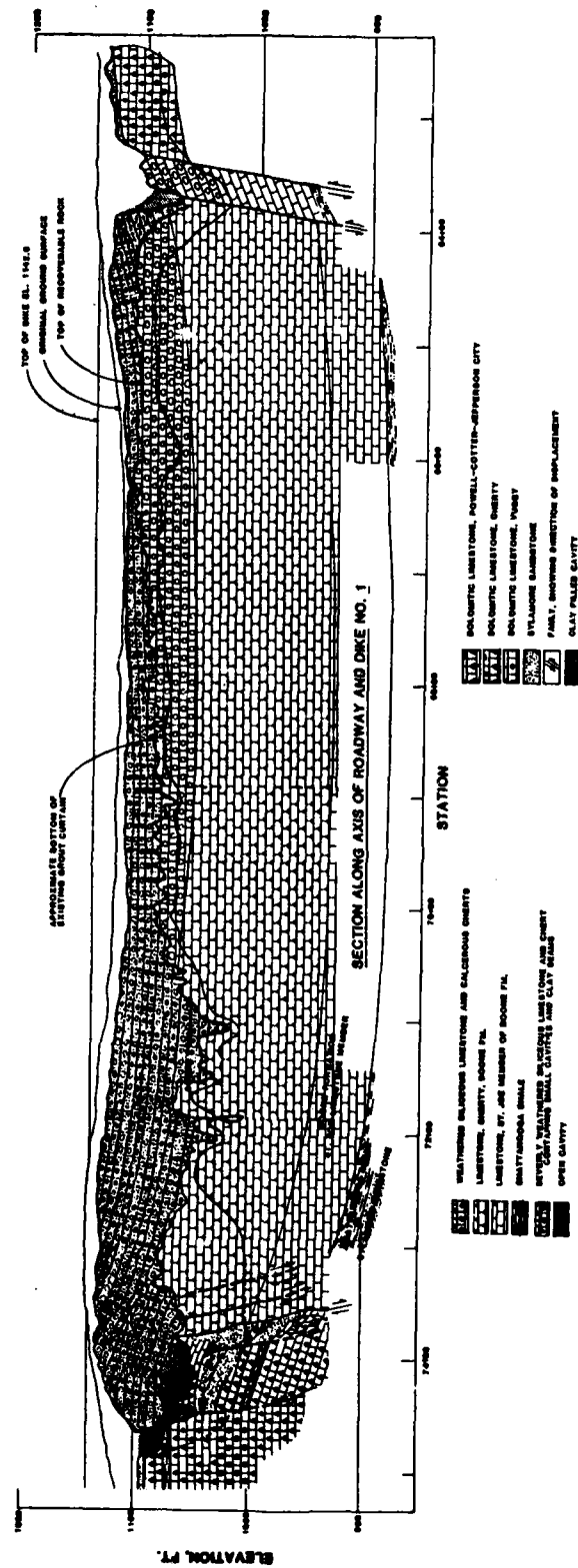
Figure 4. Geologi profile, Dike 1
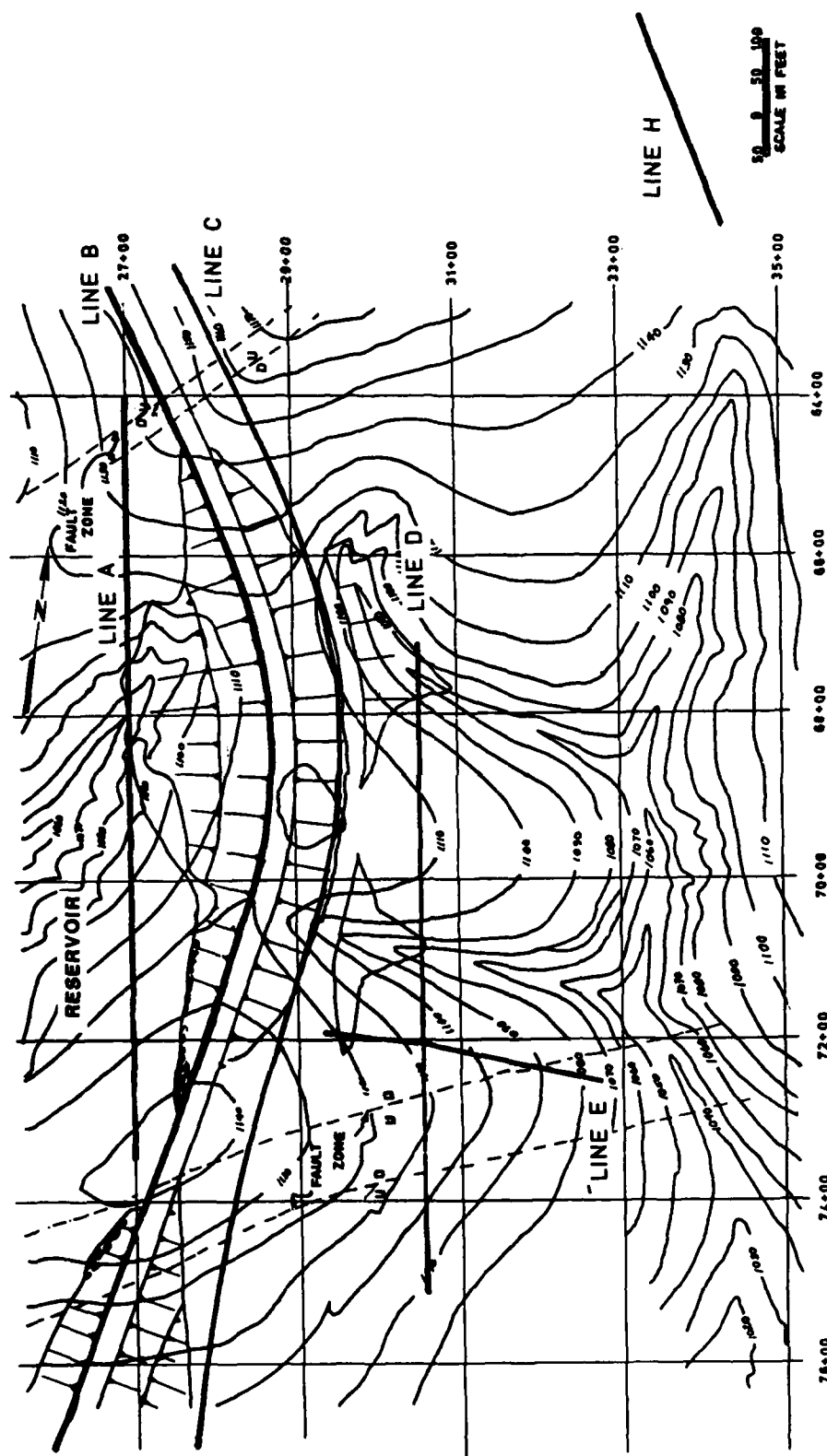
Figure 5. Location of geophysical survey lines A,B,C,D,E, and H

Figure 6. Idealized SP anomaly generation
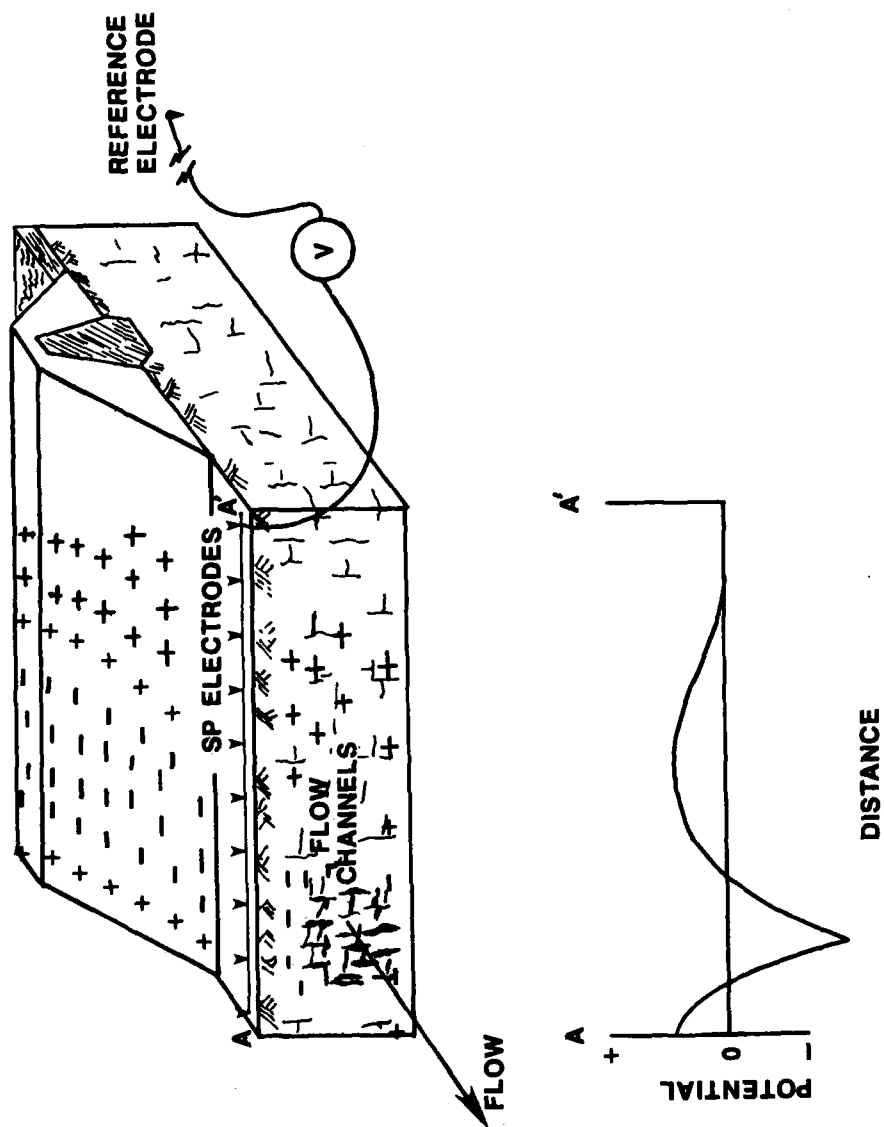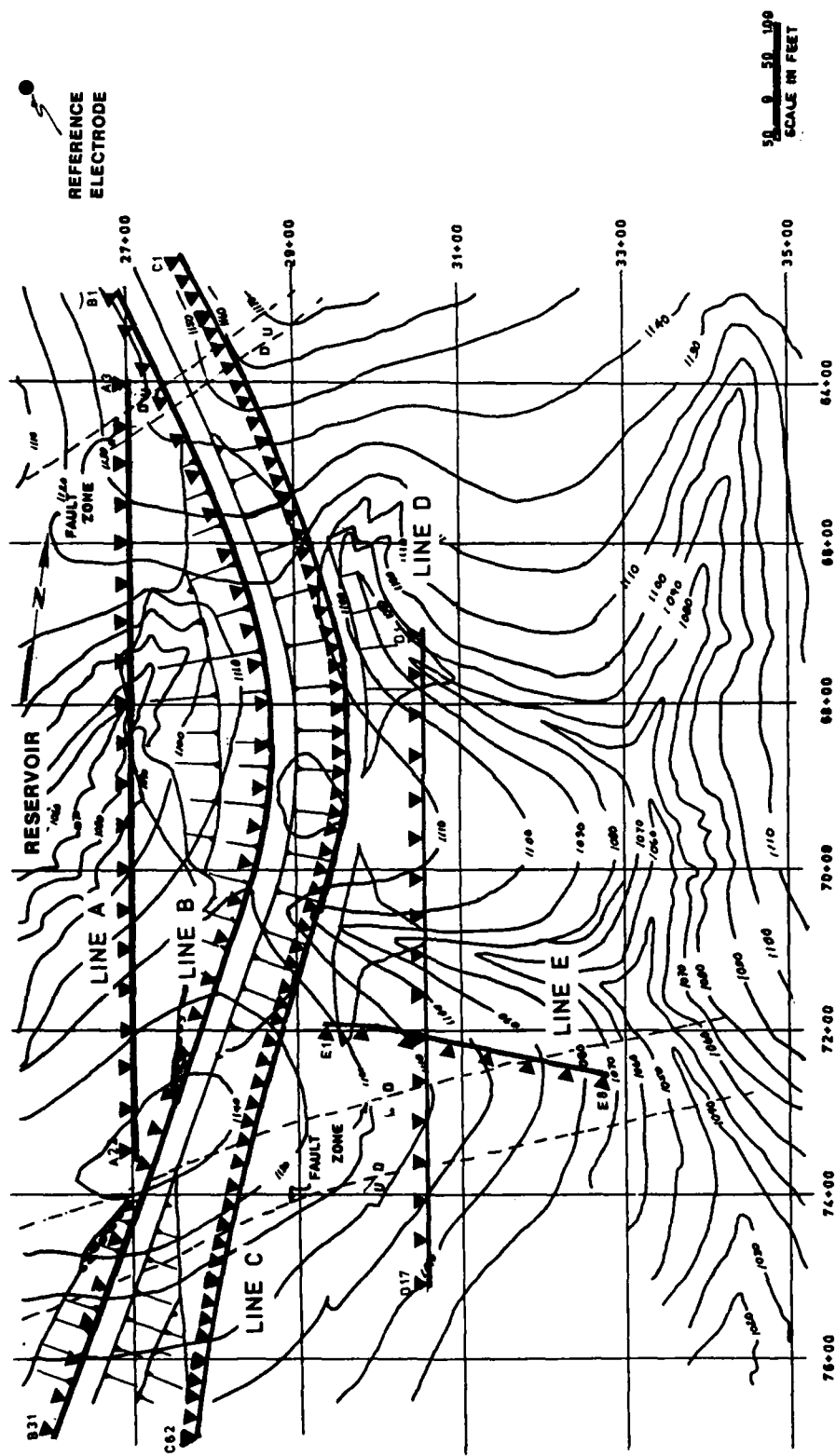
Figure 7. Location of SP survey lines
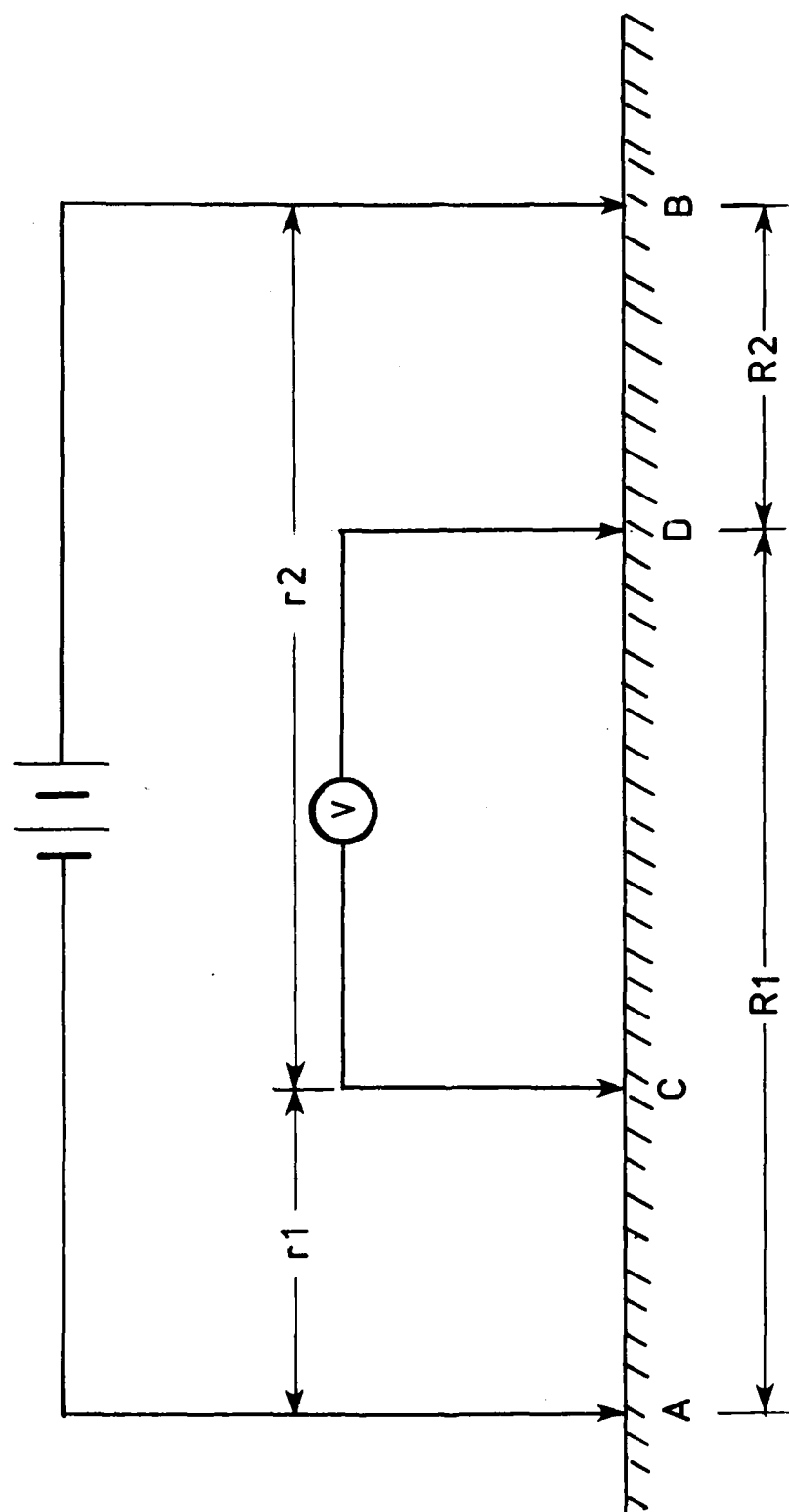
Figure 8. Arrangement of current electrodes (A and B) and potential electrodes (C and D)
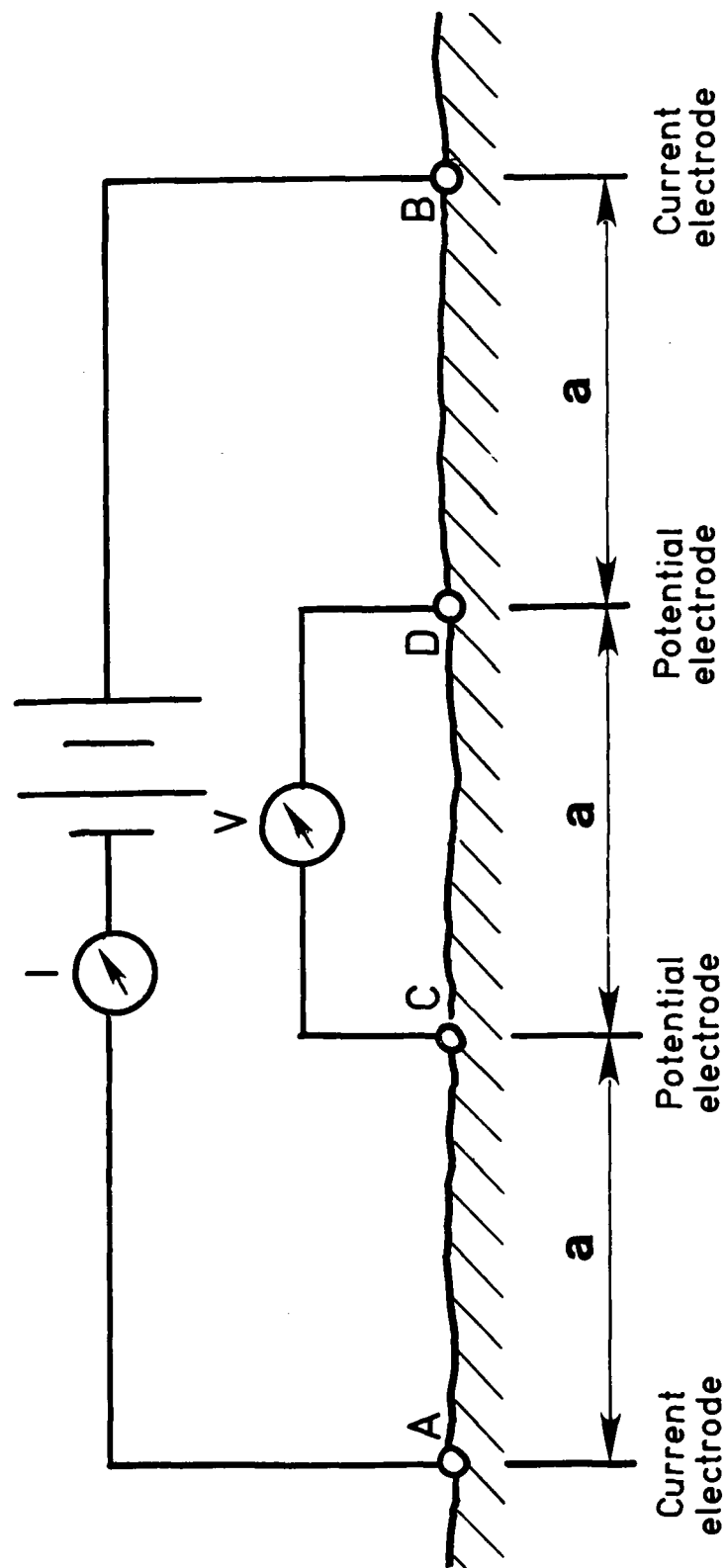
Figure 9. Wenner resistivity electrode array
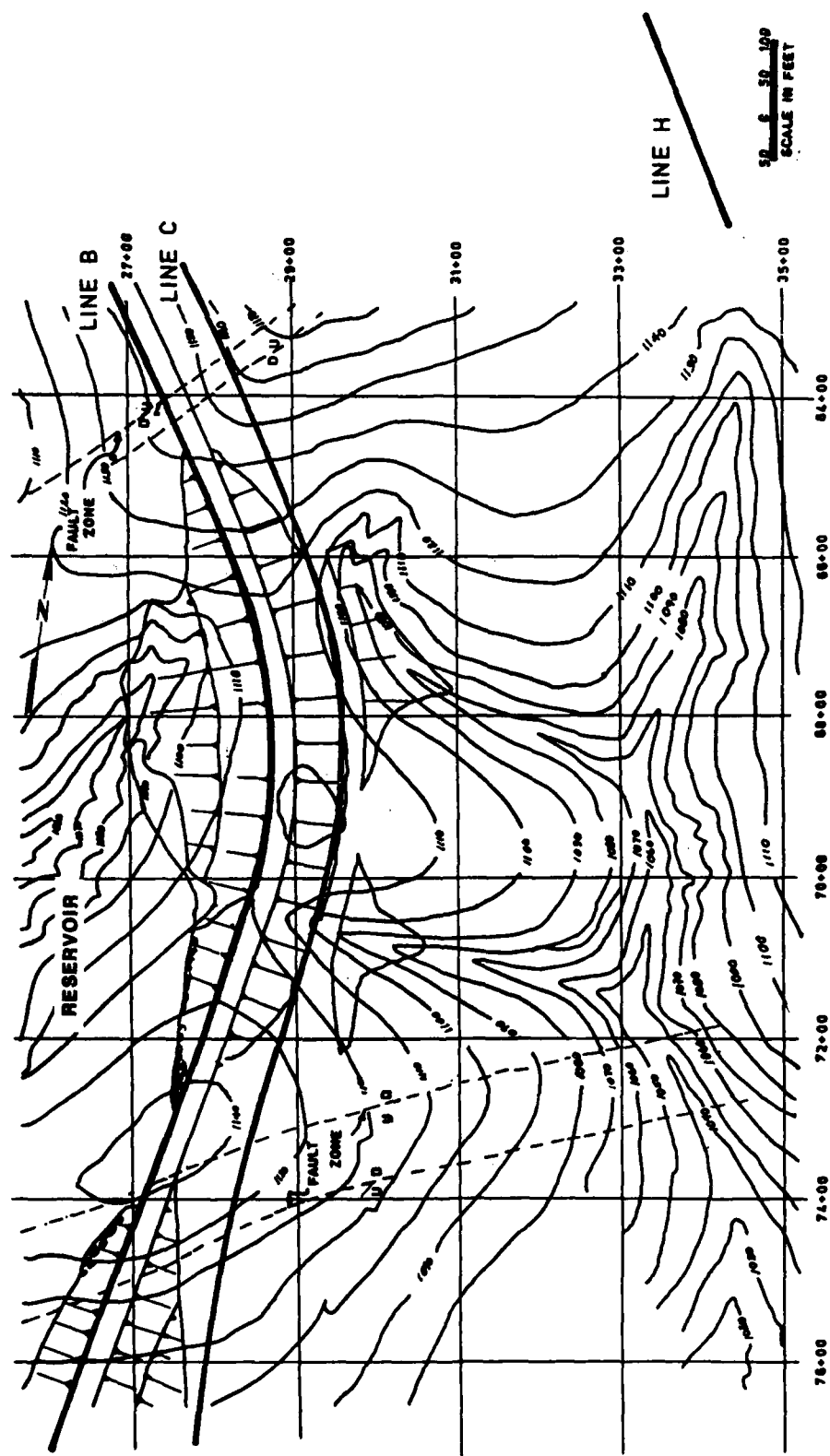
Figure 10. Location of resistivity survey lines
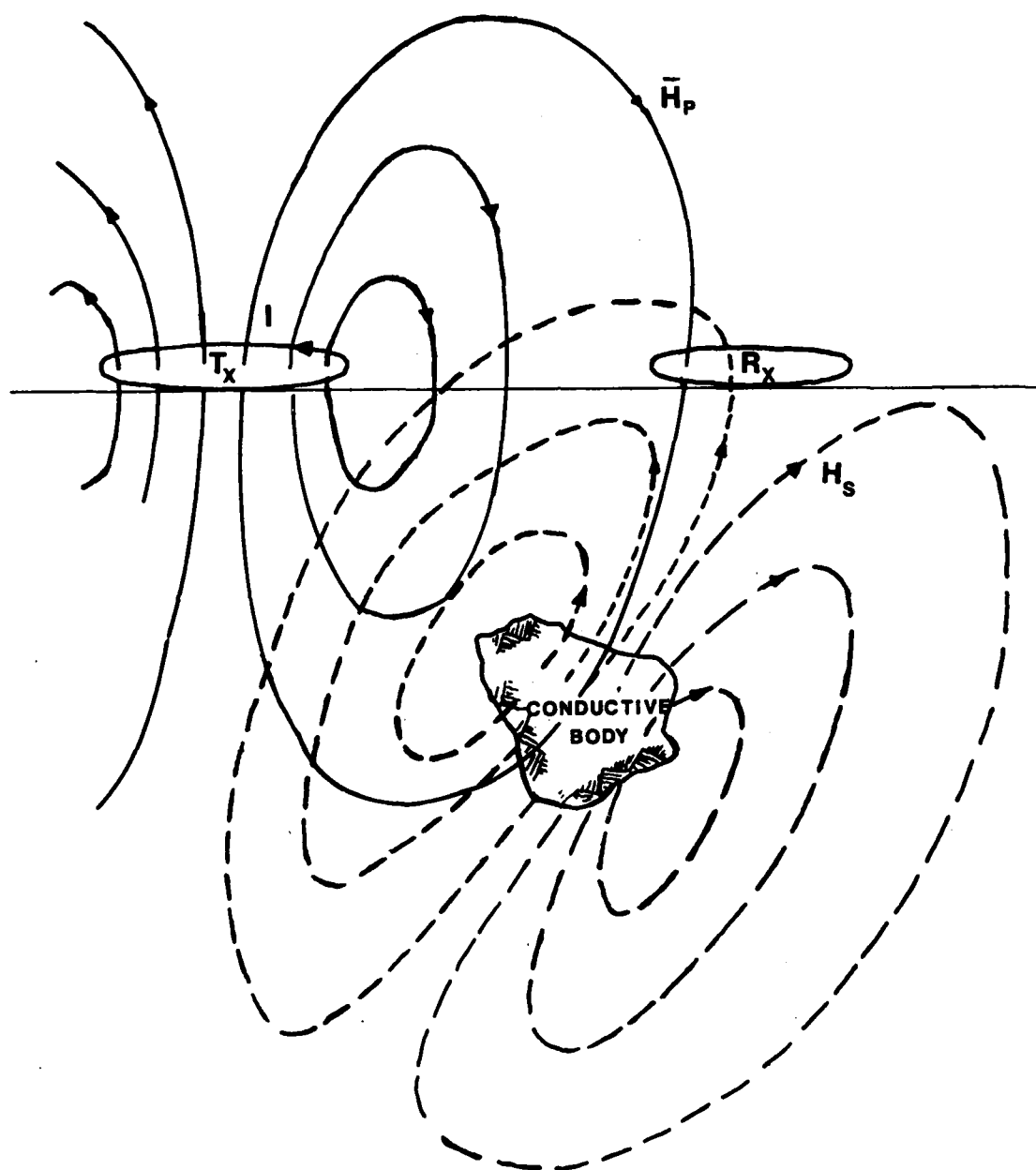
Figure 11. Inductive coupling between transmitter (Tx),
receiver (Rx), and conductive body; Hp and Hs are the
primary and secondary magnetic fields, respectively
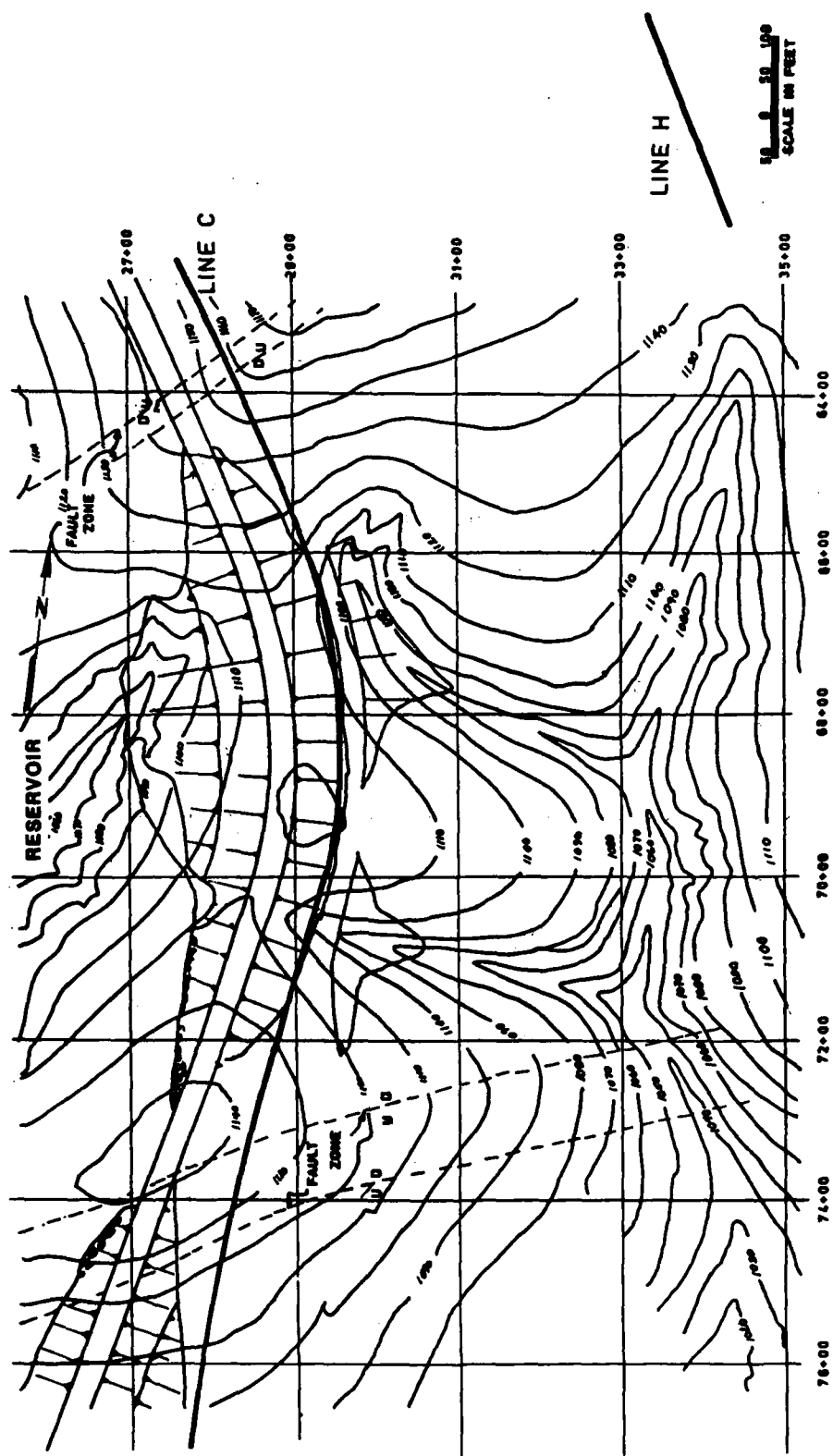
Figure 12. Location of EM survey lines

$$\text{SLOPE} = \frac{1}{V_1}$$

$$\text{SLOPE} = \frac{1}{V_0}$$

$$I_C = \text{SIN}^{-1} \frac{V_0}{V_1}$$
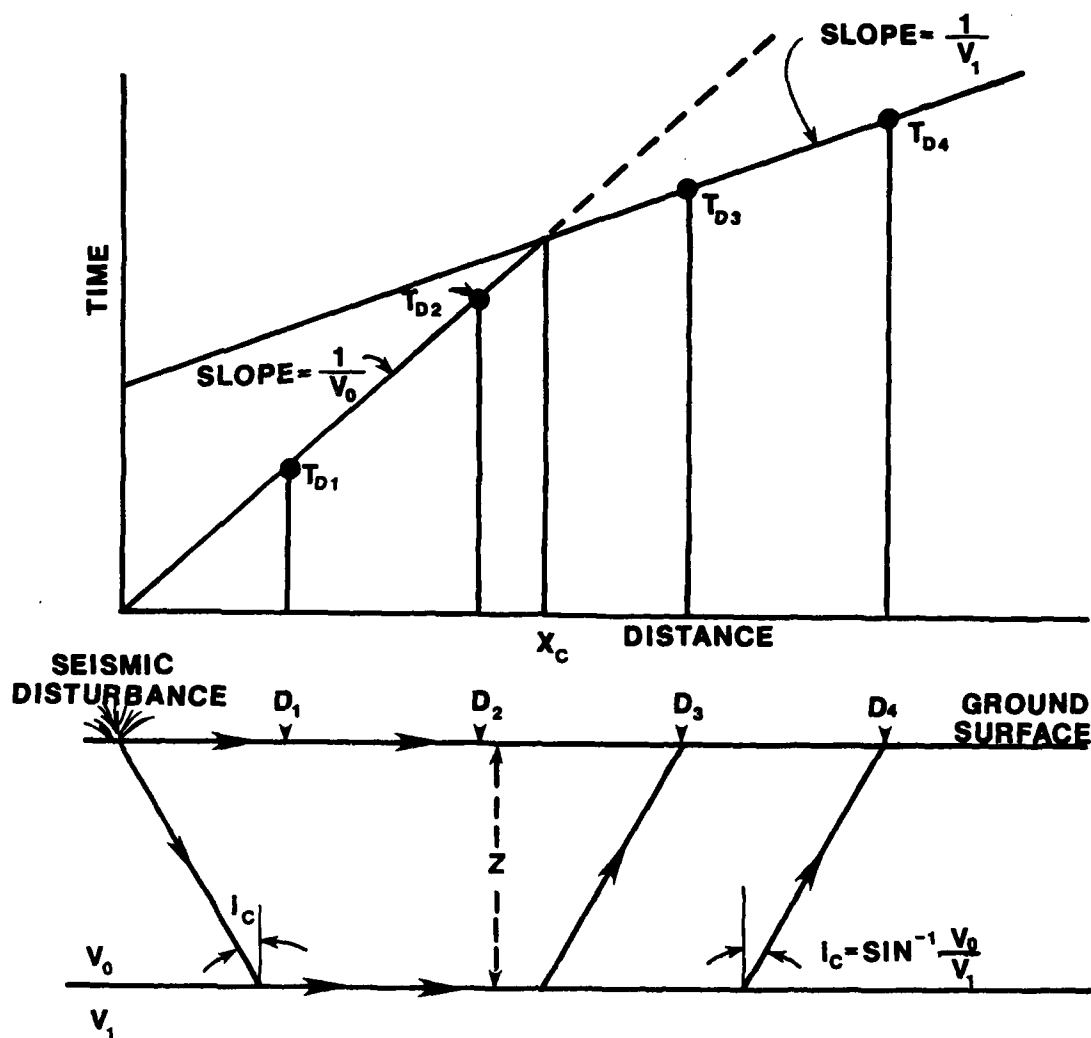
Figure 13. Example of a time-distance plot for a two layer earth model
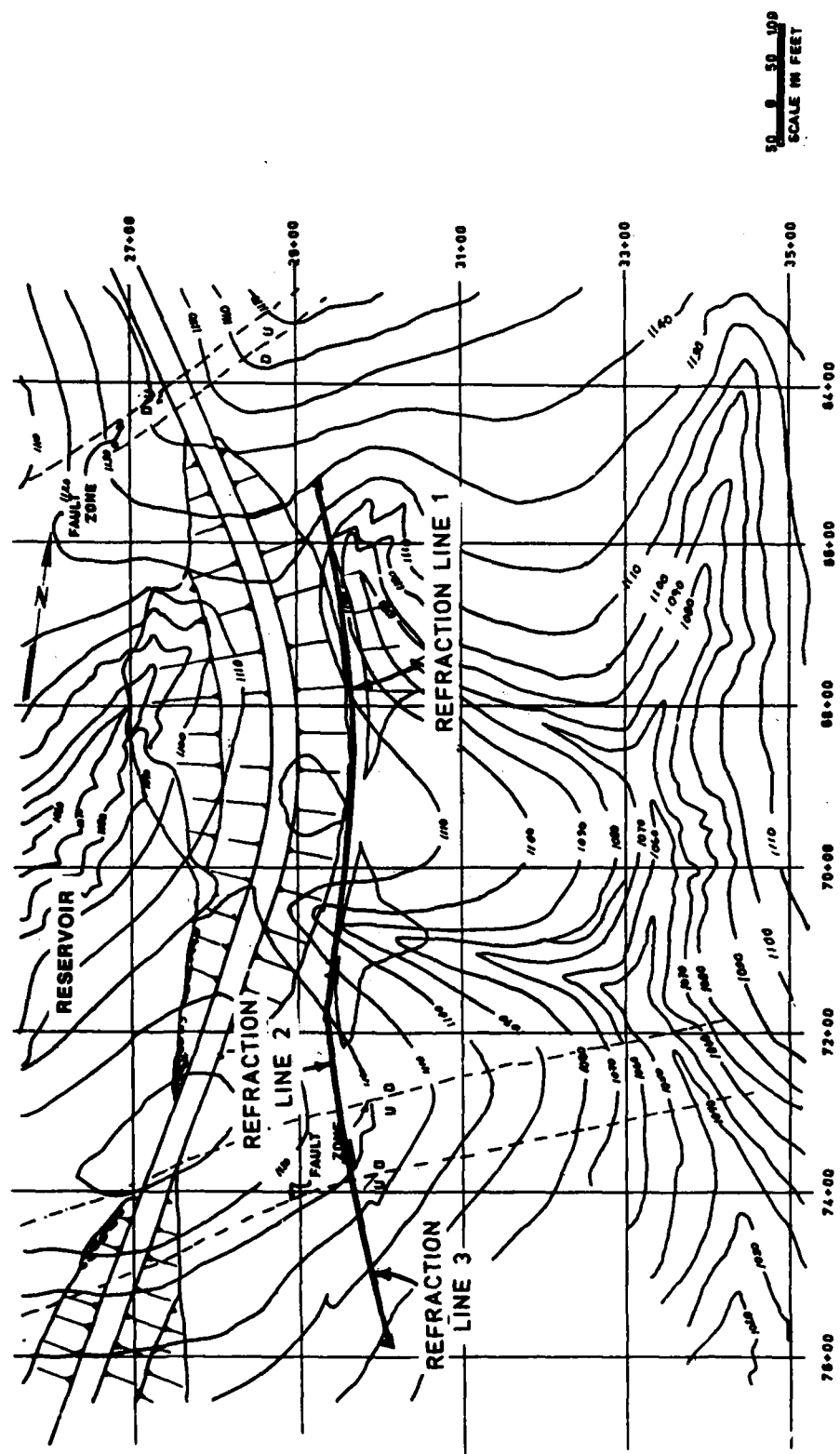
Figure 14. Location of refraction survey lines
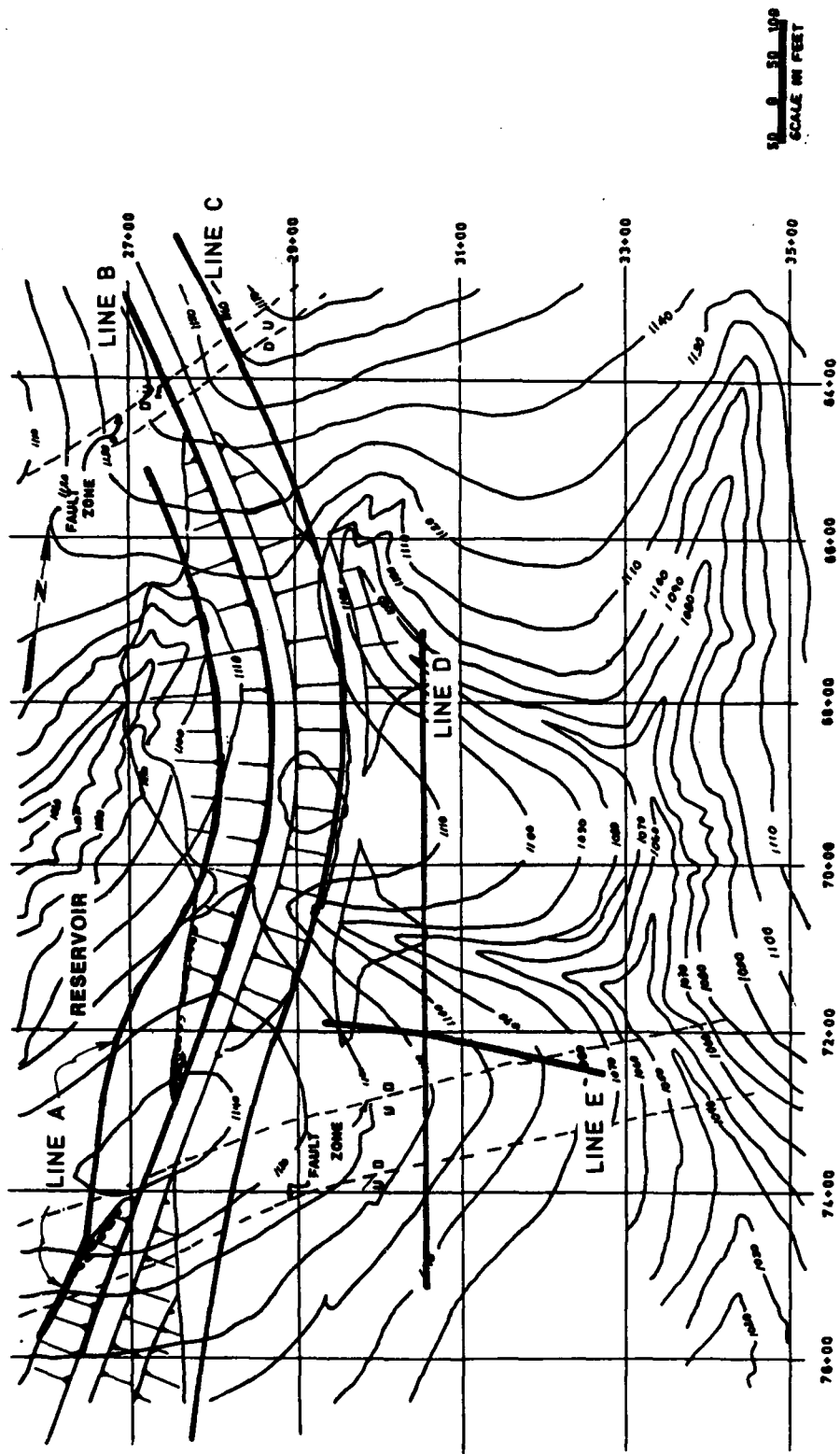
Figure 15. Location of magnetic survey lines

Figure 16. Theoretical Wenner resistivity profile
across a high-resistivity, vertical fault
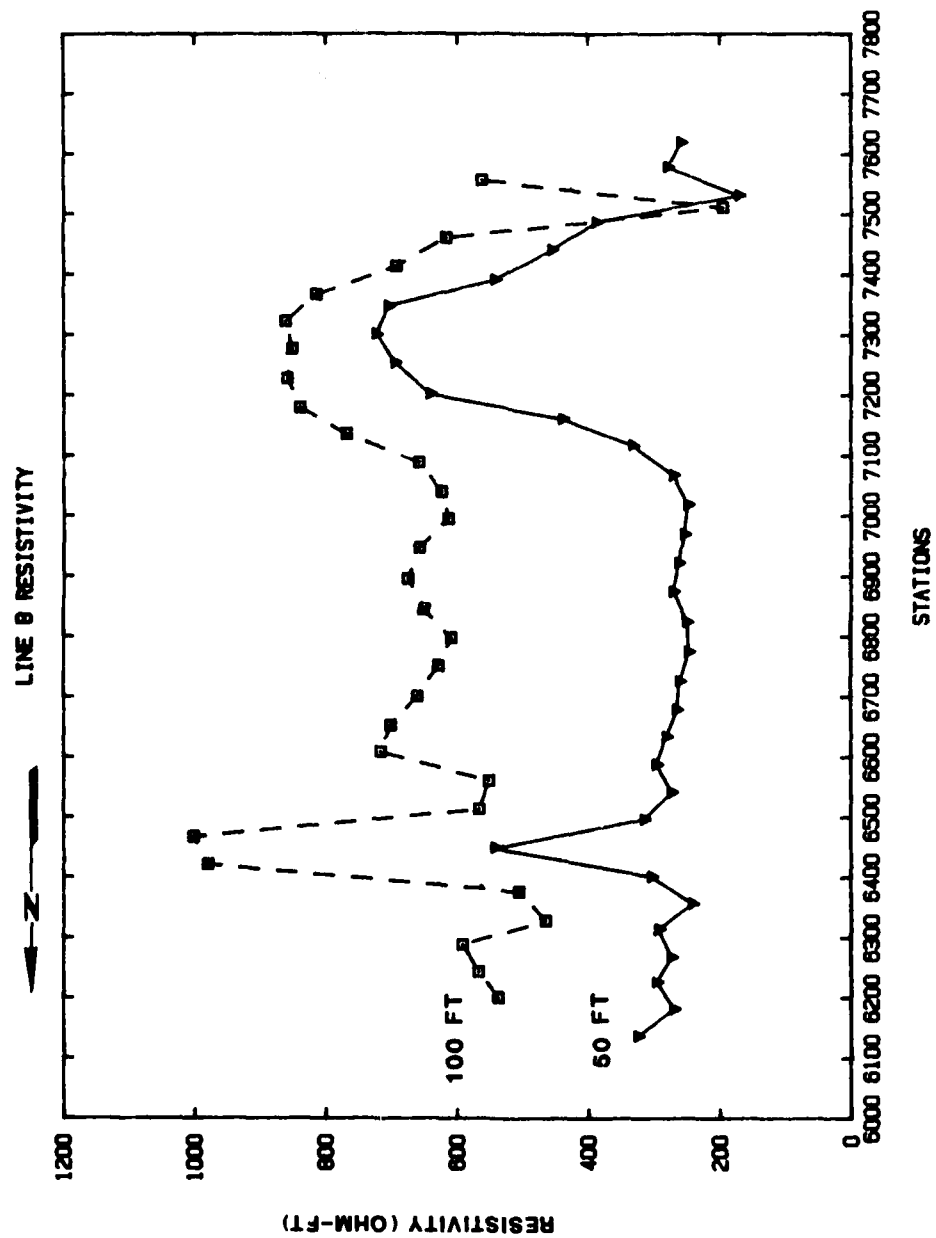
Figure 17. Wenner resistivity profile line B, crest Dike 1
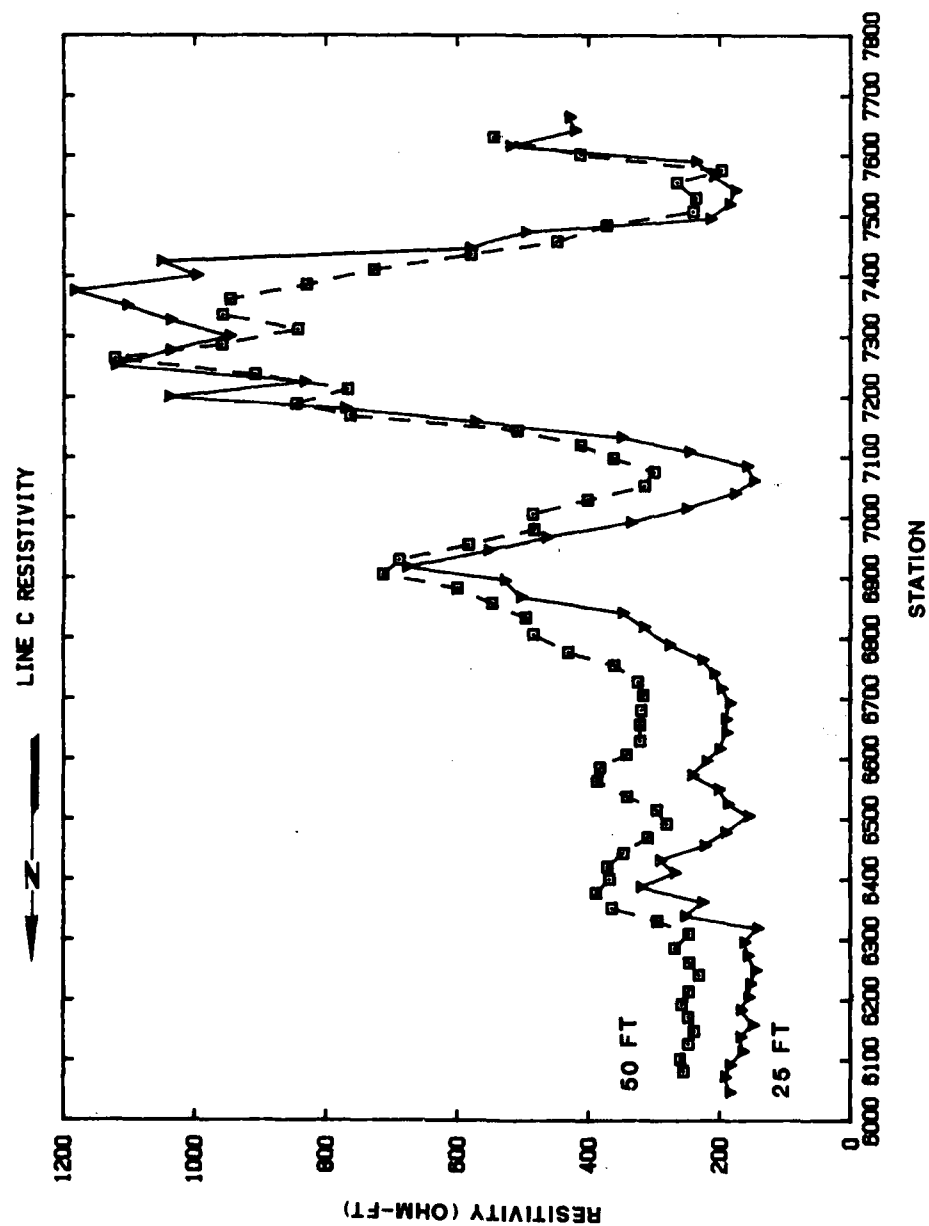
Figure 18. Wenner resistivity profile line C, downstream berm Dike 1
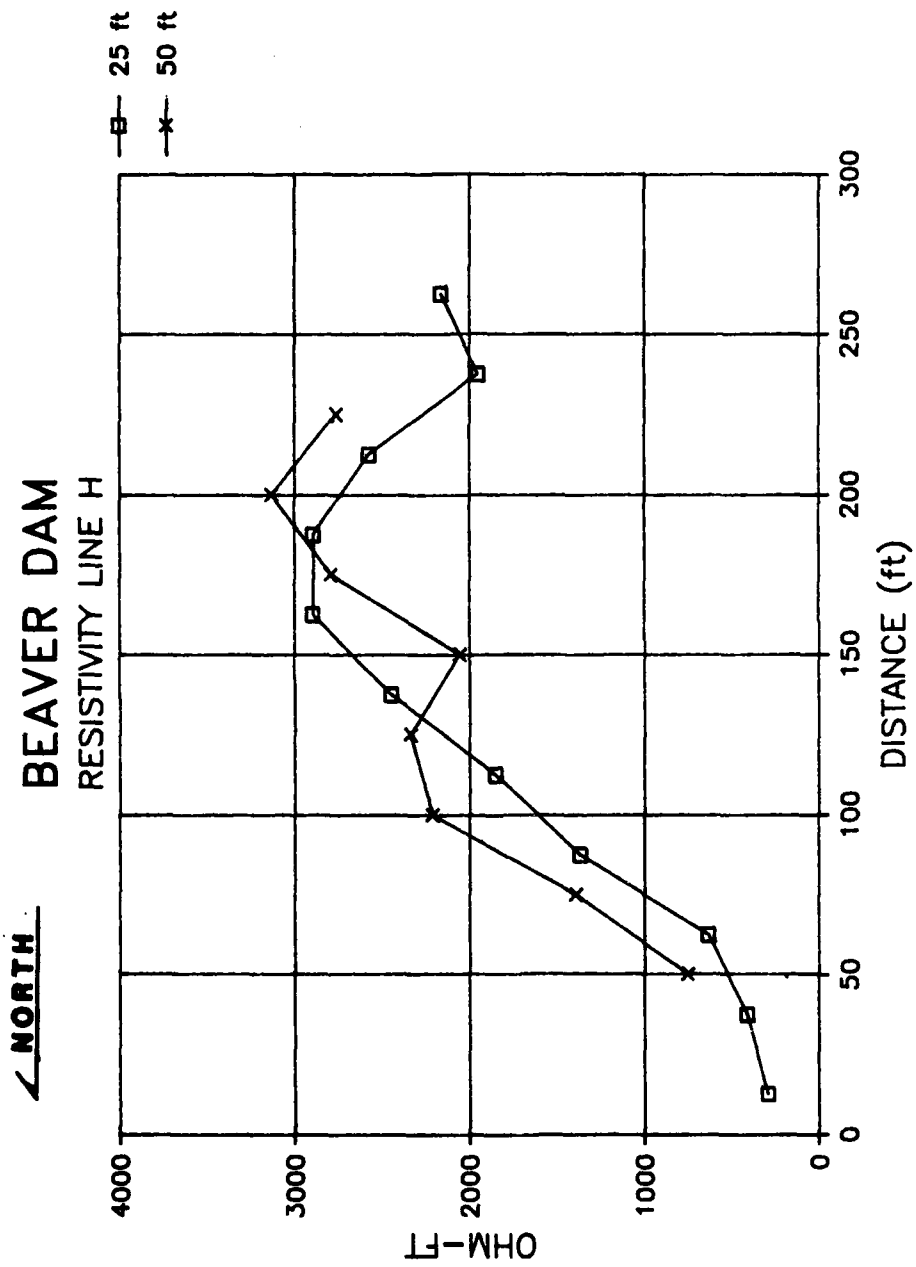
Figure 19. Wenner resistivity profile line H, downstream - Left Abutment Dike 1
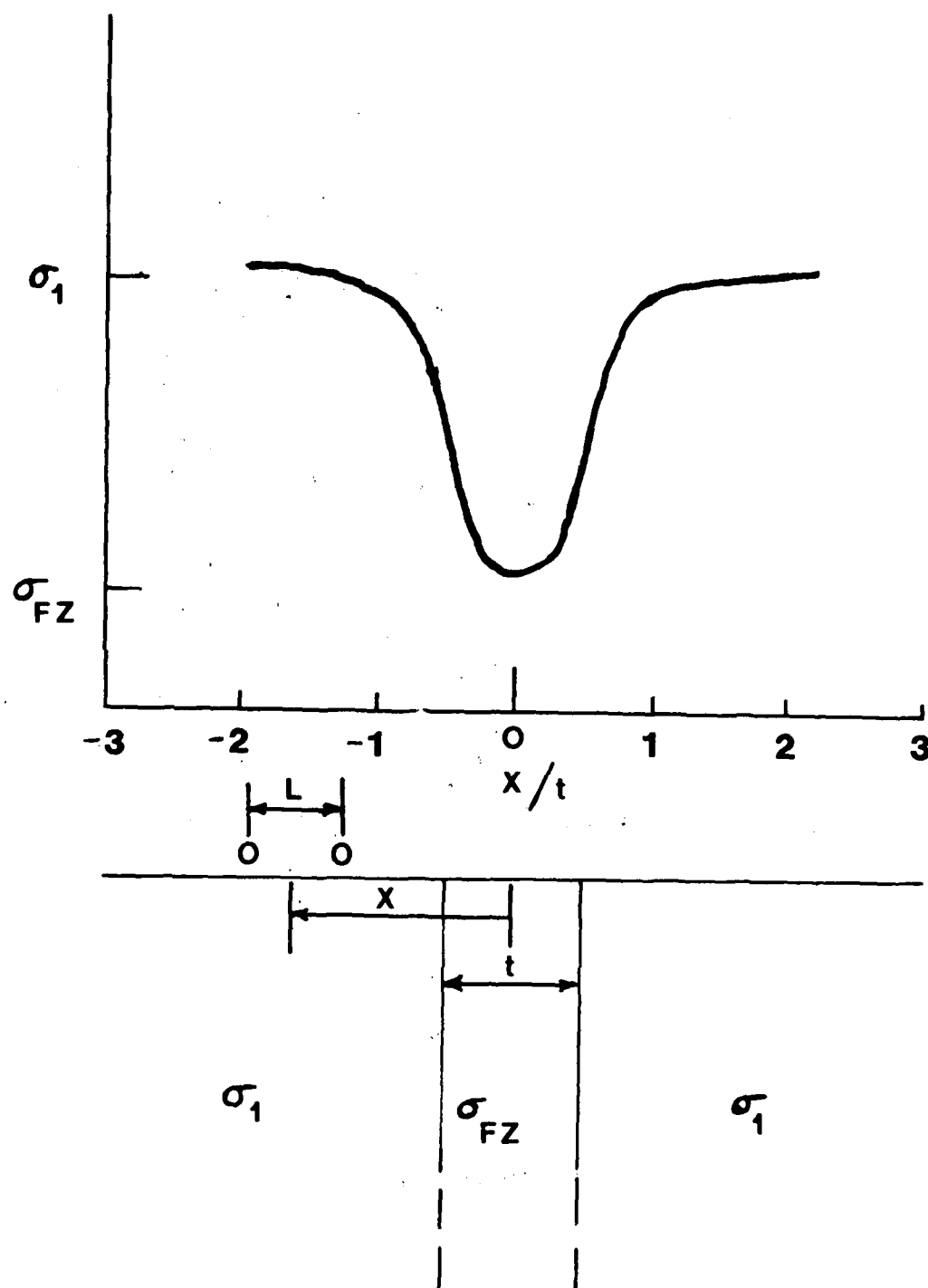
Figure 20. Theoretical electromagnetic profile across
a high-resistivity, vertical fault
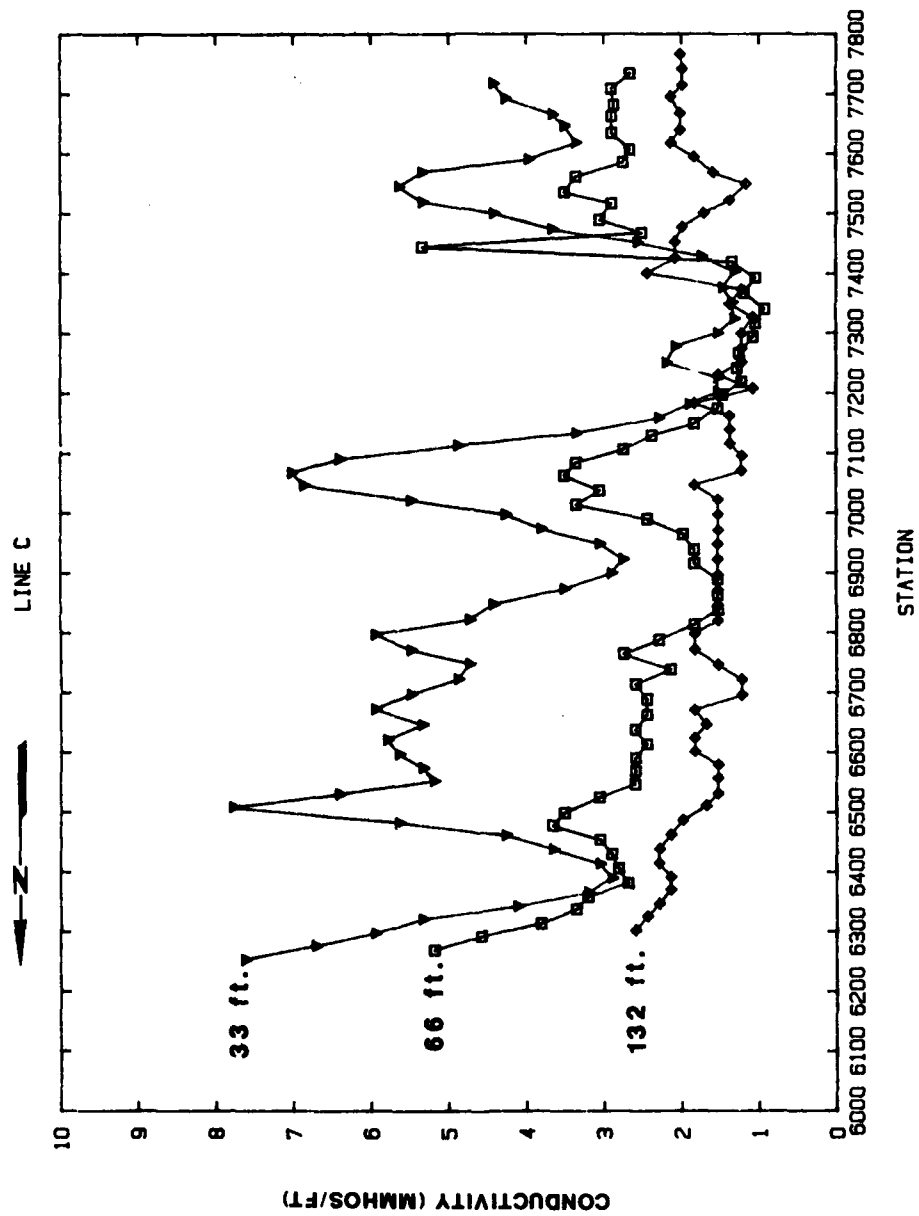
Figure 21. EM profile line C, downstream berm Dike 1
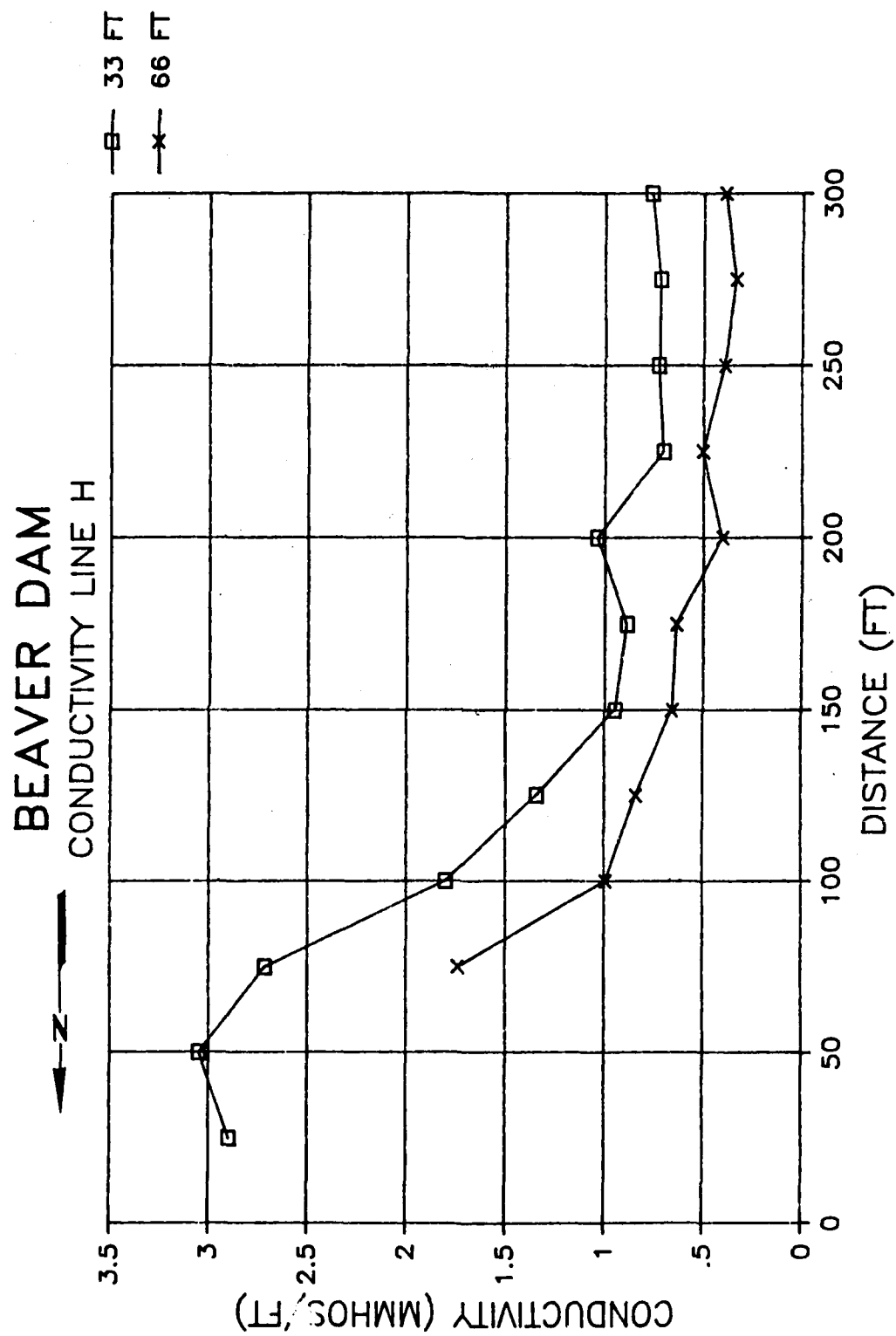
Figure 22. EM profile line H, downstream - Left Abutment Dike 1
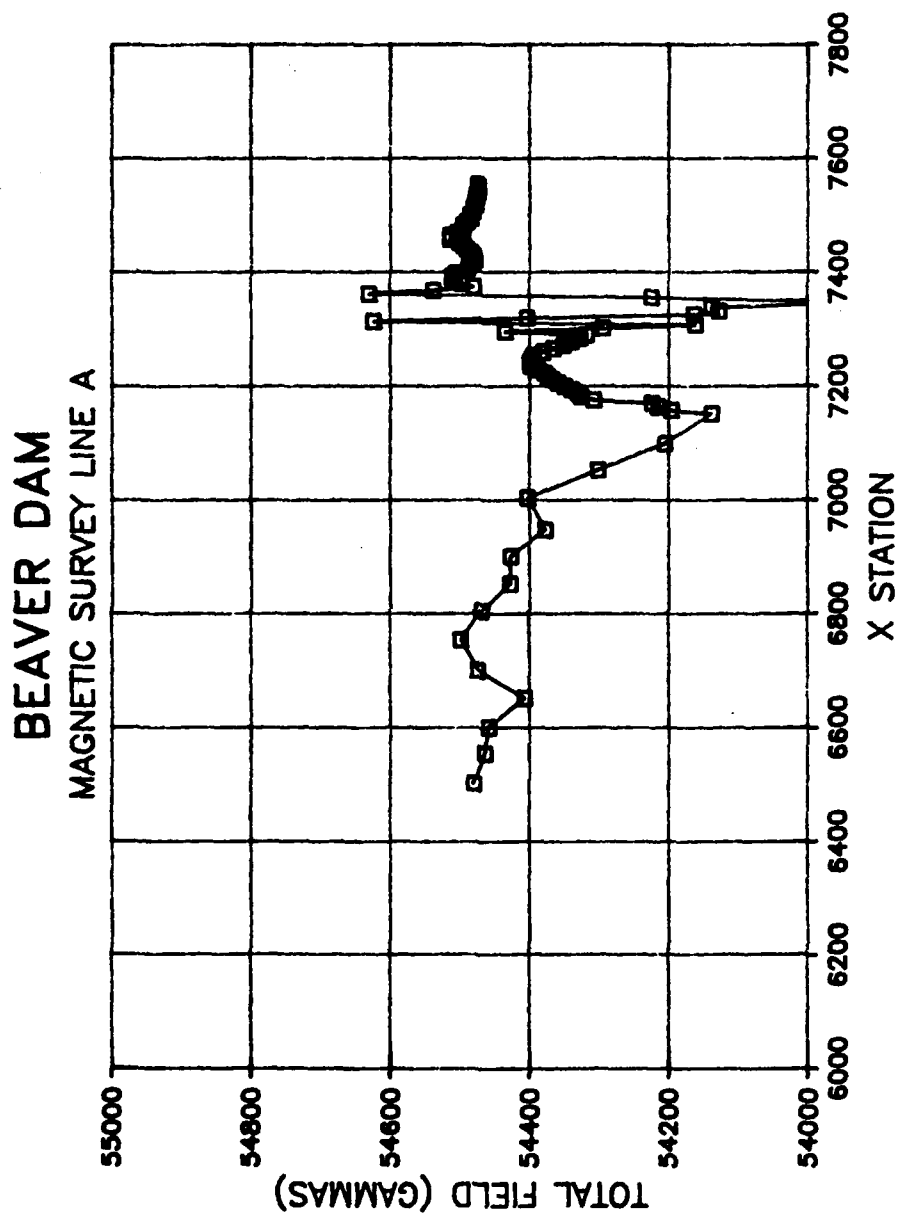
Figure 23. Magnetic survey line A, upstream toe Dike 1
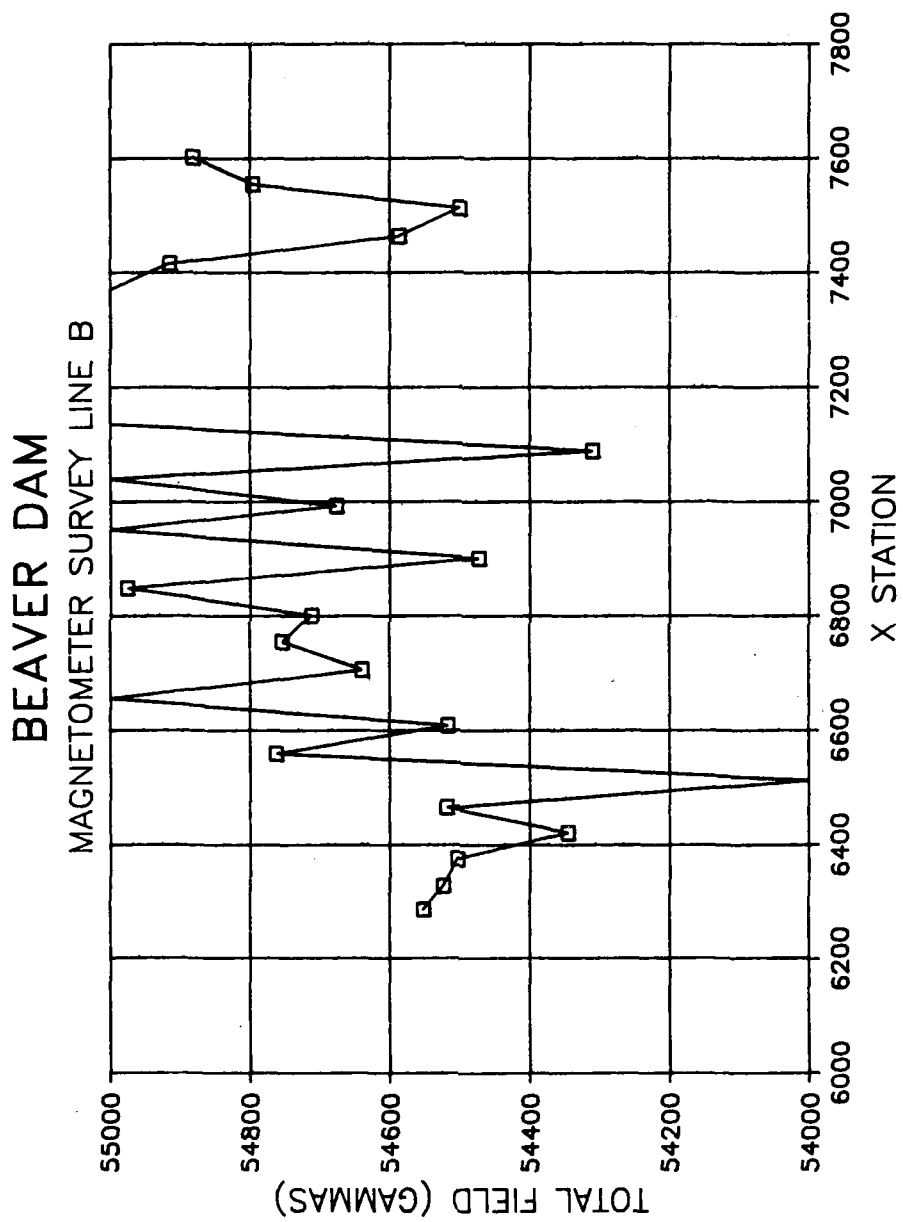
Figure 24. Magnetic survey line B, crest Dike 1
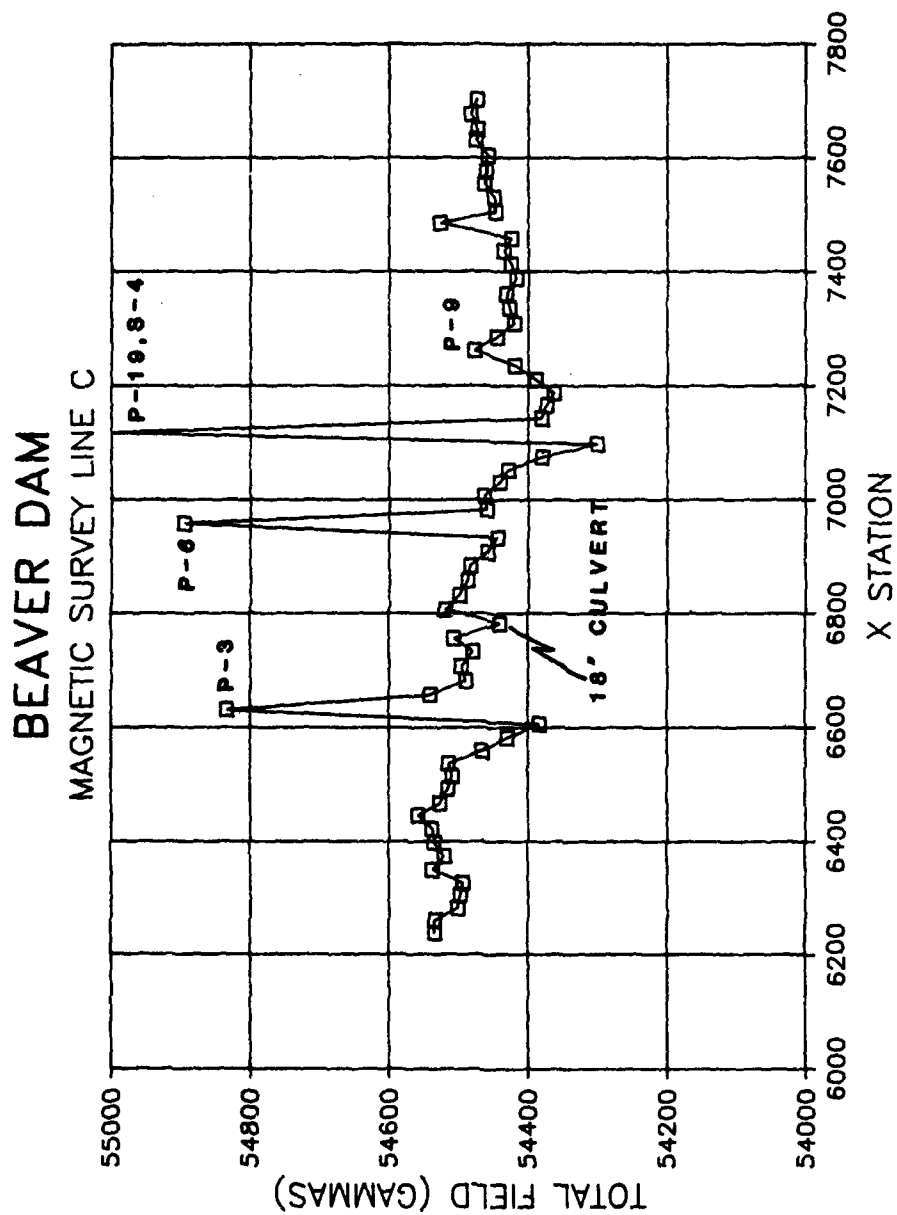
Figure 25. Magnetic survey line C, downstream berm Dike 1
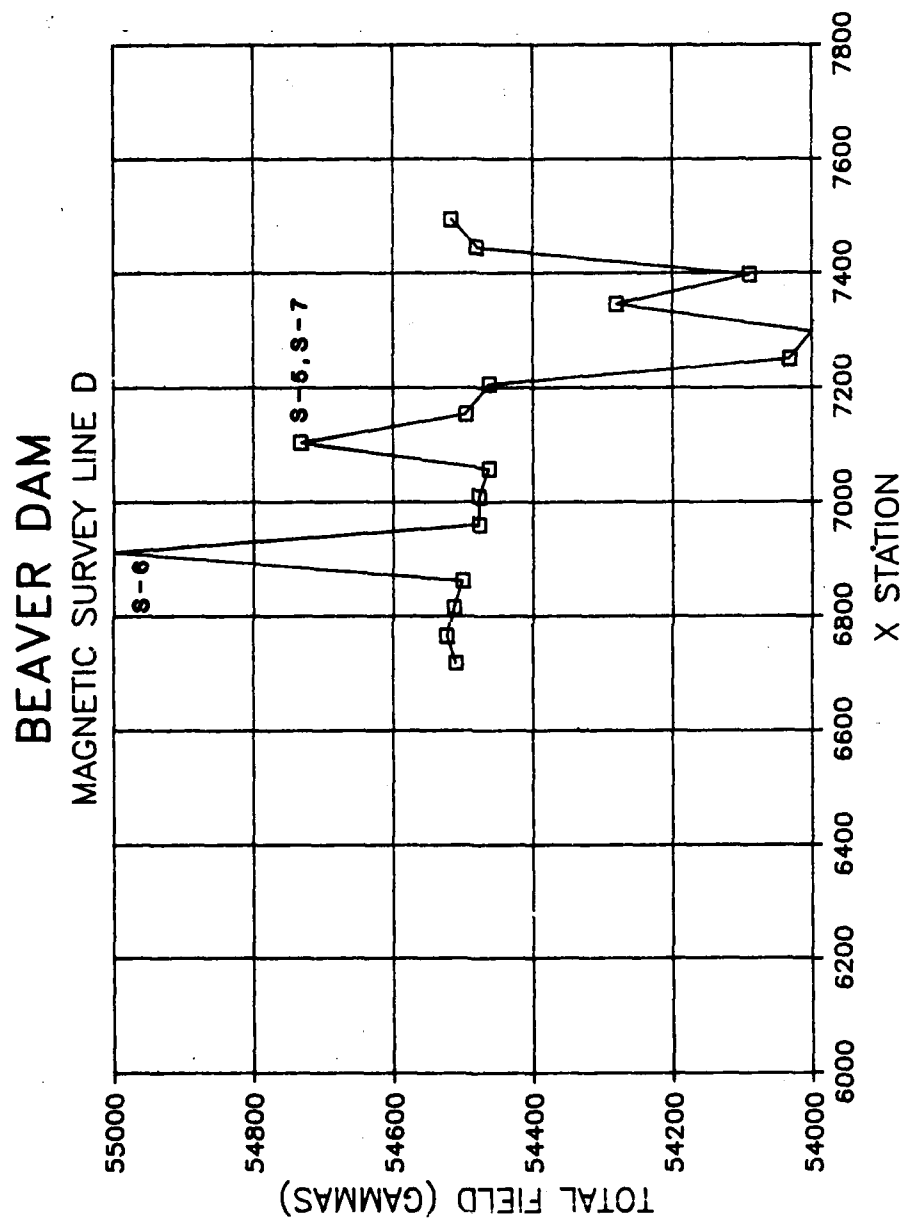
Figure 26. Magnetic survey line D, downstream Dike 1
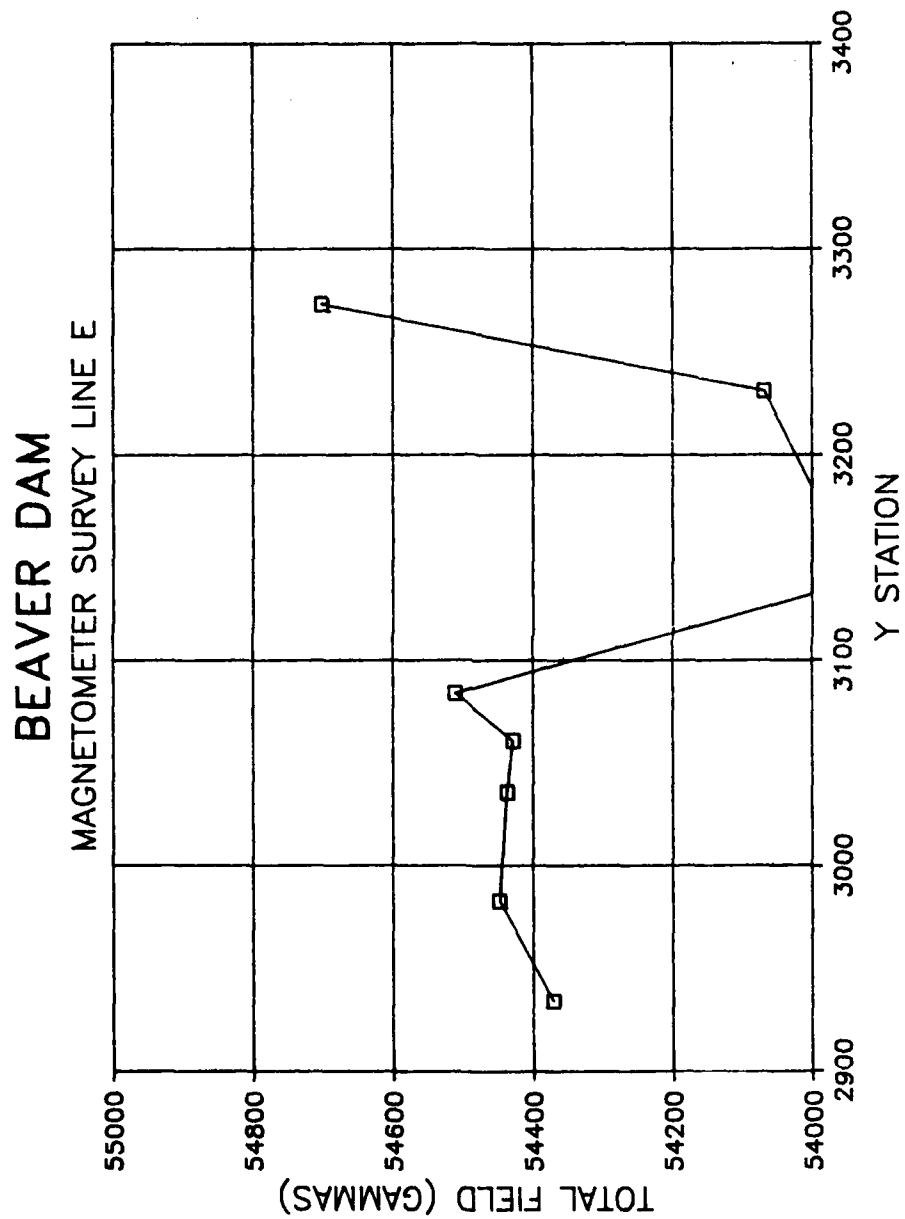
Figure 27. Magnetic survey line E, downstream Dike 1
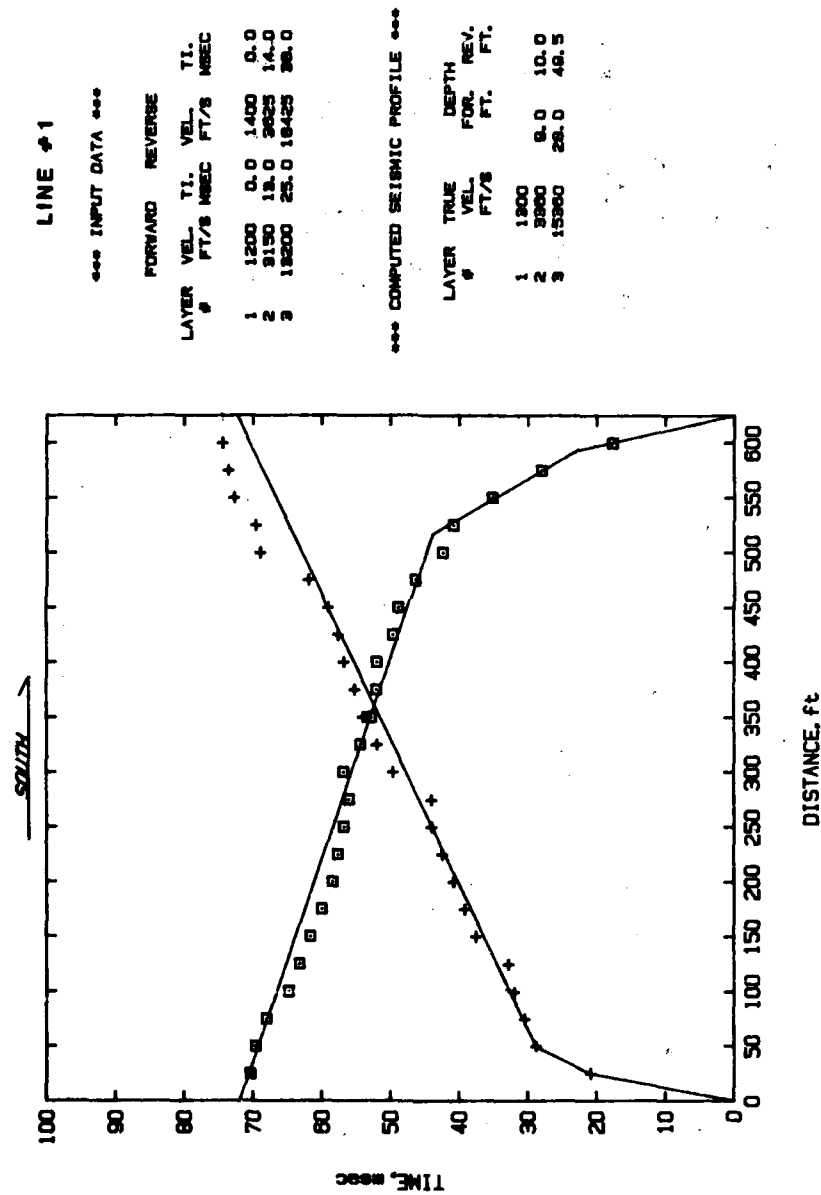
Figure 28. Time versus distance plot for seismic refraction line 1
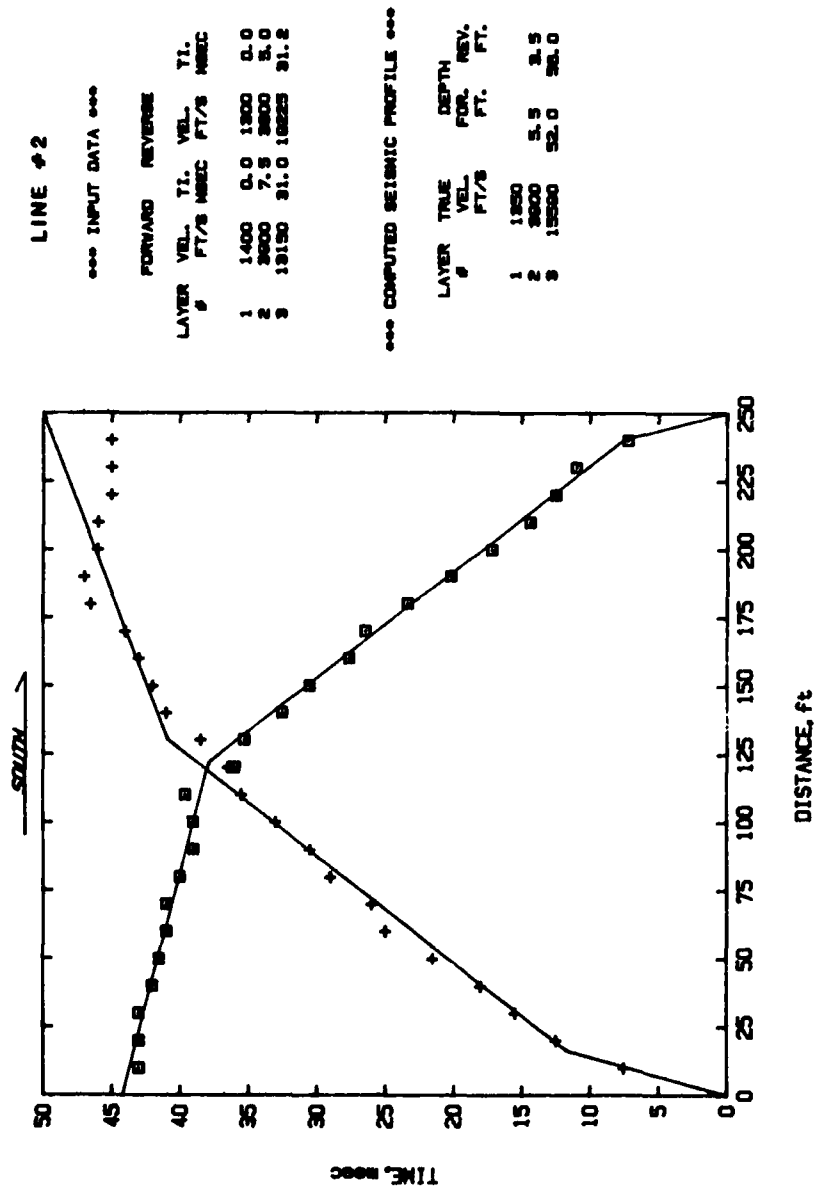
Figure 29. Time versus distance plot for seismic refraction line 2
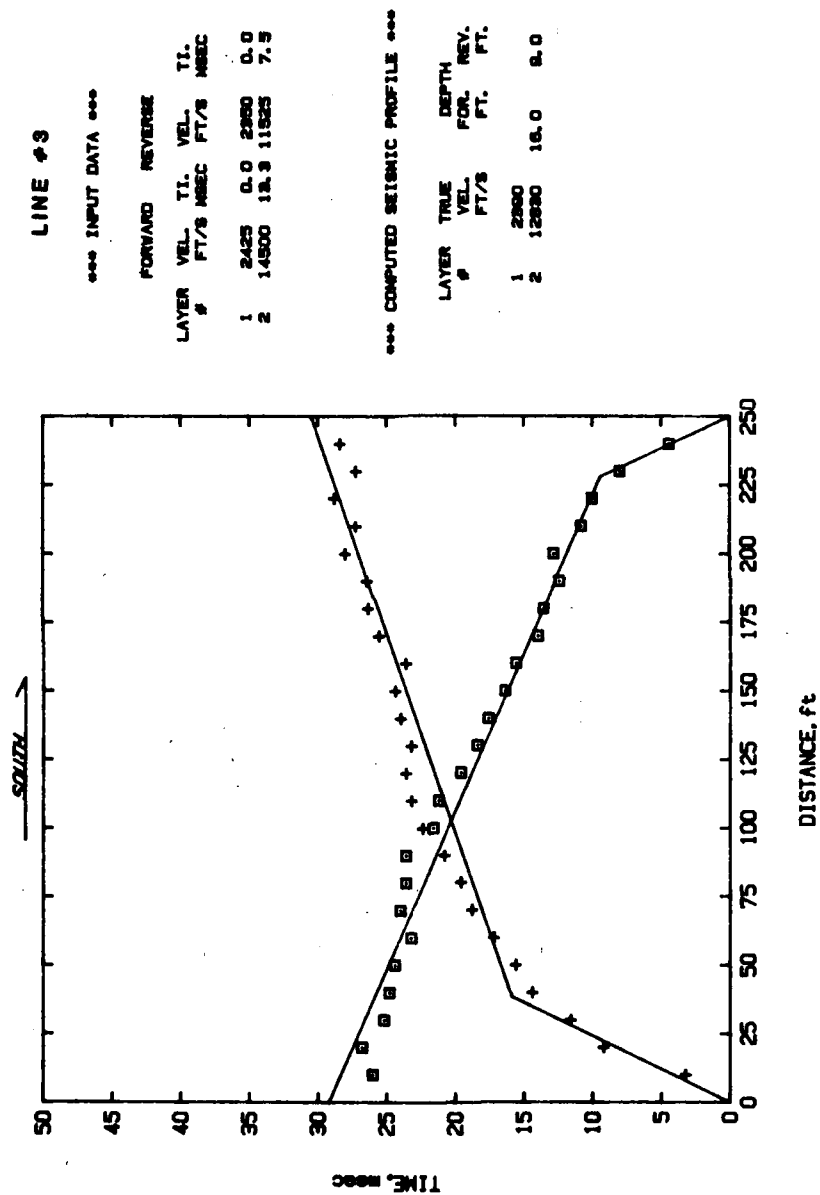
Figure 30. Time versus distance plot for seismic refraction line 3
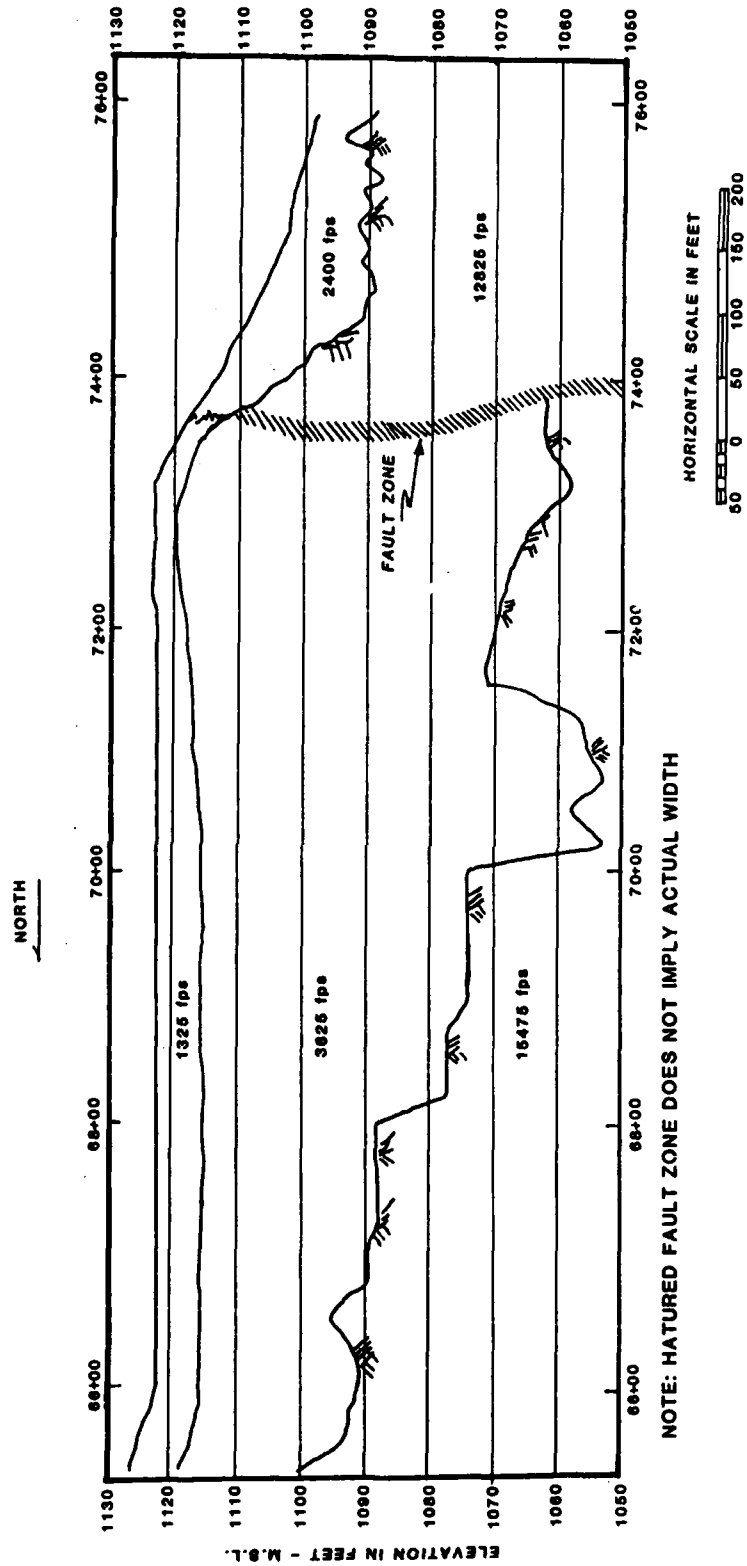
Figure 31. P-wave velocity cross section for Dike 1
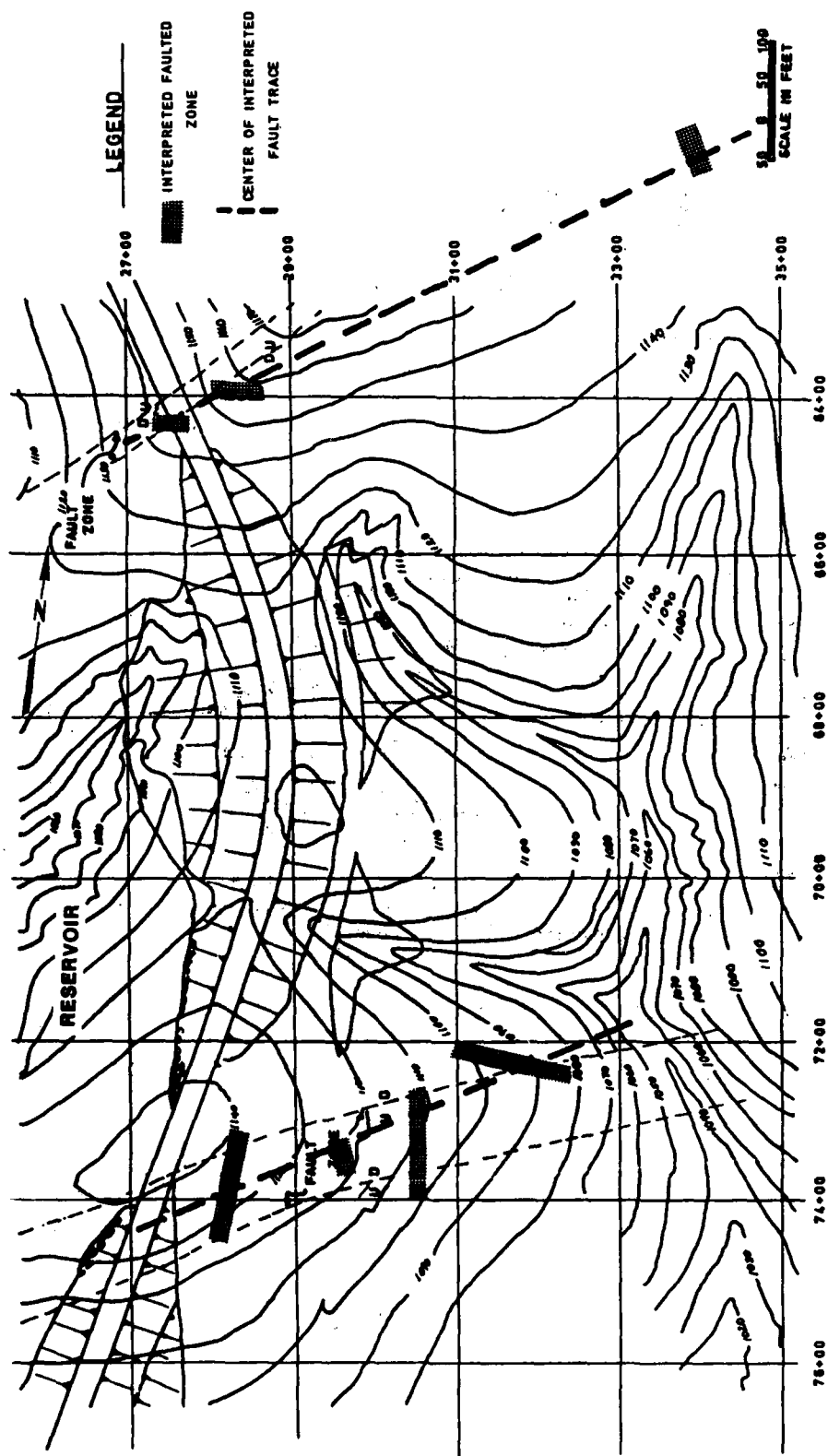
Figure 32. Fault zone locations interpreted from results of geophysical testing
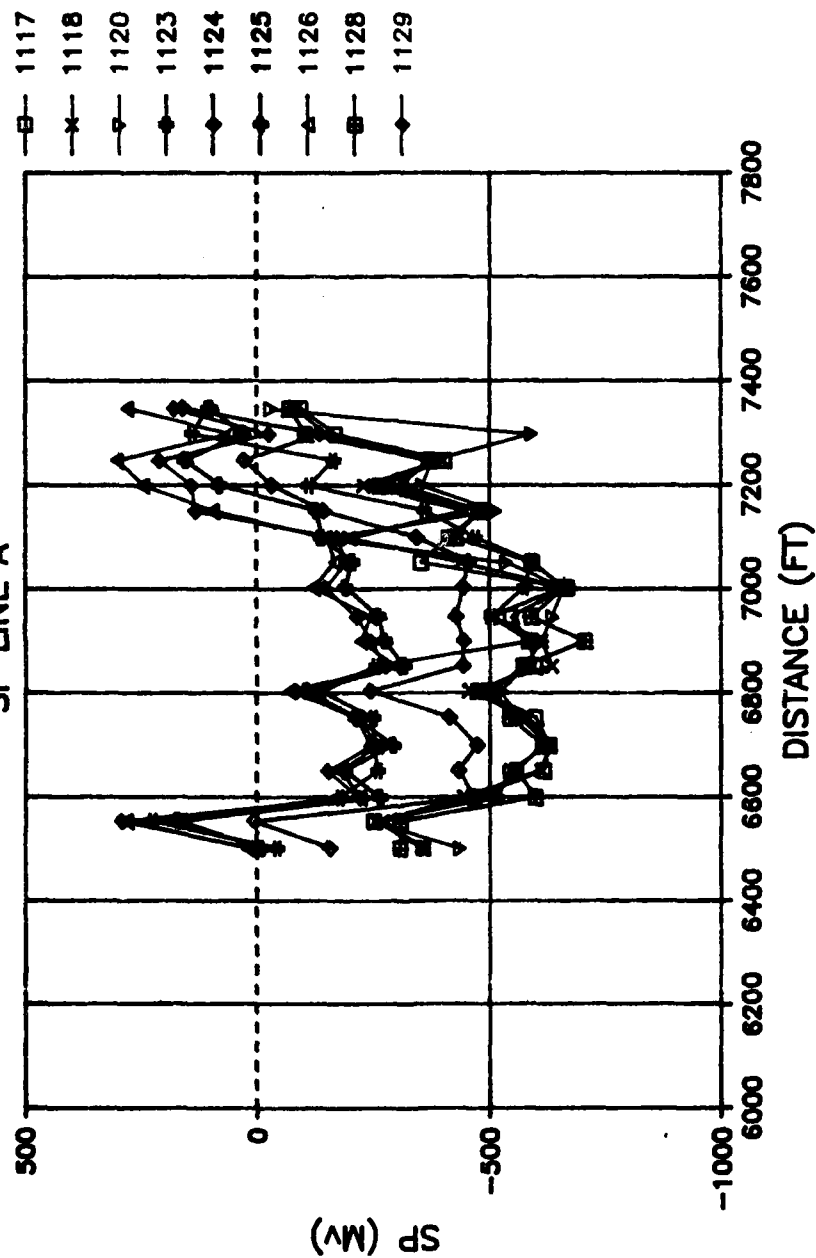
Figure 33. Unprocessed SP readings for SP line A, upstream Dike 1
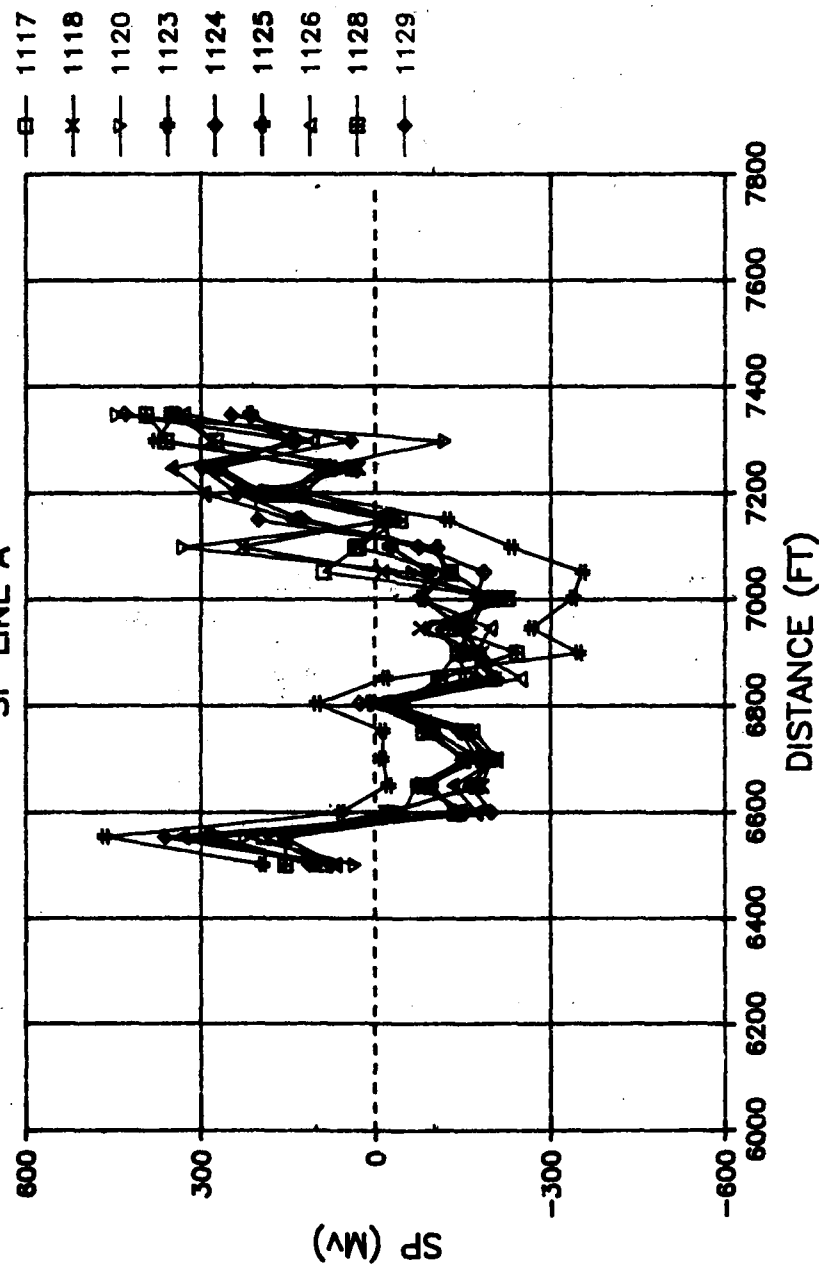
Figure 34. Static SP profile, SP line A, upstream Dike 1
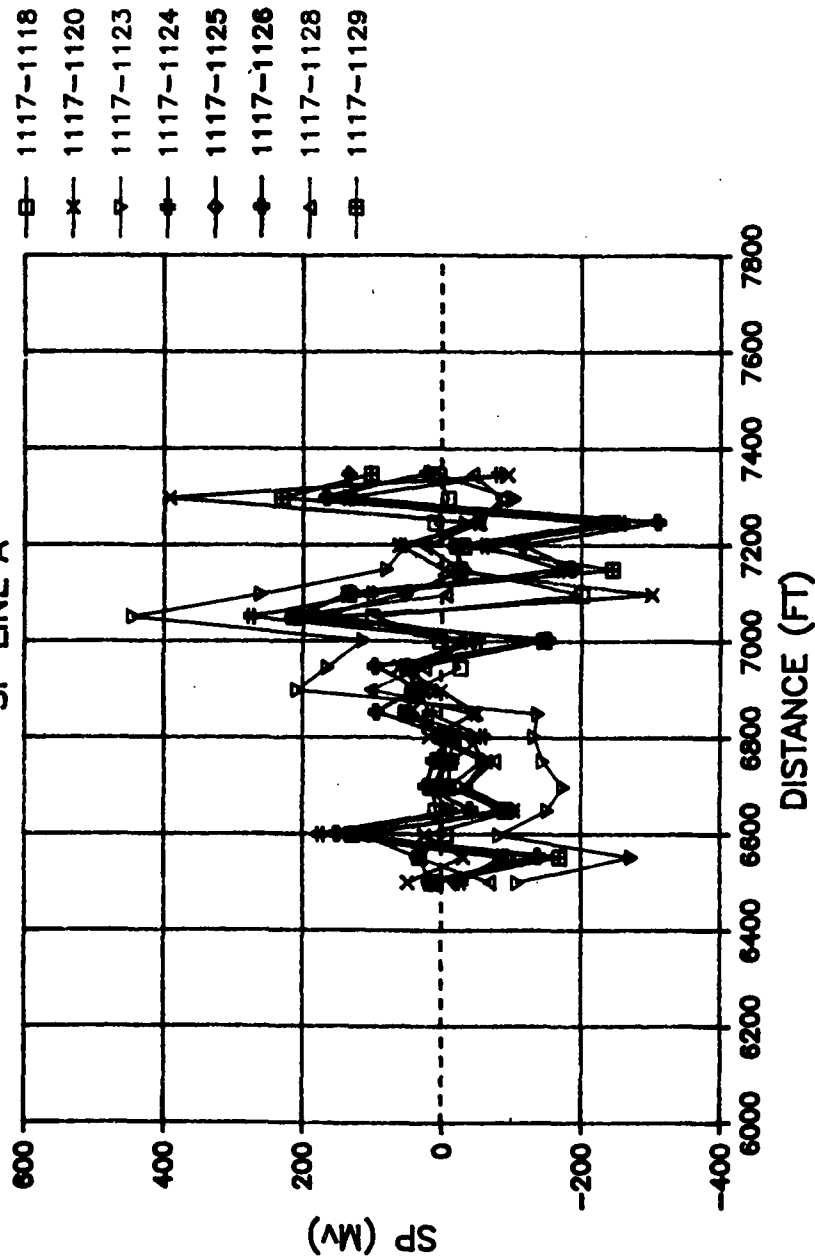
Figure 35. SP difference plot, SP line A, upstream Dike 1
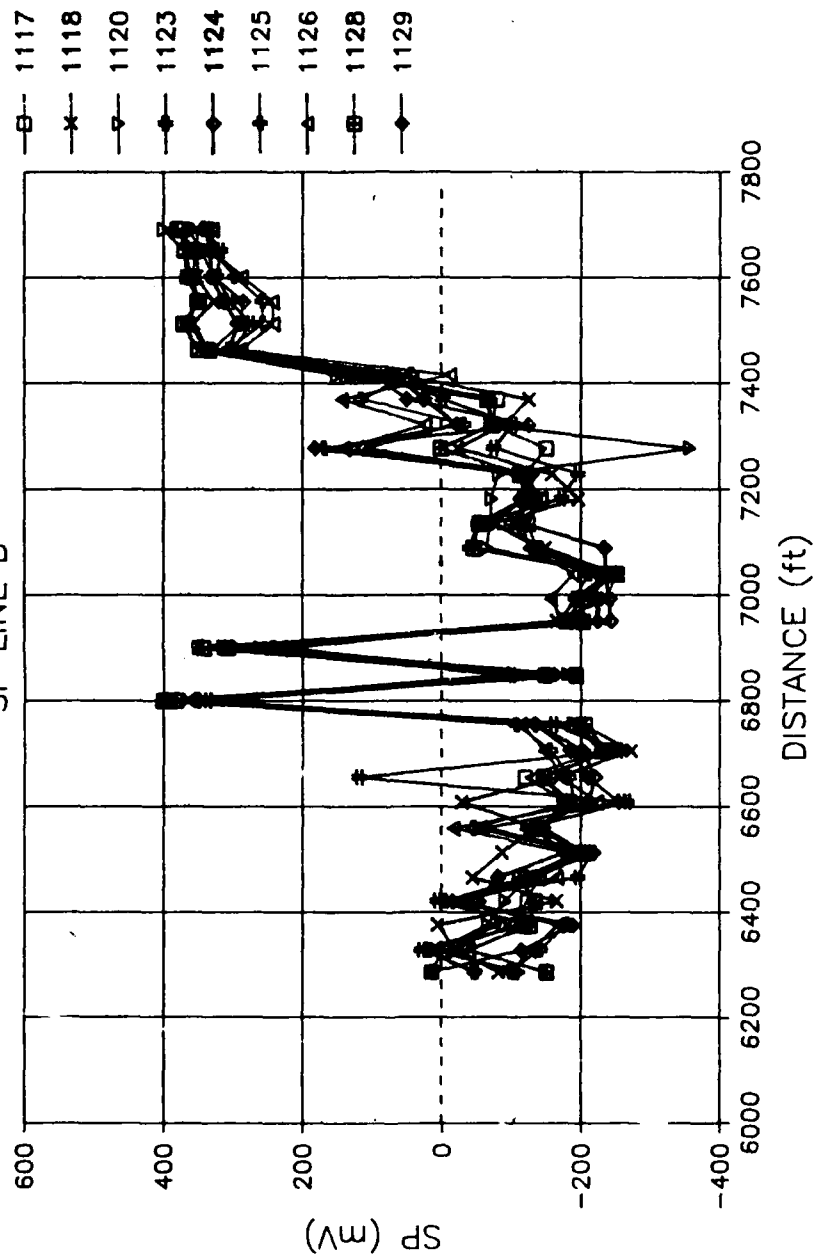
Figure 36. Static SP profile, SP line B, crest Dike 1
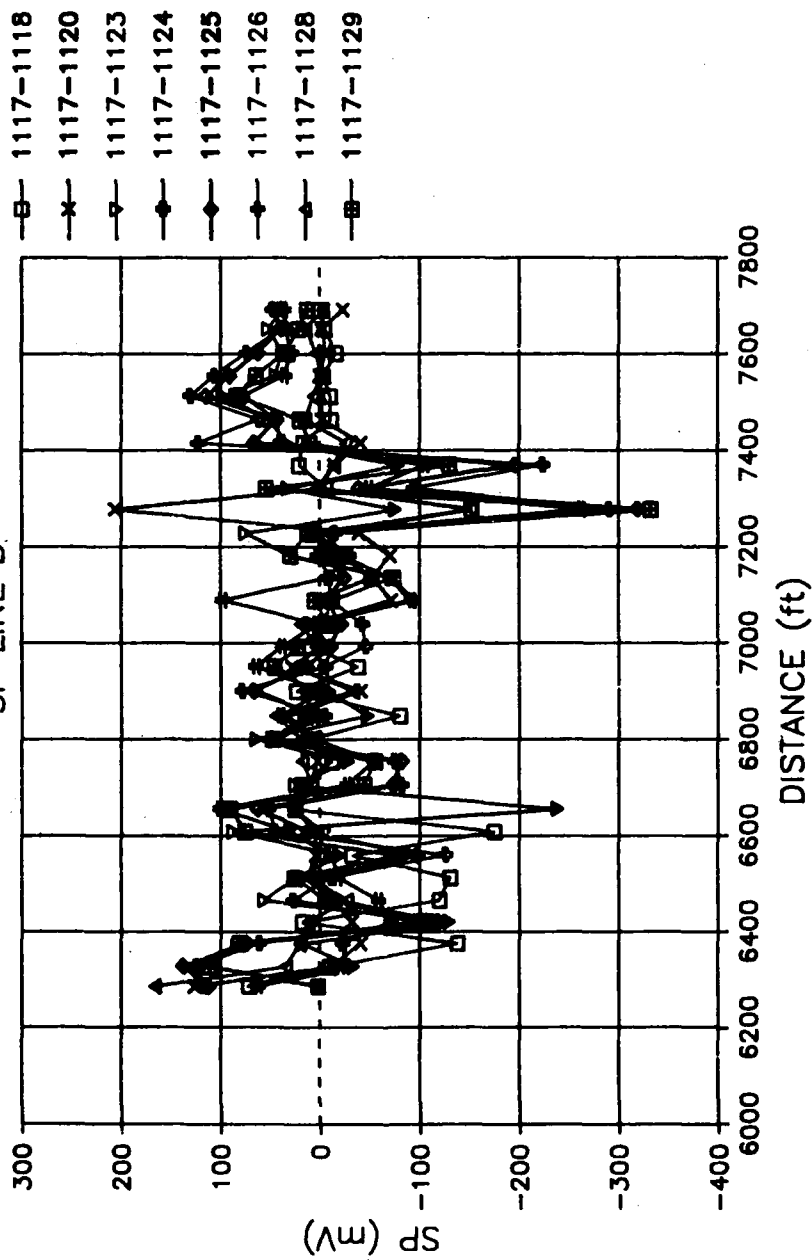
Figure 37. SP difference plot, SP line B, crest Dike 1
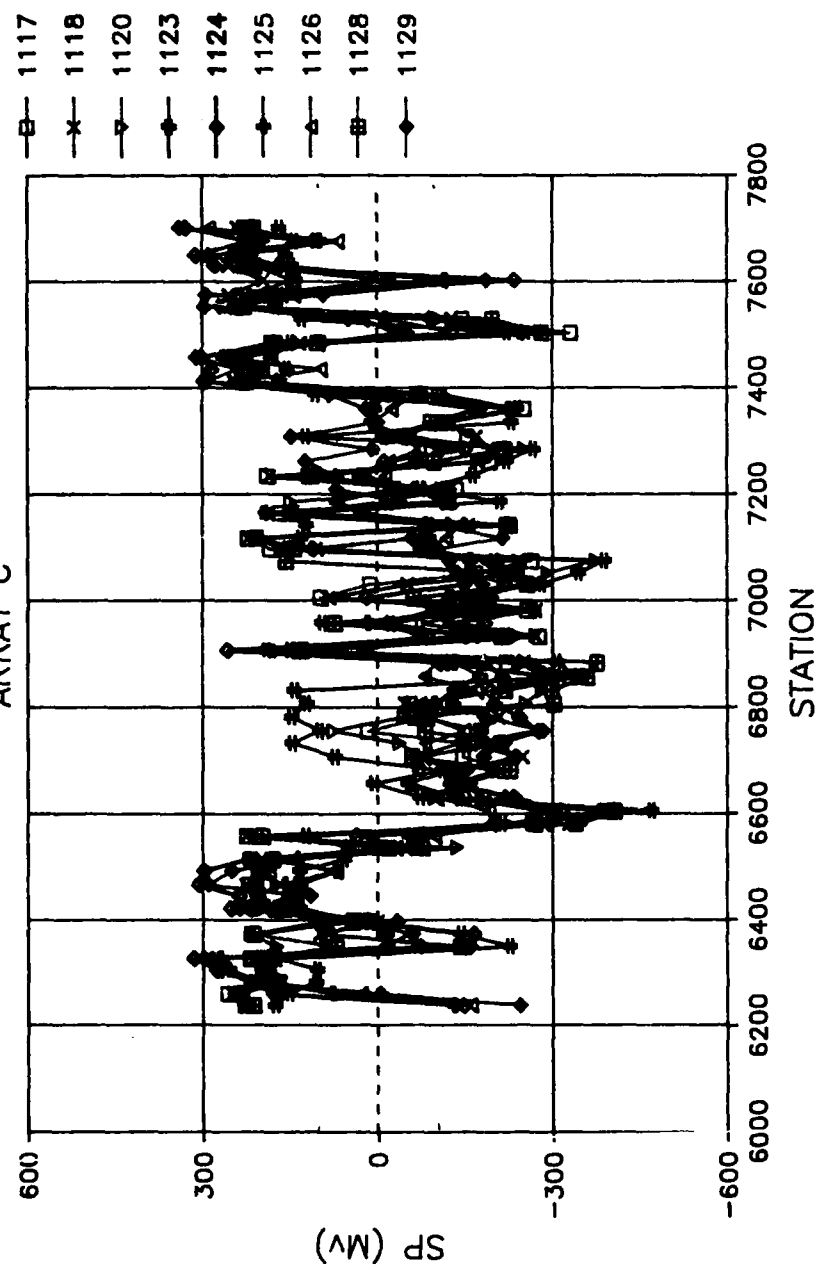
Figure 38. Static SP profile, SP line C, downstream berm Dike 1
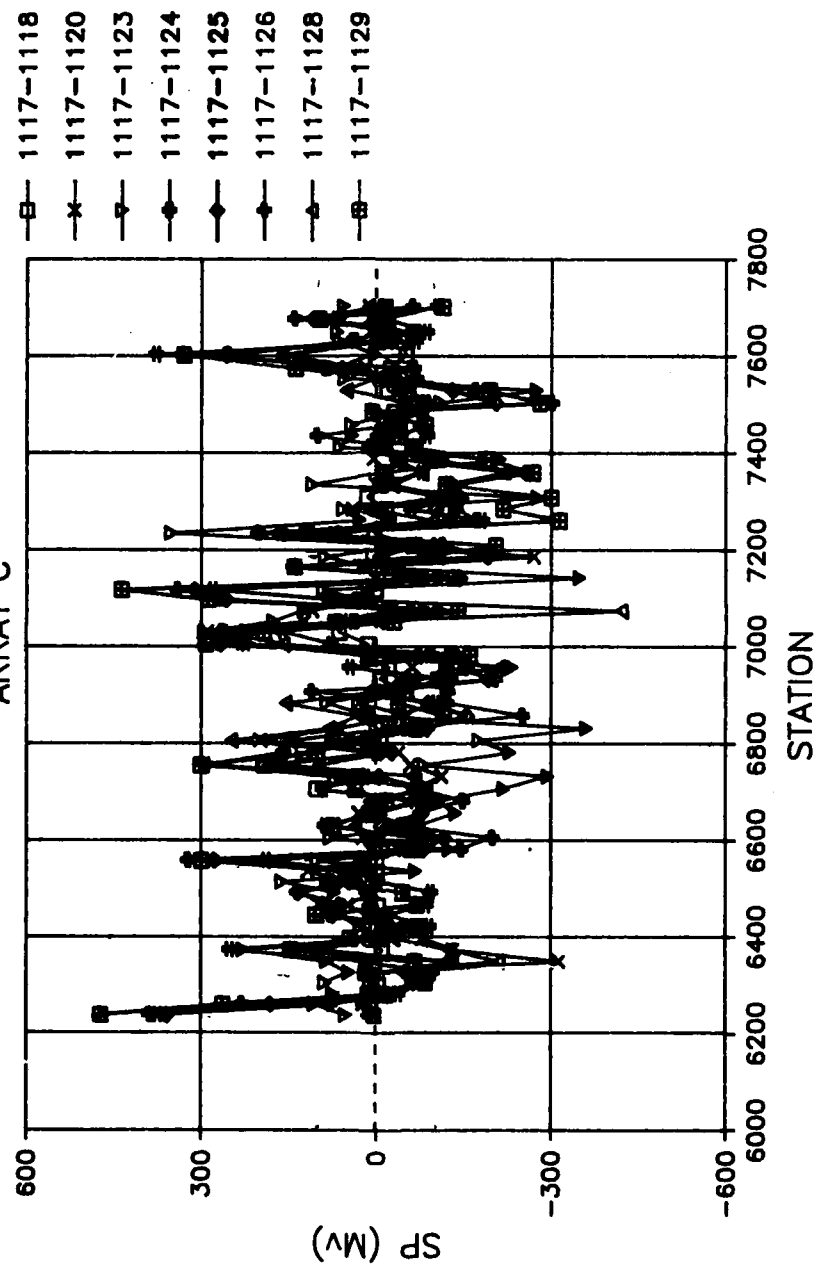
Figure 39. SP difference plot, SP line C, downstream berm Dike 1
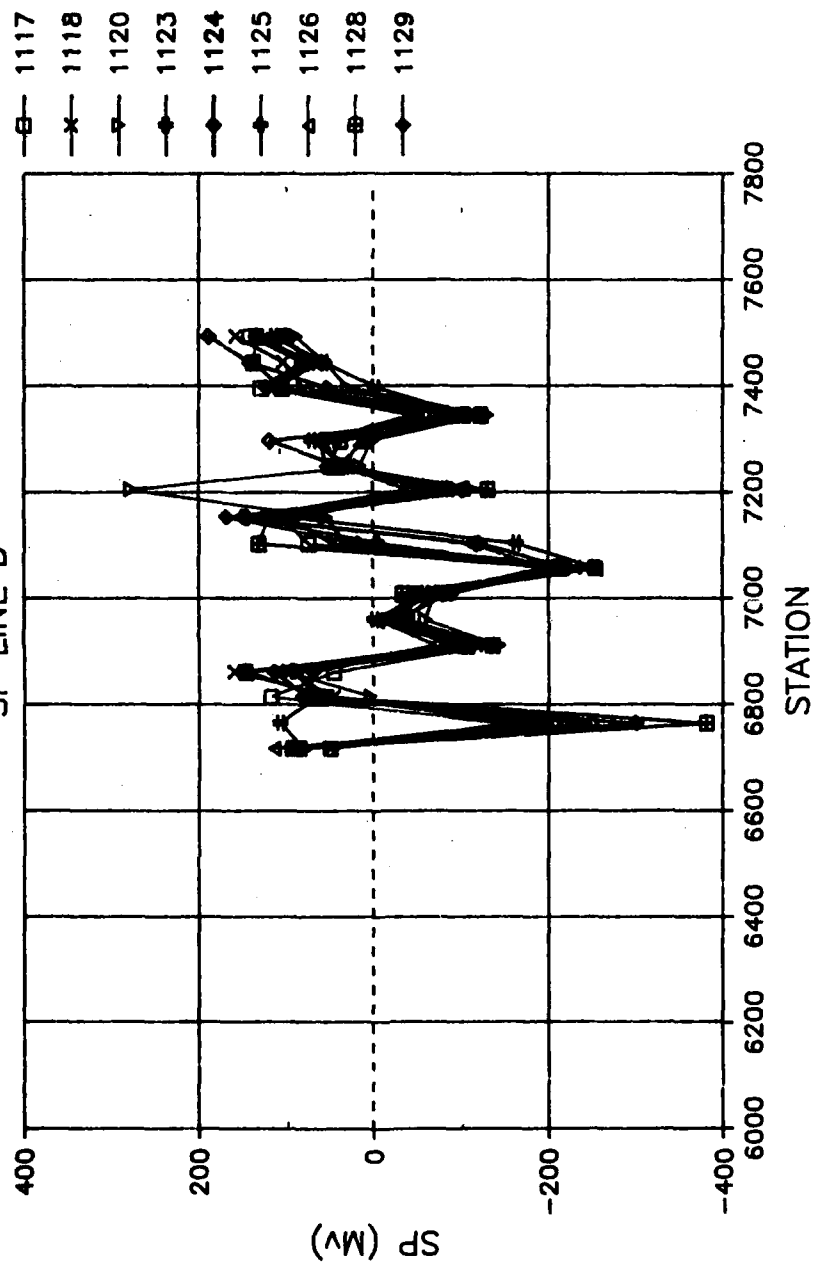
Figure 40. Static SP profile, SP line D, downstream Dike 1
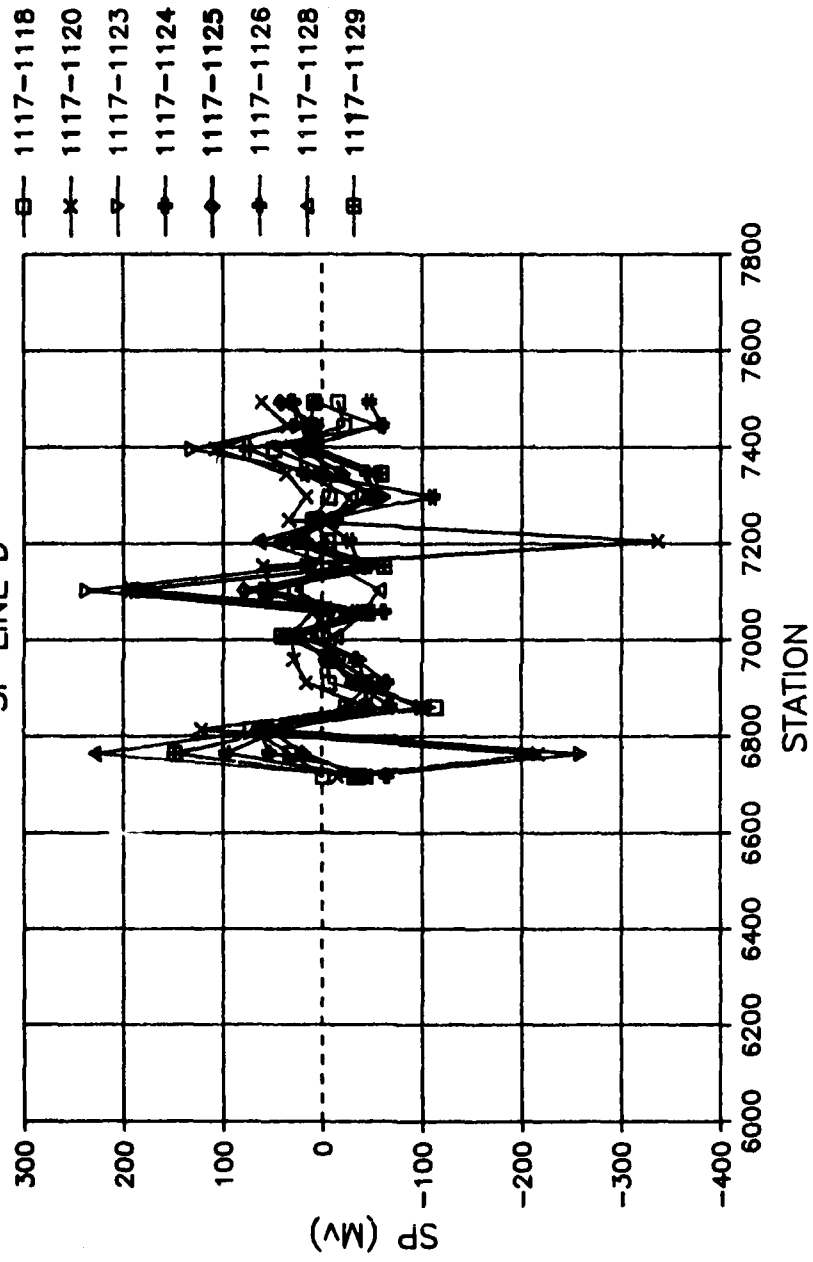
Figure 41. SP difference plot, SP line D, downstream Dike 1
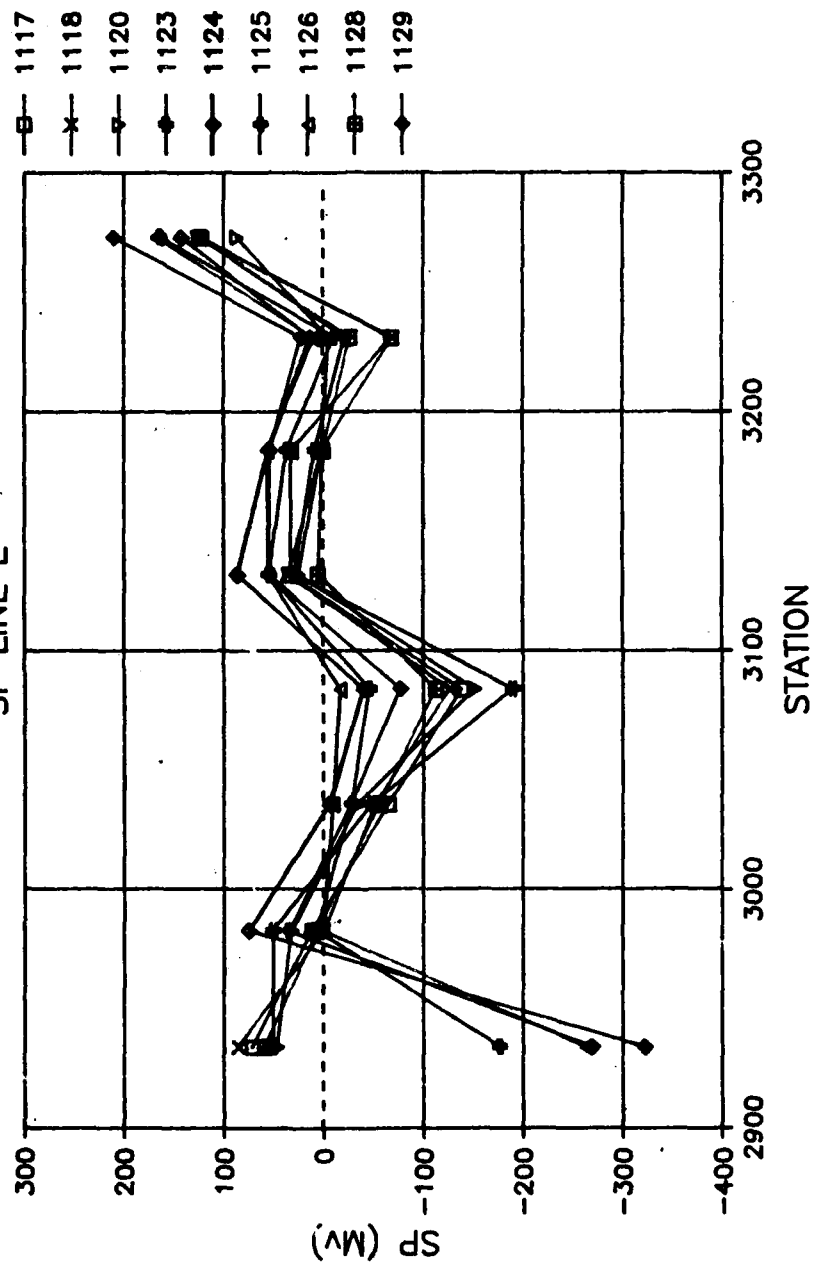
Figure 42. Static SP plot, SP line E, downstream Dike 1
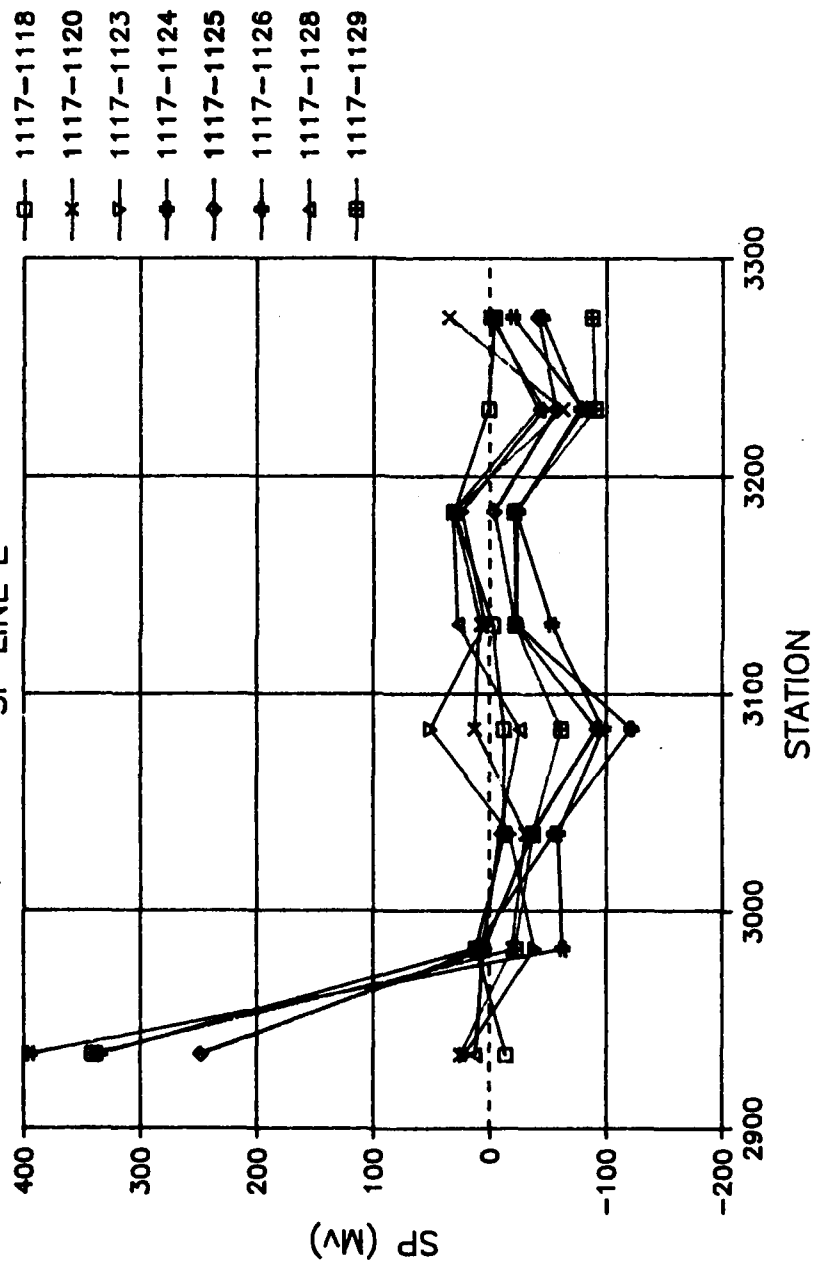
Figure 43. SP difference plot, SP line E, downstream Dike 1
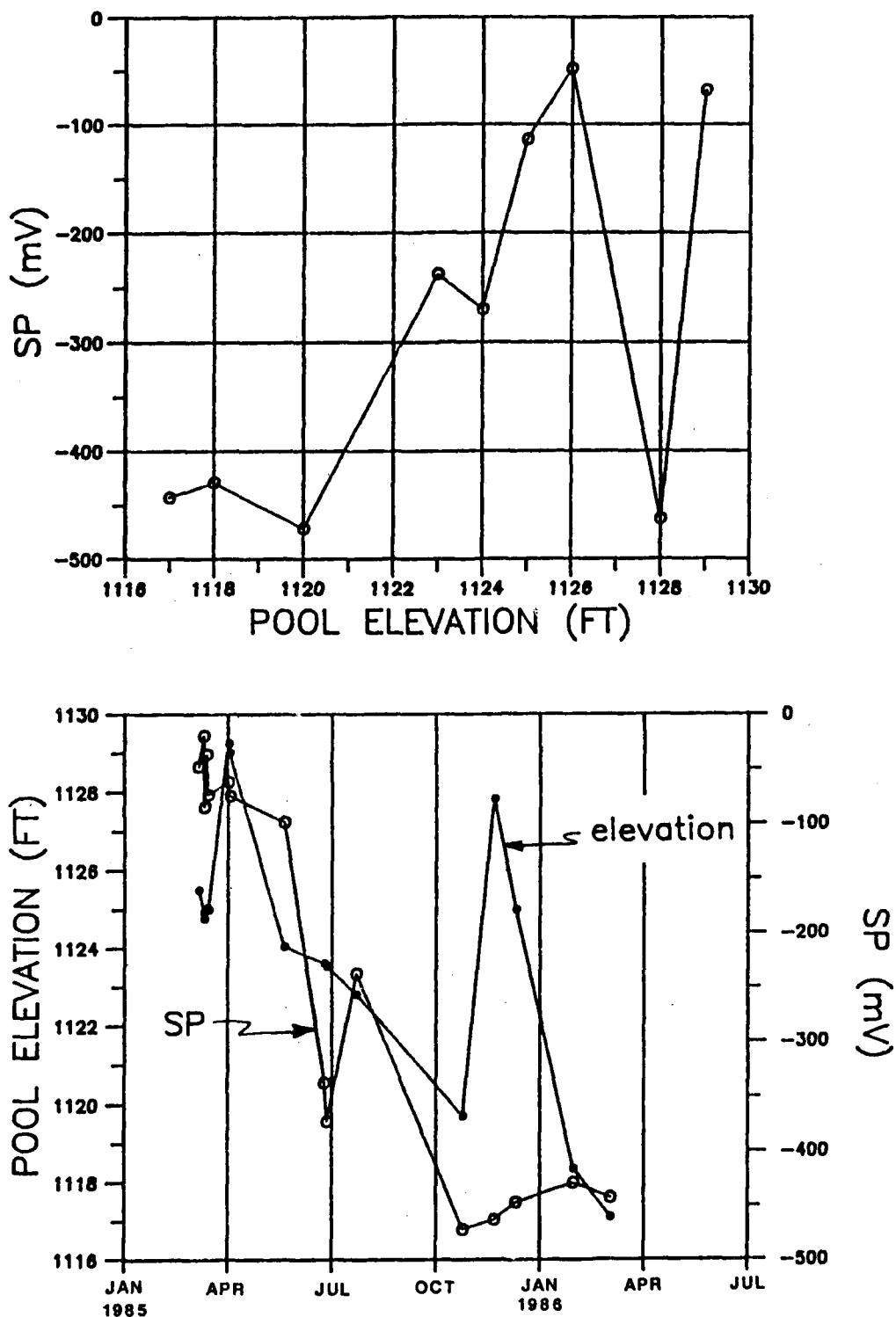
Figure 44. SP versus pool elevation, SP versus time, and
pool elevation versus time, for SP line A, upstream of Dike 1
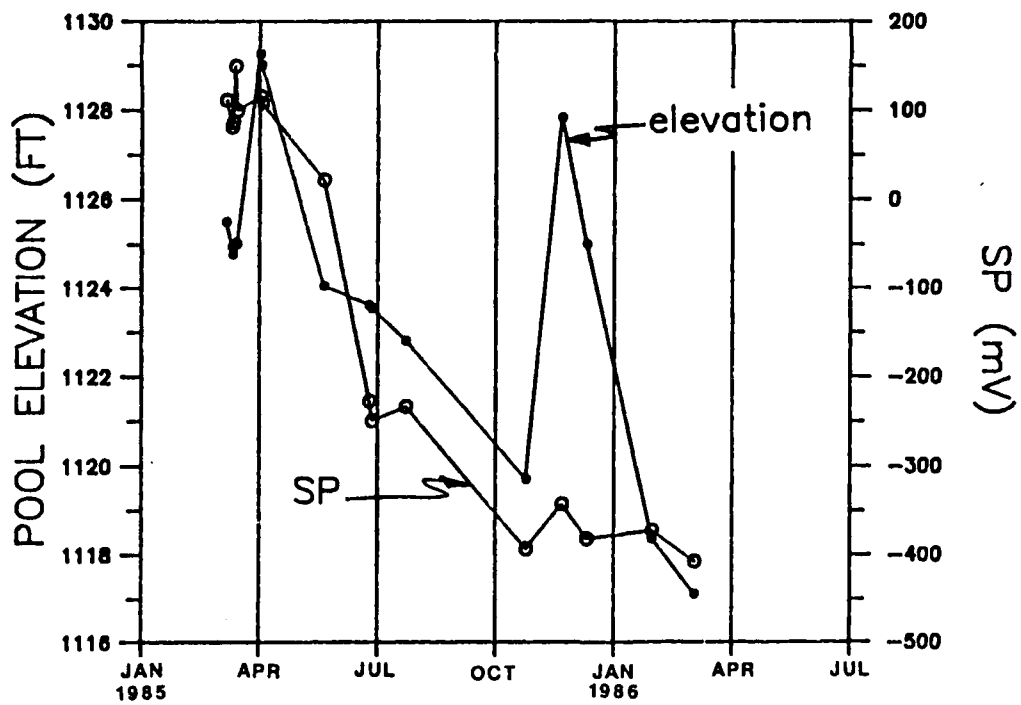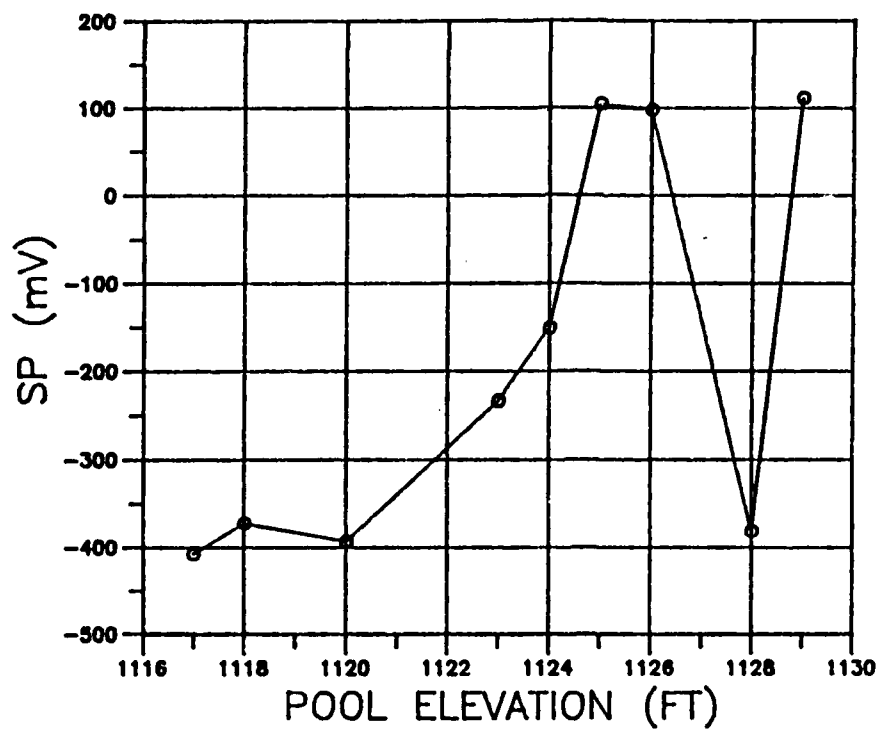
Figure 45. SP versus pool elevation, SP versus time, and pool elevation versus time, for SP line B, crest of Dike 1
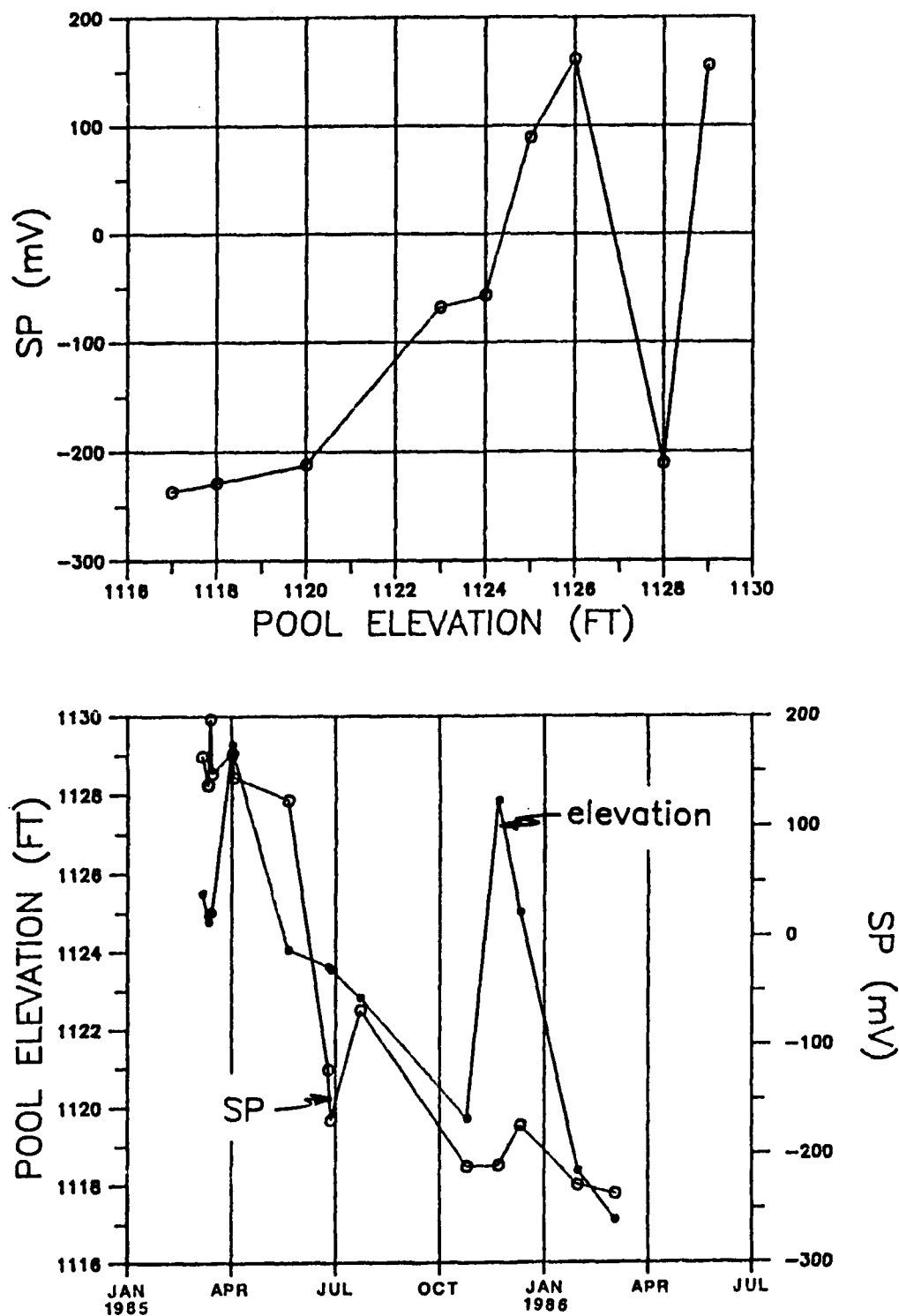
Figure 46. SP versus pool elevation, SP versus time, and pool elevation versus time, for SP line C, downstream berm Dike 1
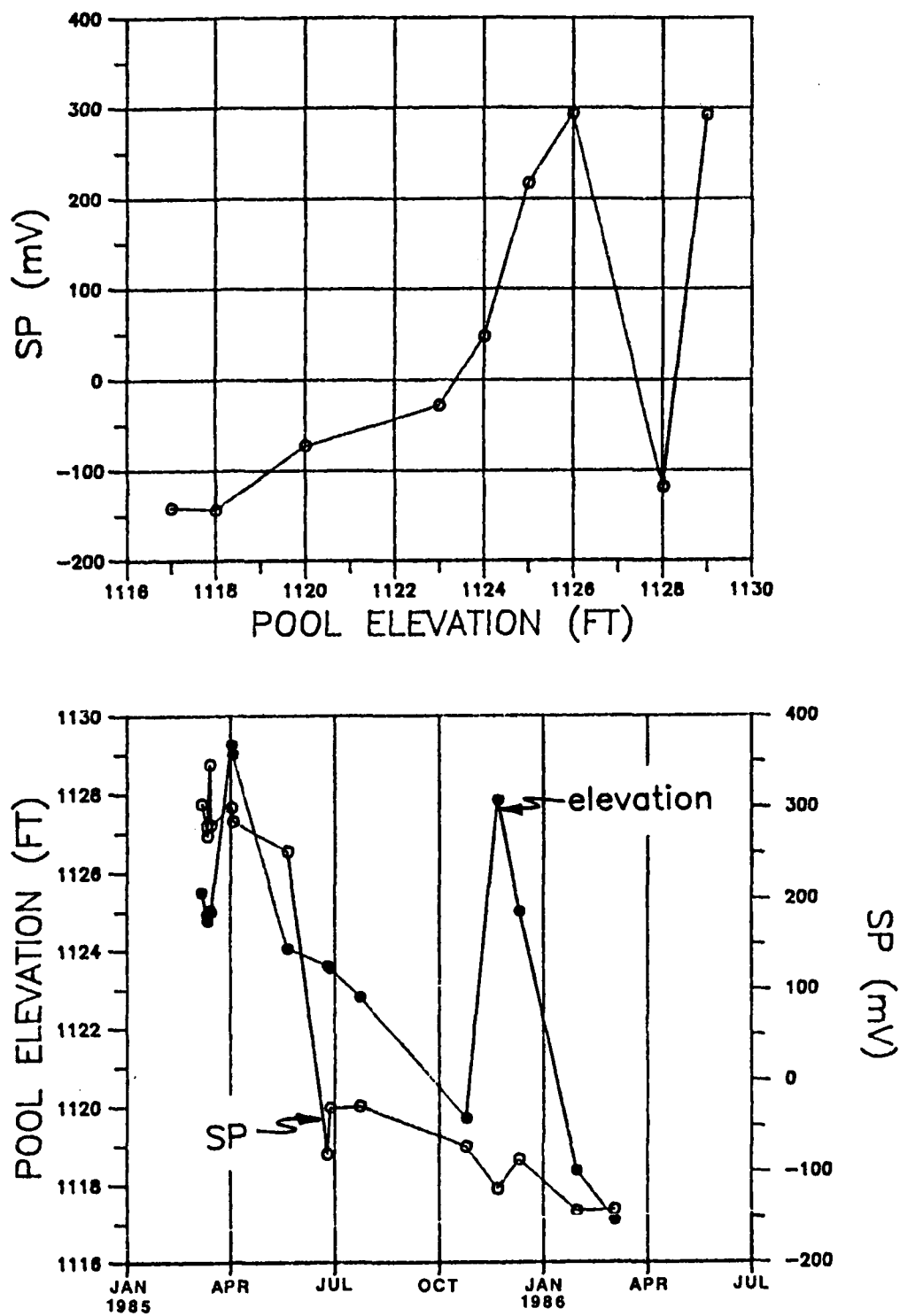
Figure 47. SP versus pool elevation, SP versus time, and pool elevation versus time, for SP line D, downstream of Dike 1
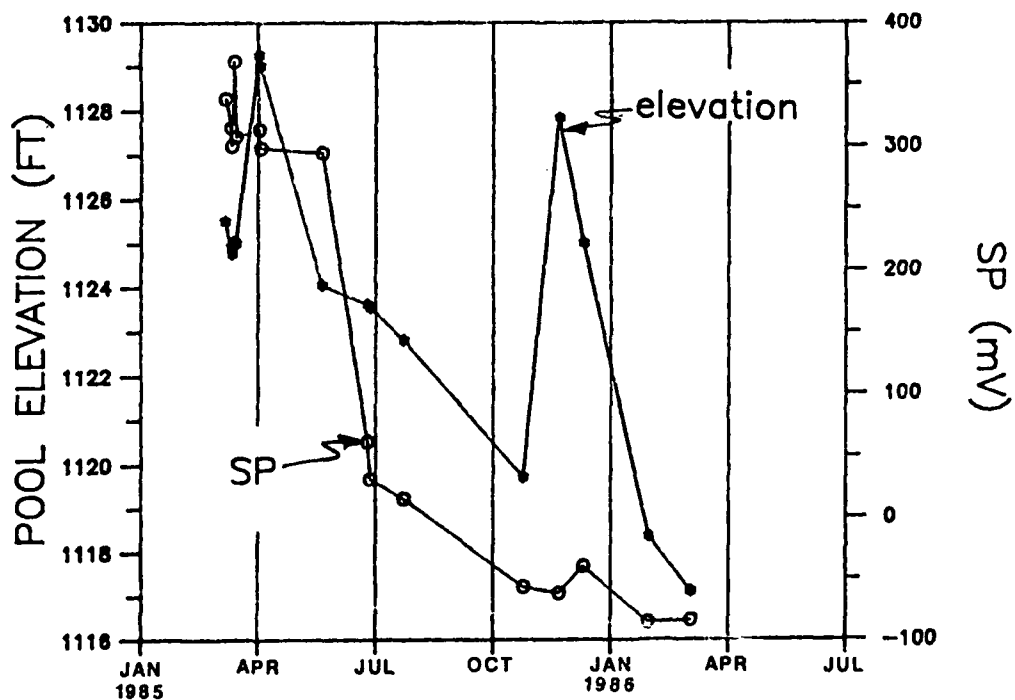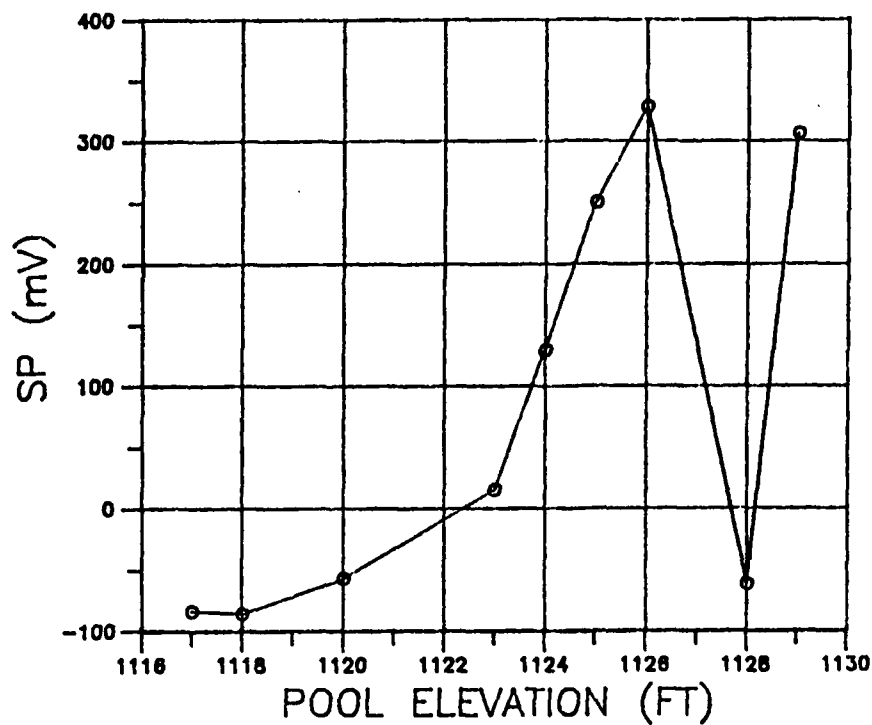
Figure 48. SP versus pool elevation, SP versus time, and pool elevation versus time, for SP line E, downstream of Dike 1

Figure 49. Results of November 1984 downhole water conductivity survey

END
9-88

1.0

4.5
50
56
6.3
7.1
80

2.8

3.2

3.6

4.0

2.5

2.2

2.0

1.1

1.8

1.25

1.4

1.6
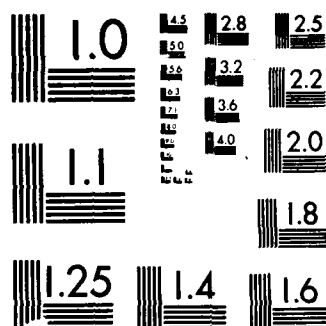
UTION TEST CHART
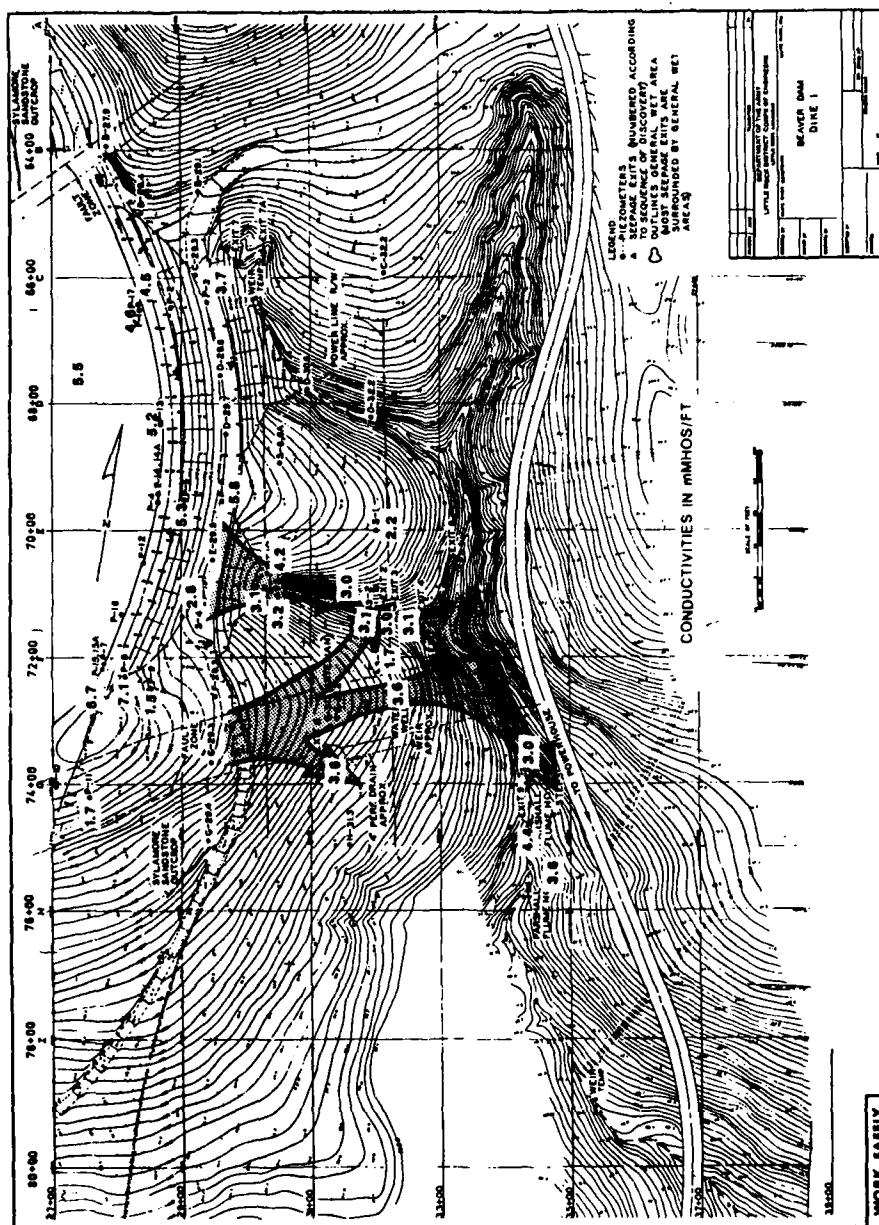
Figure 50. Results of March 1985 downhole water conductivity survey
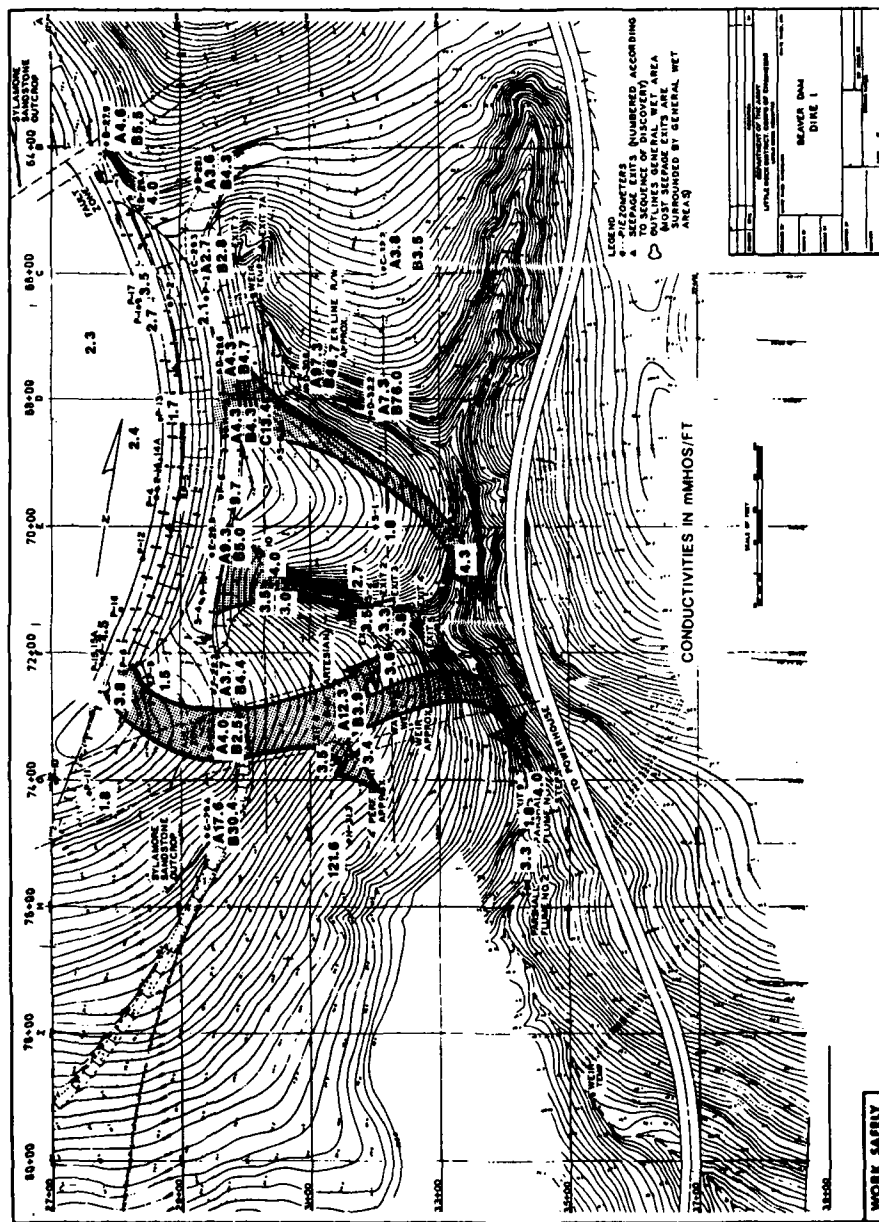
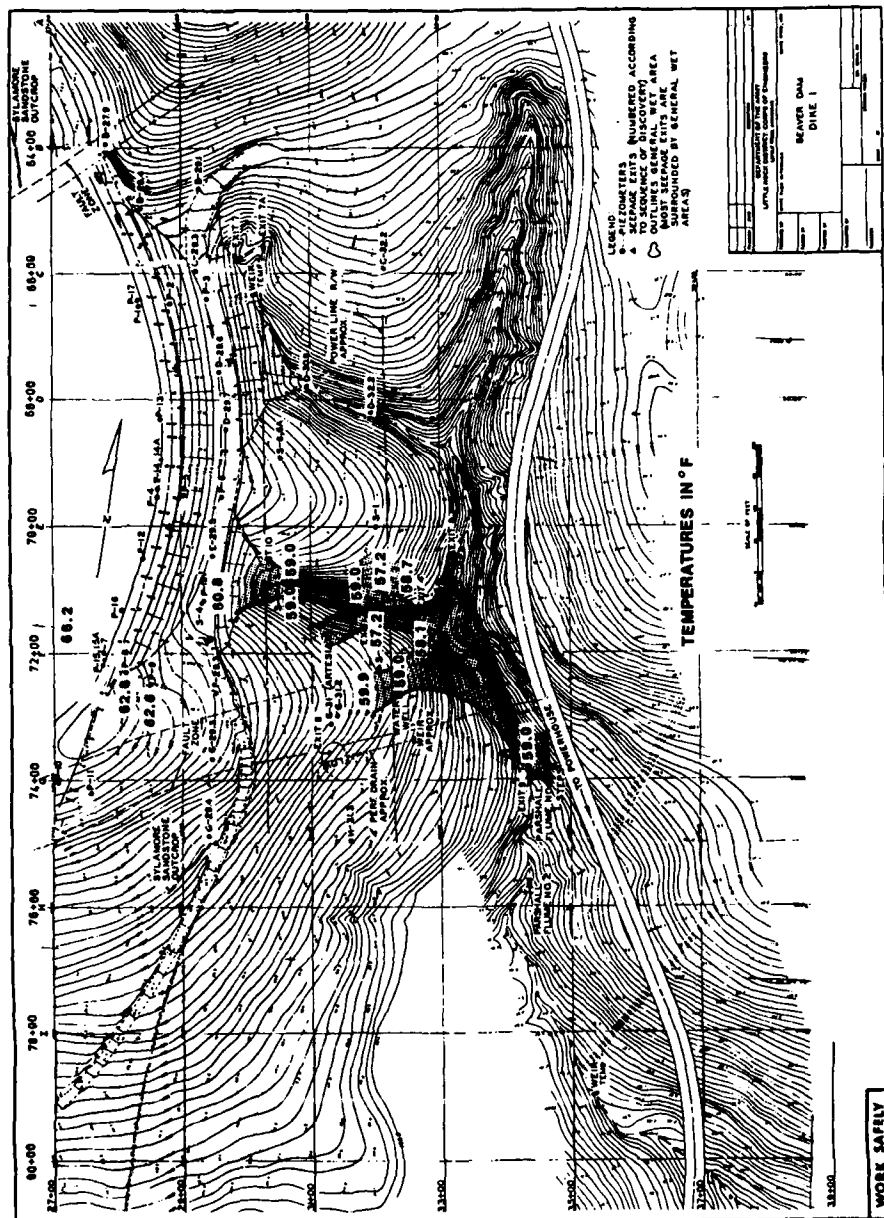Figure 51. Results of January 1986 downhole water conductivity survey

Figure 52. Results of November 1984 downhole water temperature survey

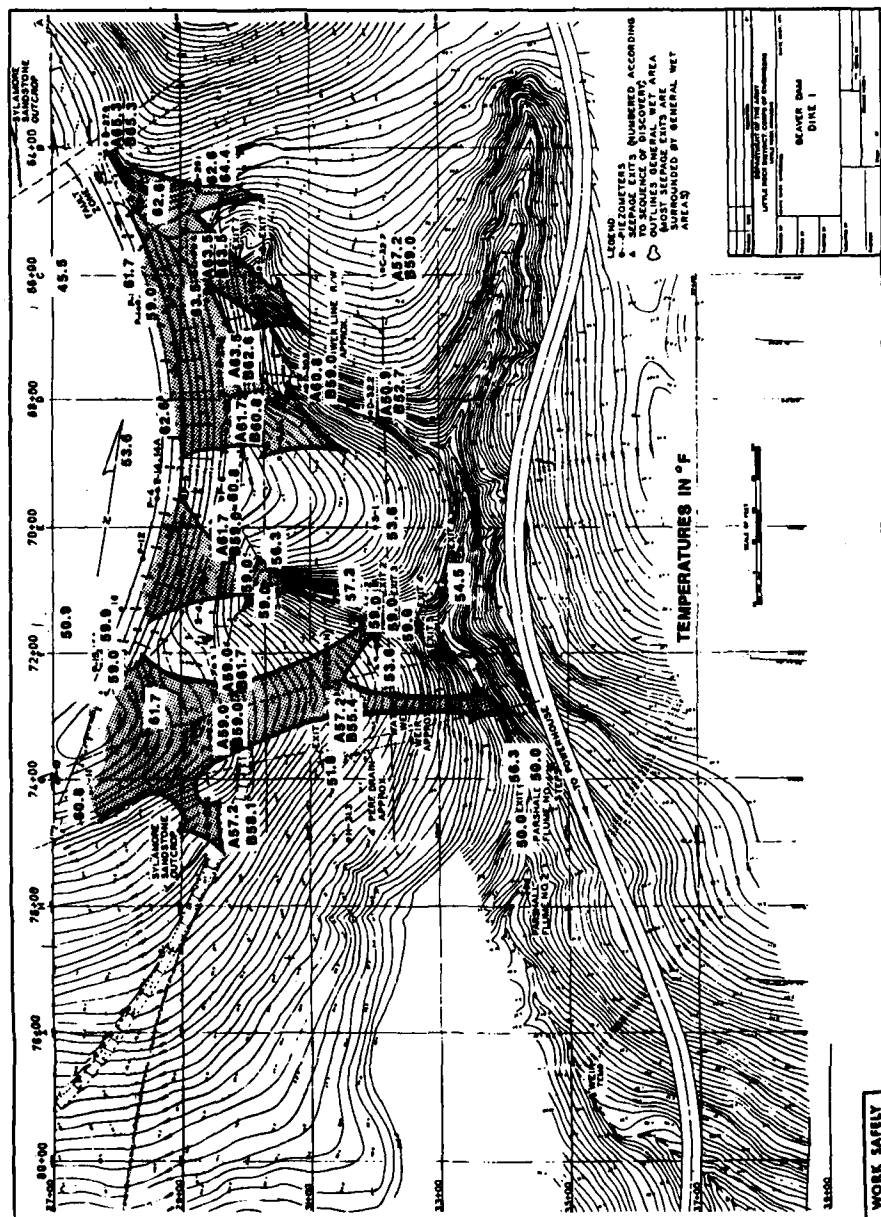Figure 53. Results of March 1985 downhole water temperature survey

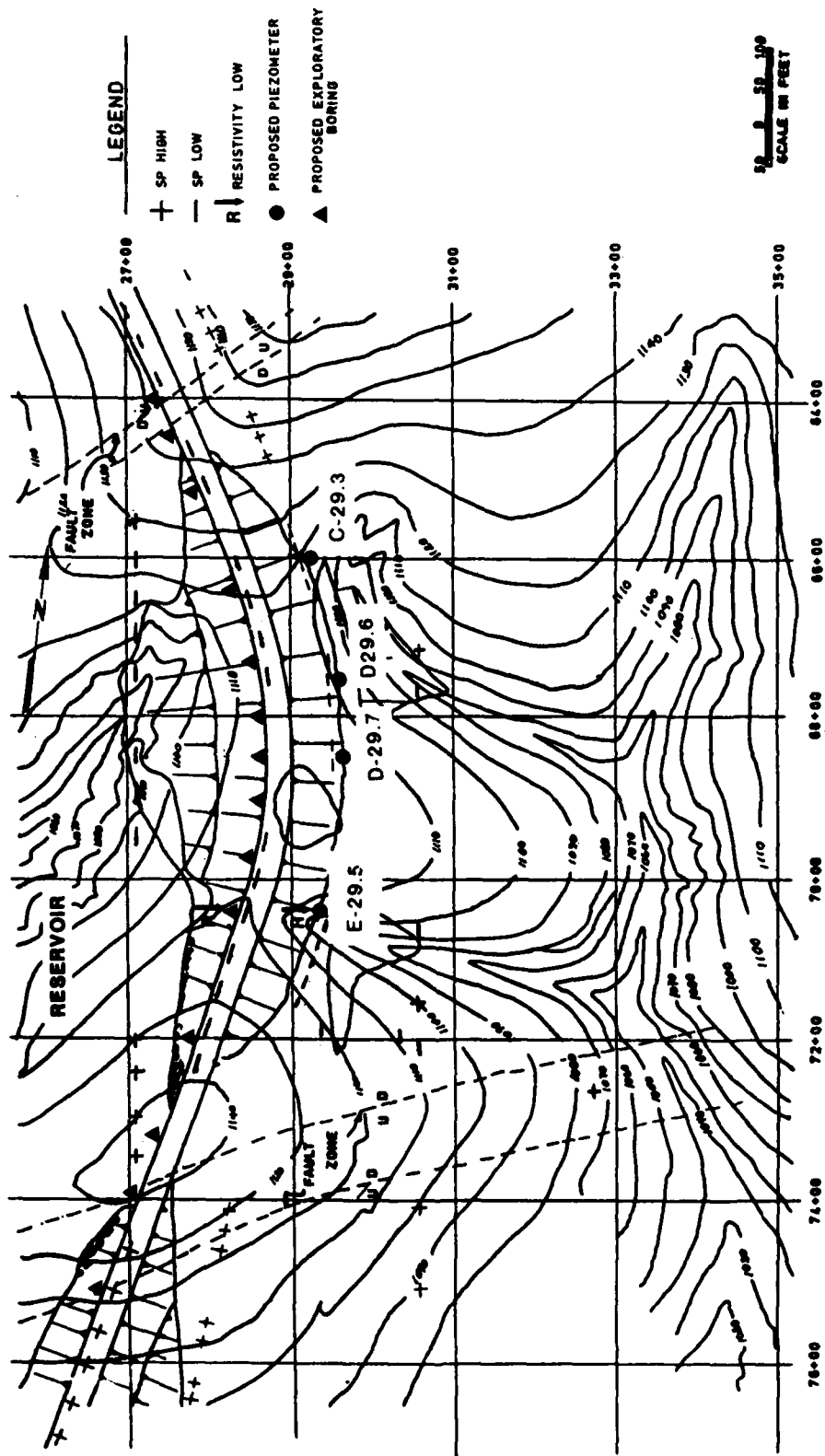Figure 54. Results of January 1986 downhole water temperature survey

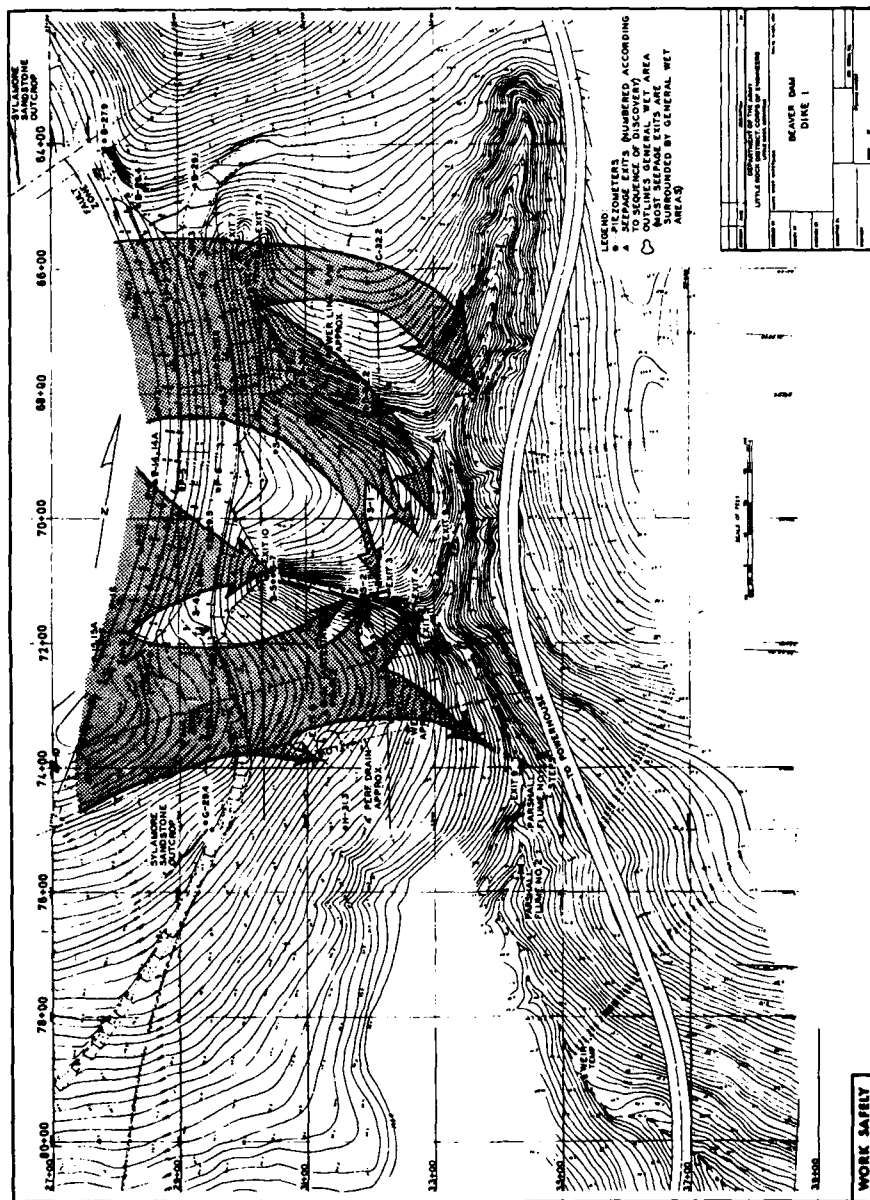Figure 55. WES-recommended piezometer and exploratory boring locations

Figure 56. Integrated methods seepage map